

**Lehmann:
Gold deposits**

SS 2009



Gold London PM Fix 2000 present



Silver - London PM Fix 2000 - present



www.kitco.com

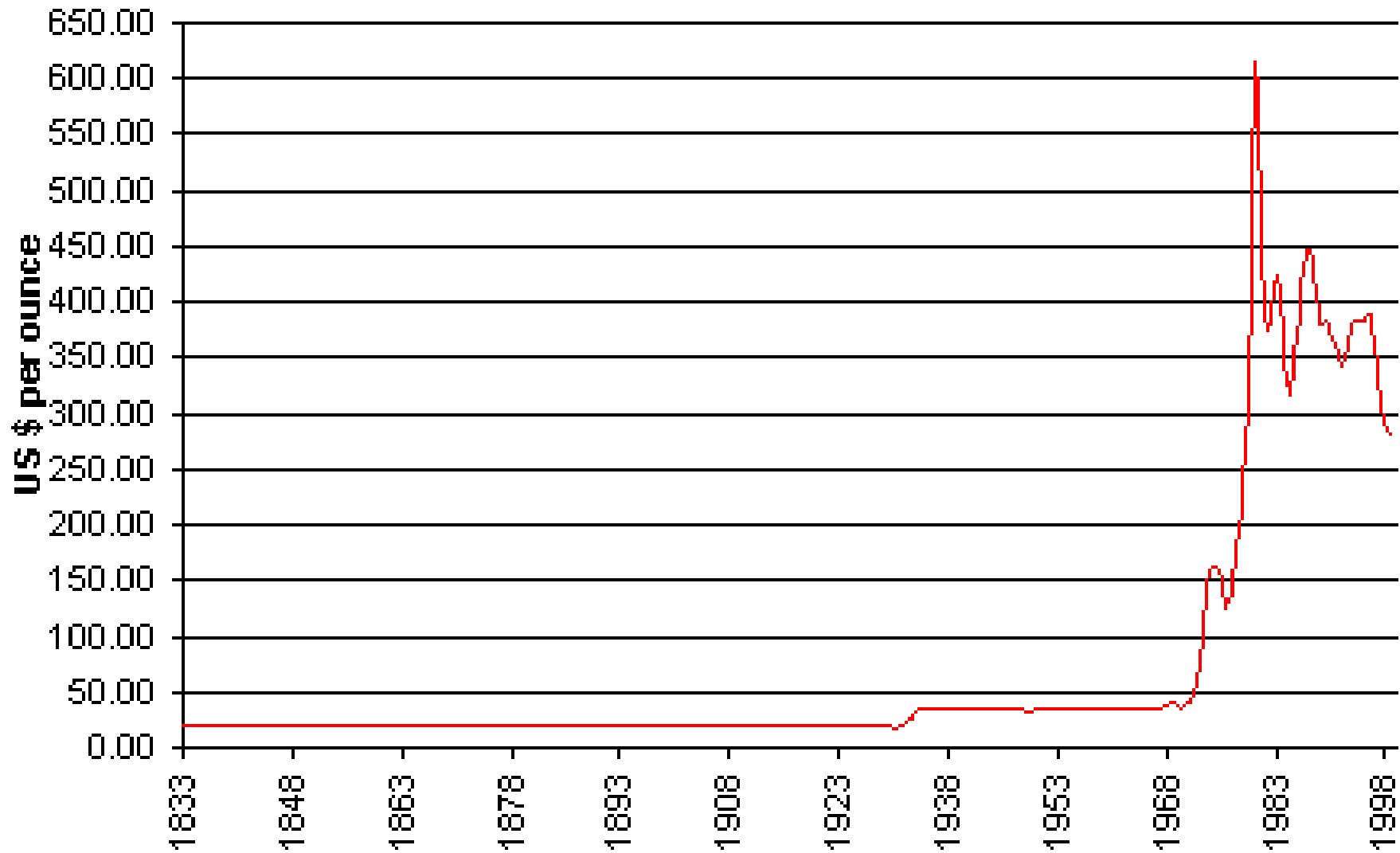
Gold - London PM Fix 1975 - present



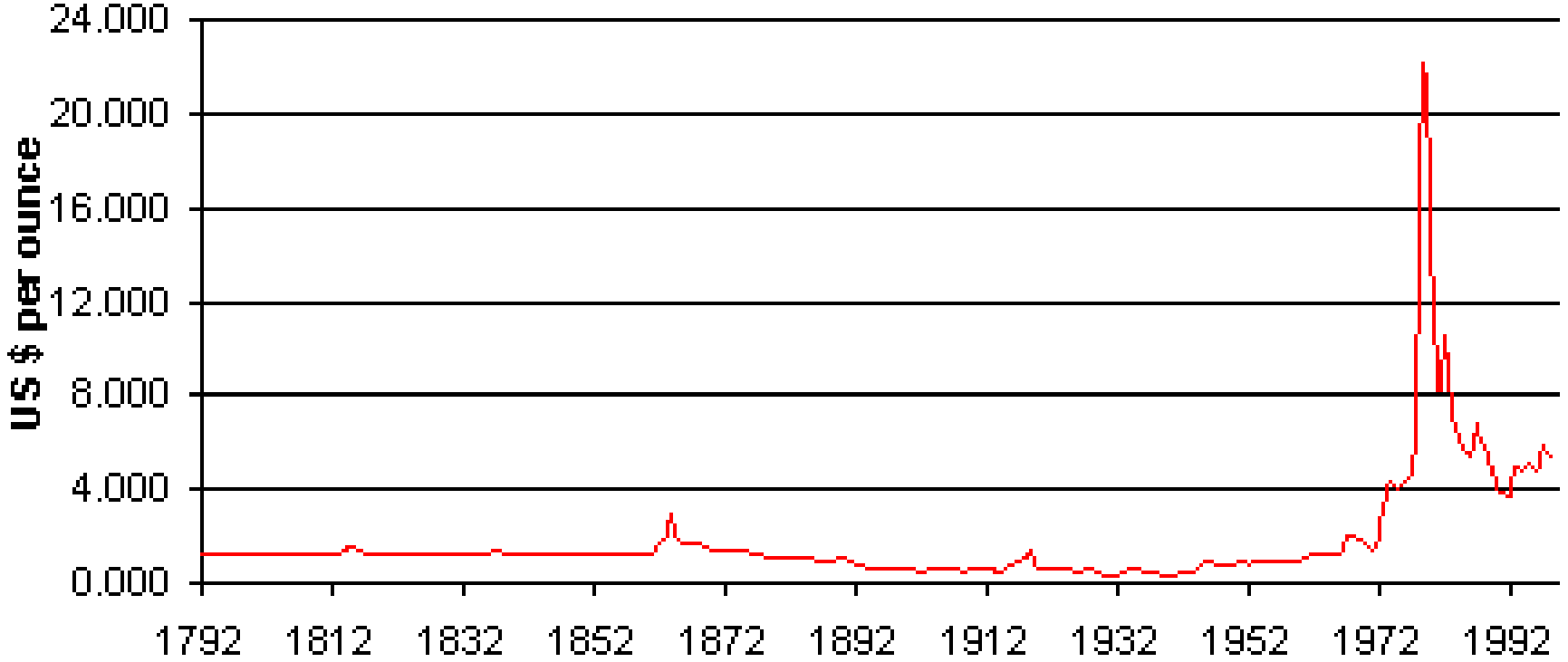
www.kitco.com

GOLD - London PM Fix Averages - 1883 - present

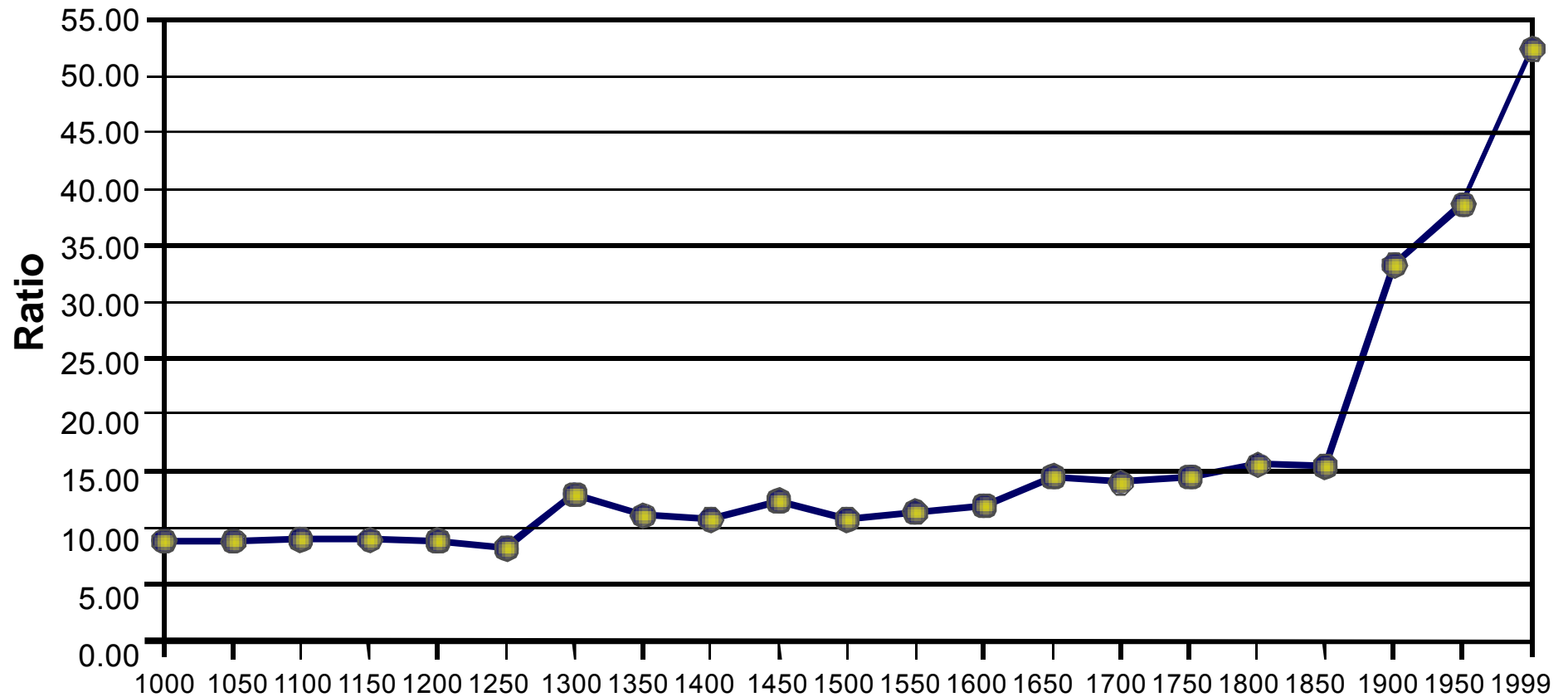
kitco.com



SILVER - London Fix - Averages - 1792 - present
kitco.com



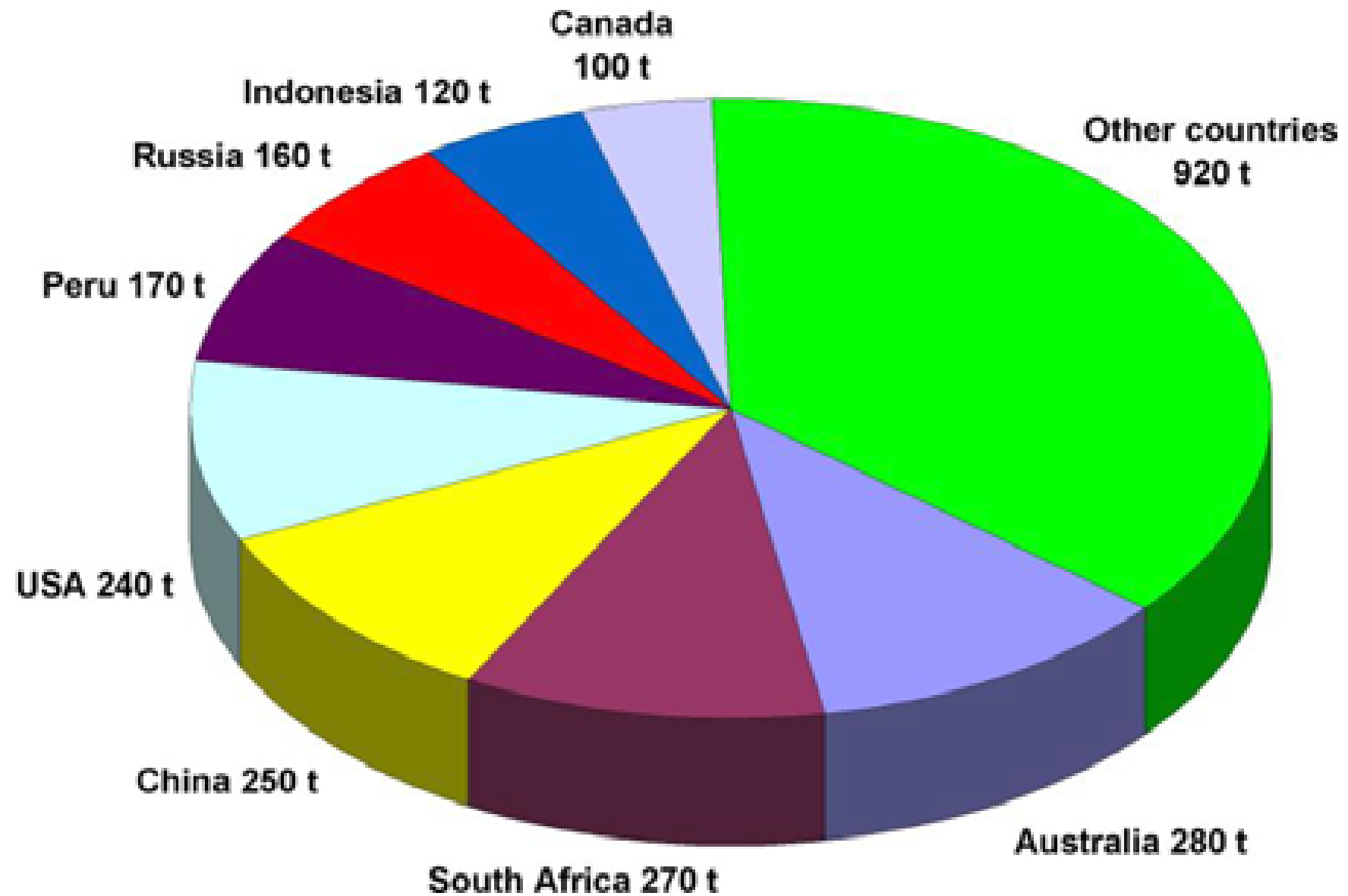
Gold/Silver Price Ratio (1000 – 1999)



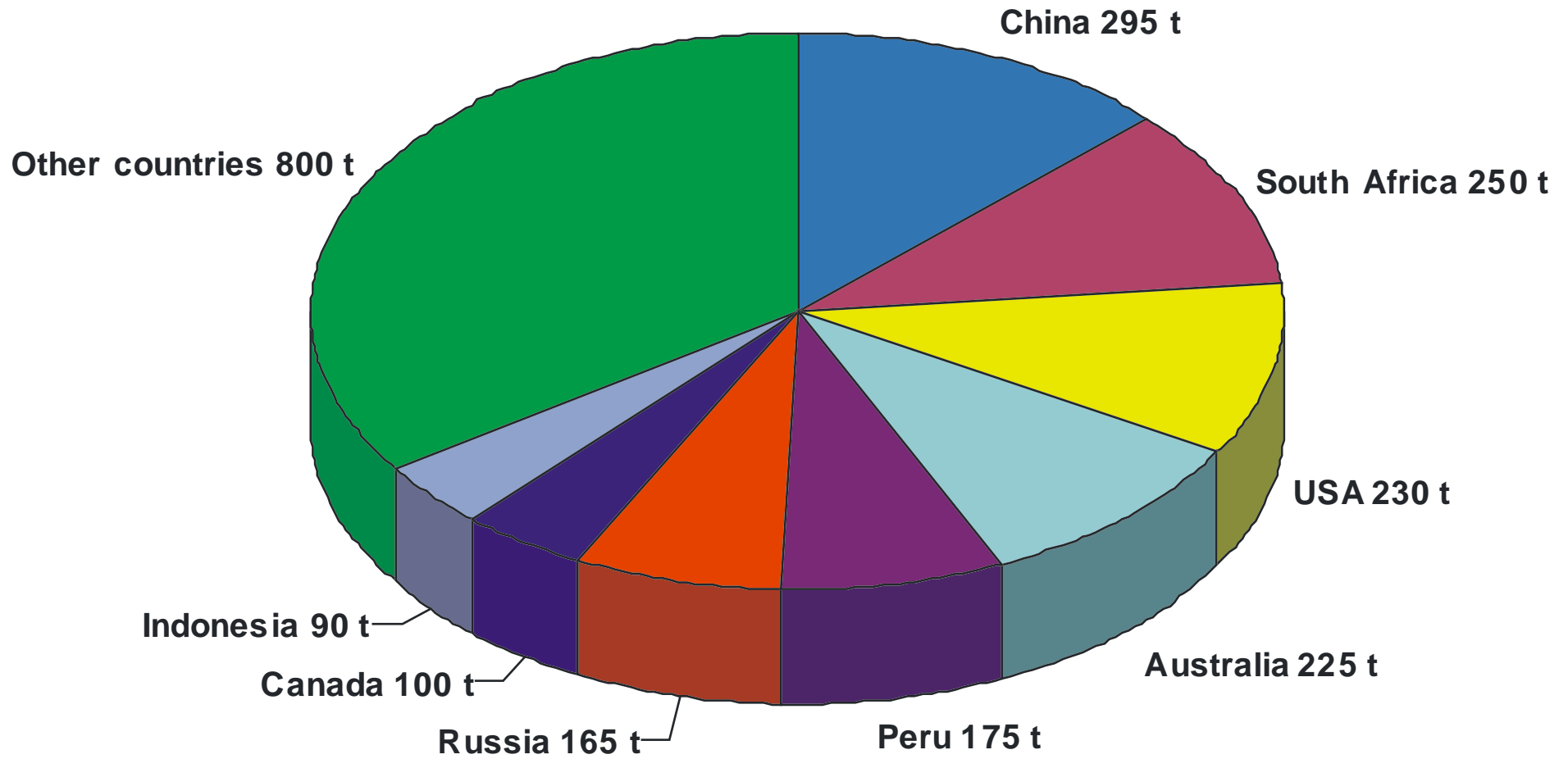
← 3500 BC: 2.5

→ 2008: 50

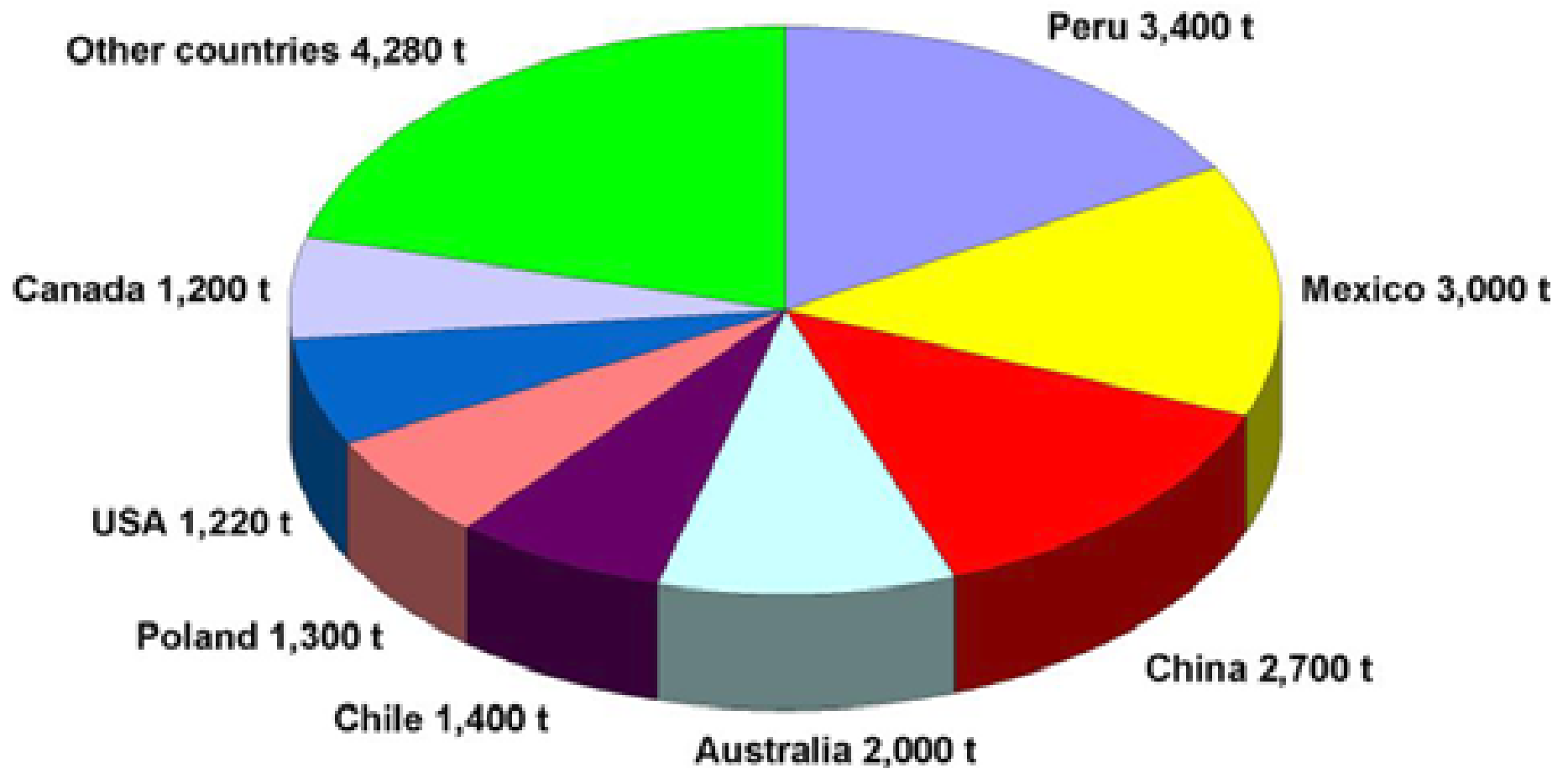
GOLD WORLD MINE PRODUCTION 2007 (2,510 t)



GOLD WORLD MINE PRODUCTION 2008 (2,330 t)



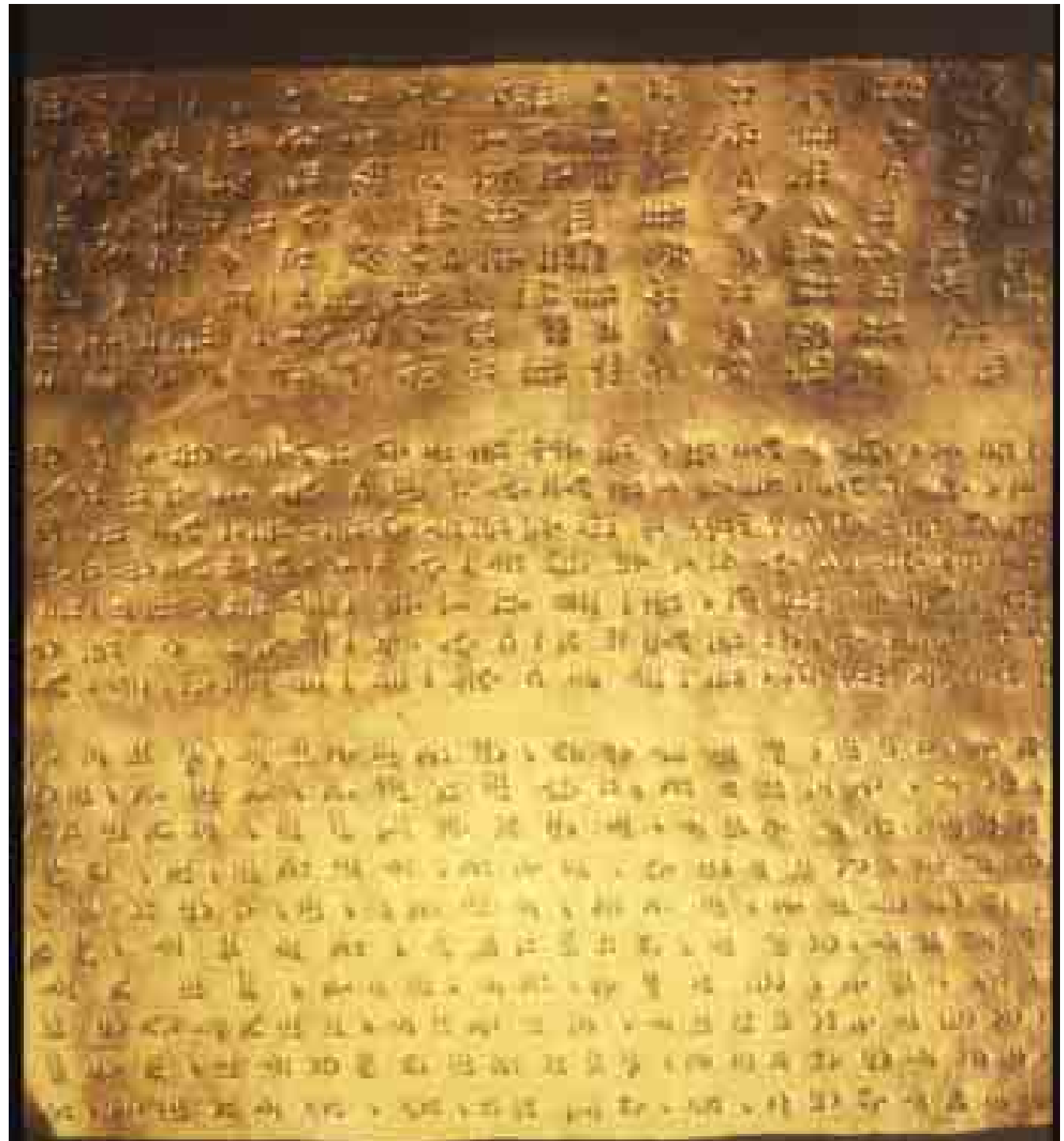
SILVER WORLD MINE PRODUCTION 2007 (20,500 t)





Gold coin with image of Justin II (c. 520 – 578 AC), 4.49 g

Darius I, Persia
6th century A.D.







0 E 50 100 cm

W



„Turin papyrus map“
Museo Egizio, Turin

Length of Wadi Hammamat
(Valley of the Many Baths)
shown is ~15 km.

Made by the well-known
‘Scribe of the Tomb’
Amennakhte in 1150 BC
First topographic and
geologic map







Mountains of gold

The shrine of Amu

The road that leads to the sea

The houses of the gold workers

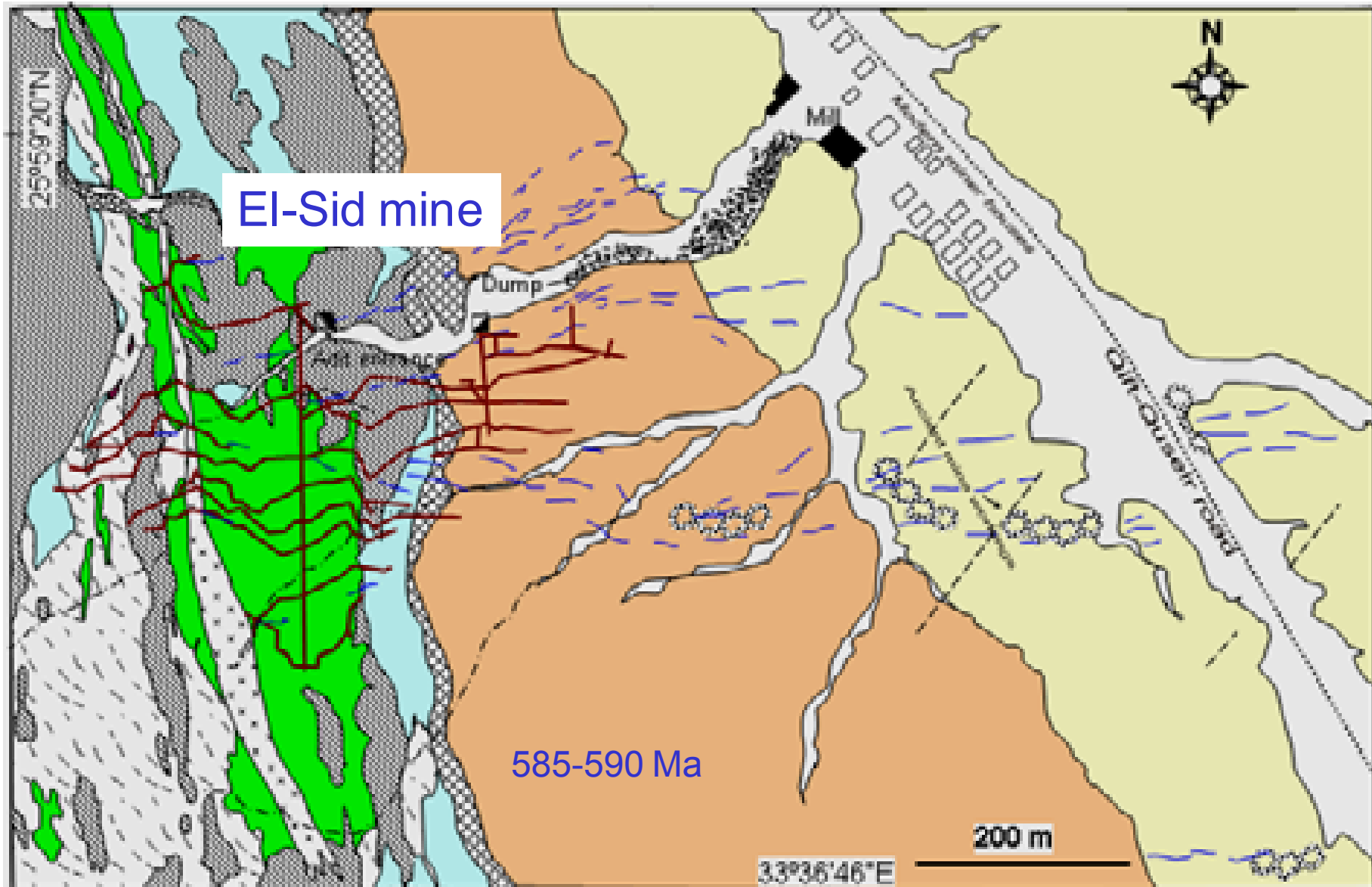
The mountains in which gold is worked, they are colored in

Mountains of gold





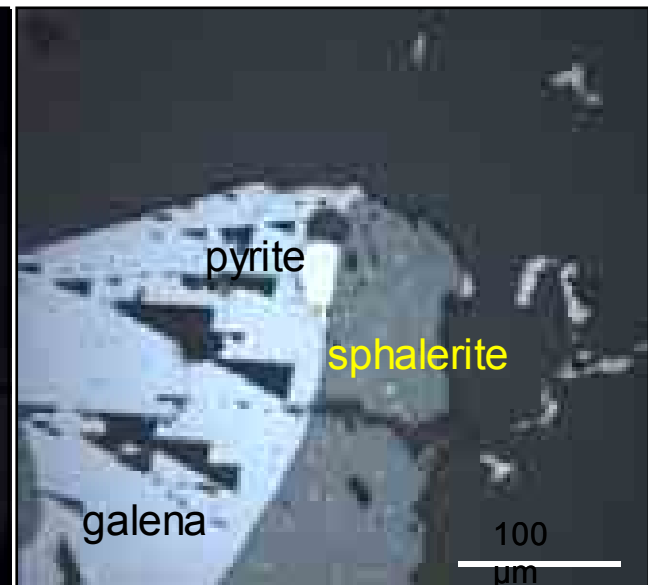
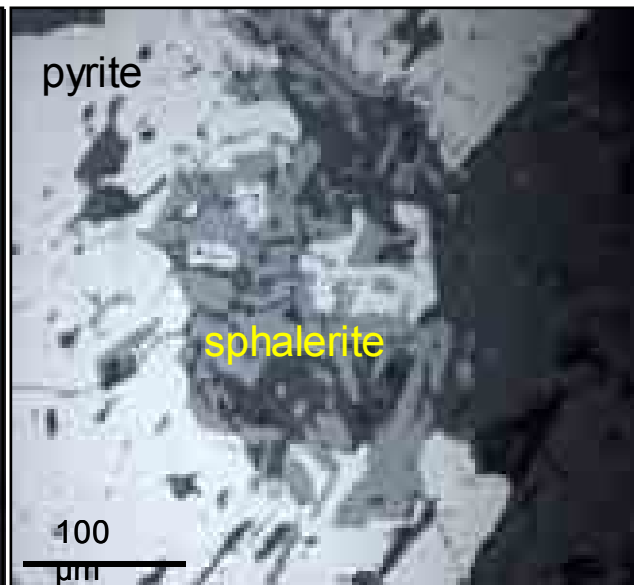
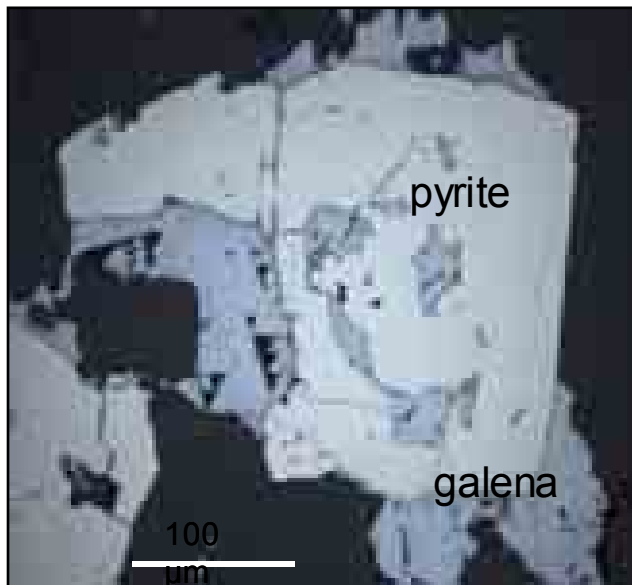
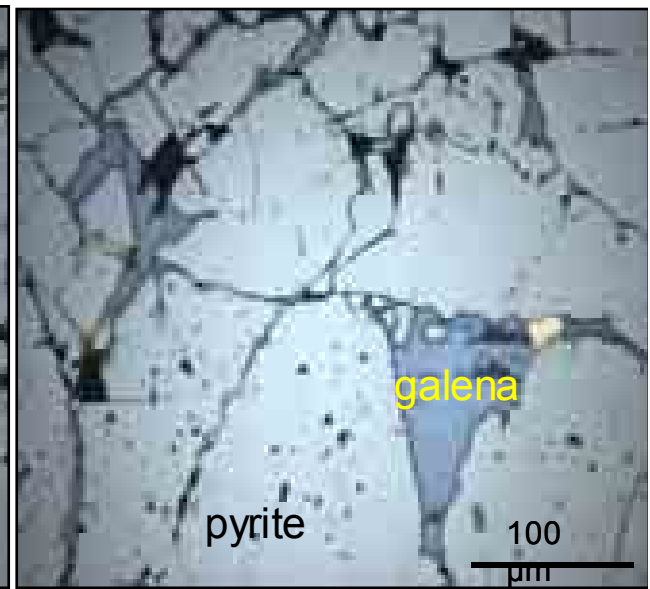
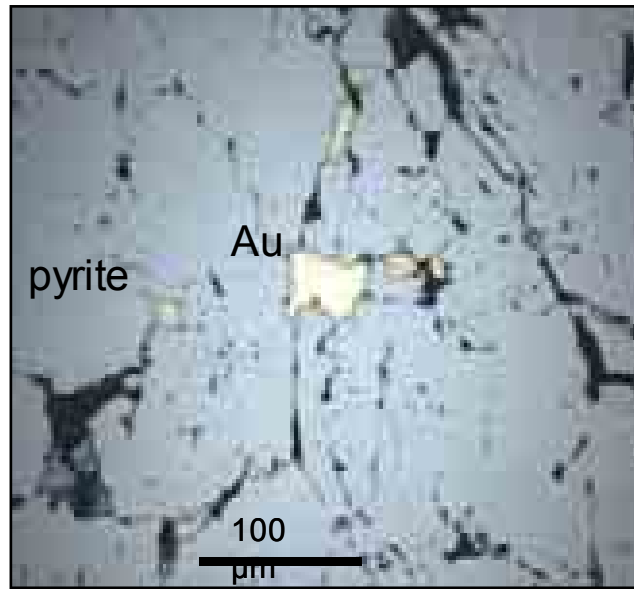
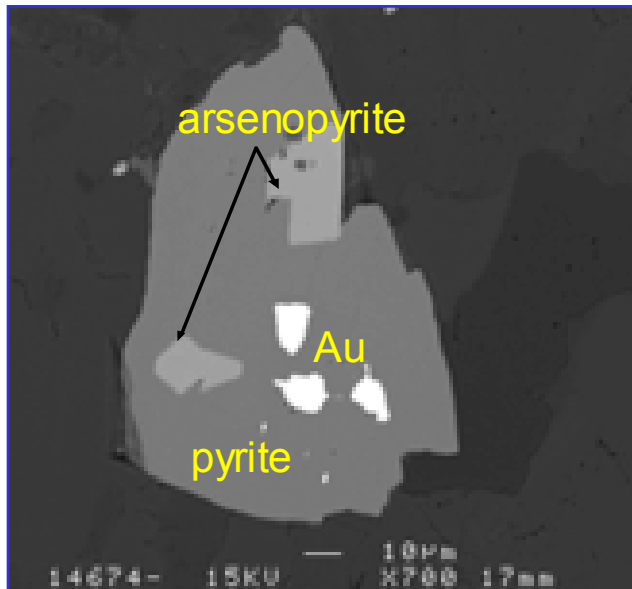
Old settlements



El-Sid mine in 1950

(produced 3 t Au from 1940-1955, with an ore grade of 28 g/t Au)





Ore microscopic features of the El-Sid deposit



Small-scale placer mining, Karen State, Burma



Karen State, Burma



Woxi,
Hunan,
China





**Pongkor,
Java,
Indonesia**





Pongkor, Java, Indonesia

**5 Mt @ 12 g/t Au + 137 g/t Ag
(cut-off 4 g/t Au)**

**Annual production:
3-4 t Au, 21-28 t Ag**

**Epithermal quartz vein system
(quartz-carbonate-adularia),
2 Ma old**



**Pongkor,
Java,
Indonesia**























Gold rush in Mongolia in 2005



Serra Pelada garimpo, Carajas, Brazil: 60-70 t gold (1980-1984)







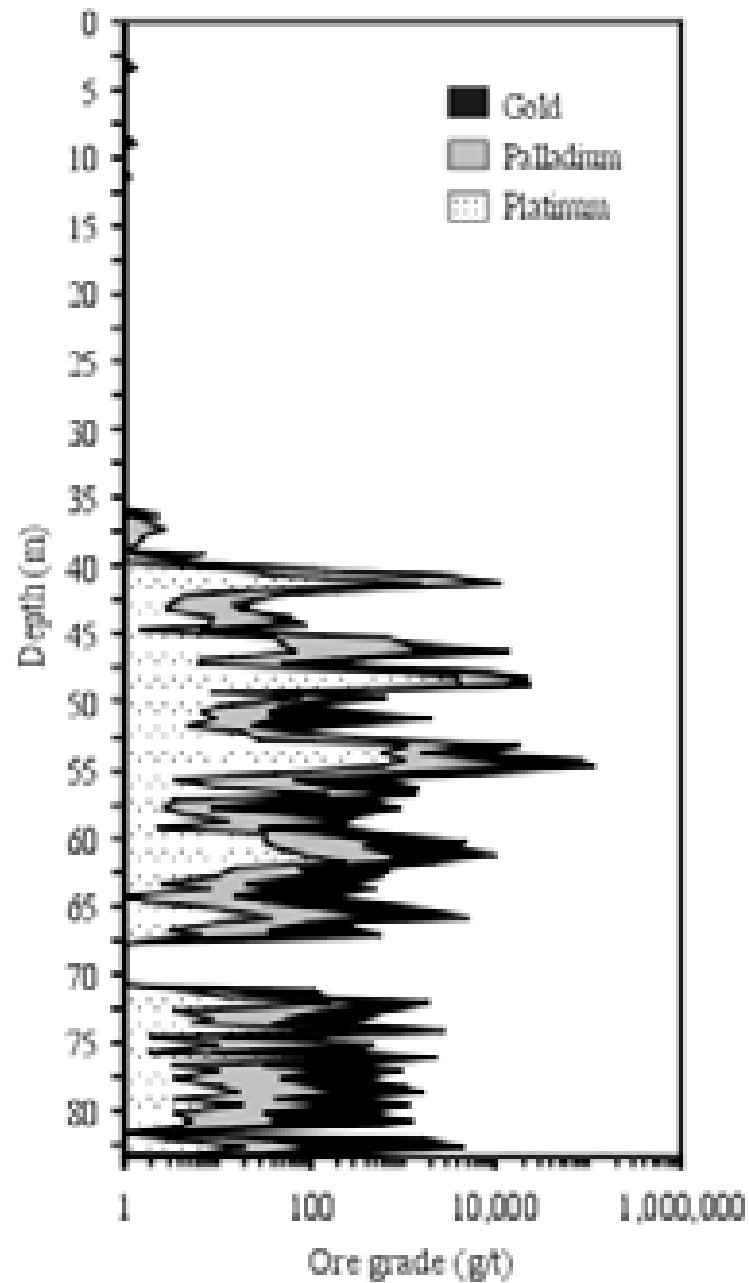


**Serra Pelada
(1983)
Carajás, Brazil**



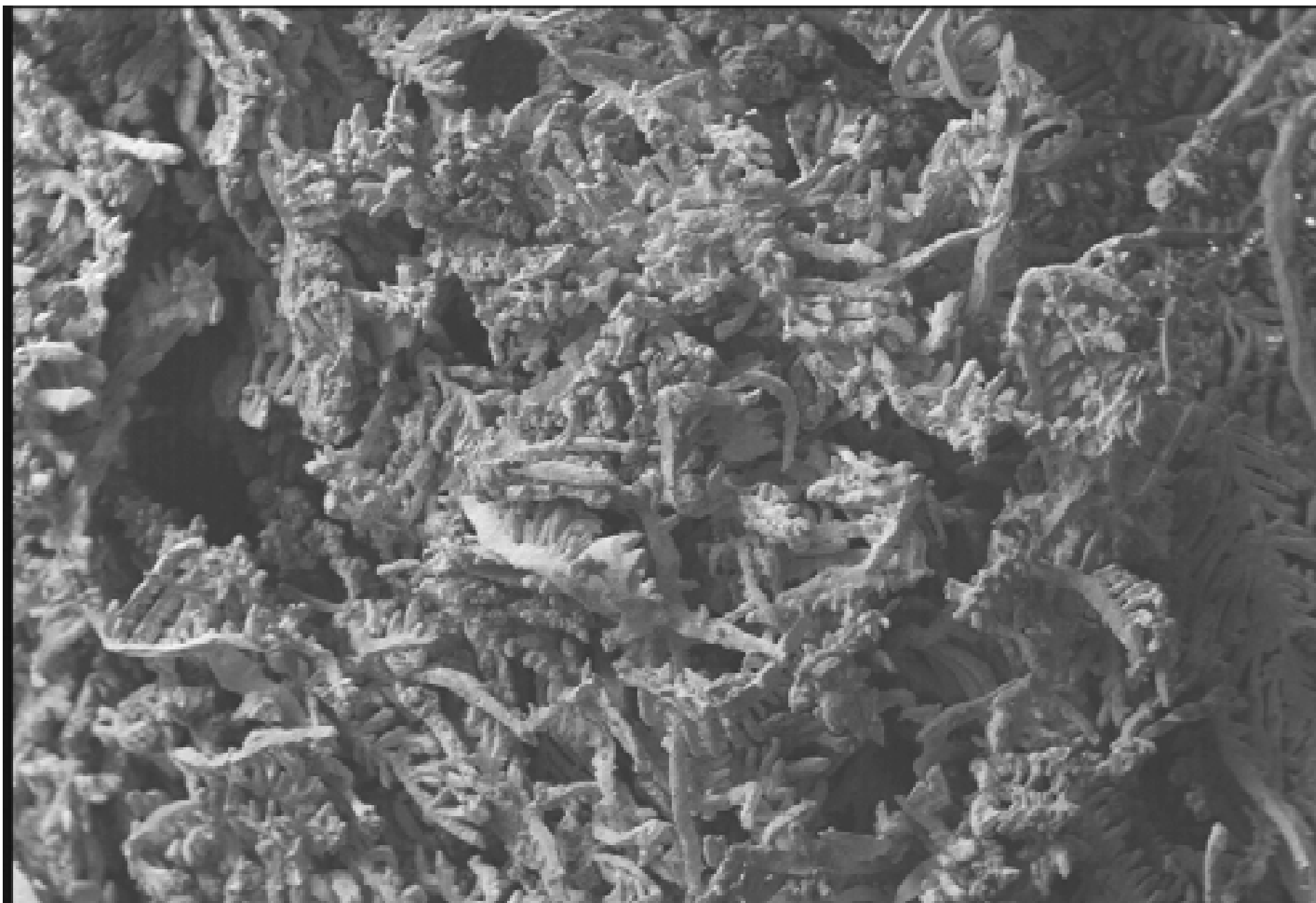






**Serra Pelada
bonanza gold,
drillcore SP-32,
sampled over 50 cm
intervals**

**Cabral et al.,
Econ Geol 97:
1132 (2002)**

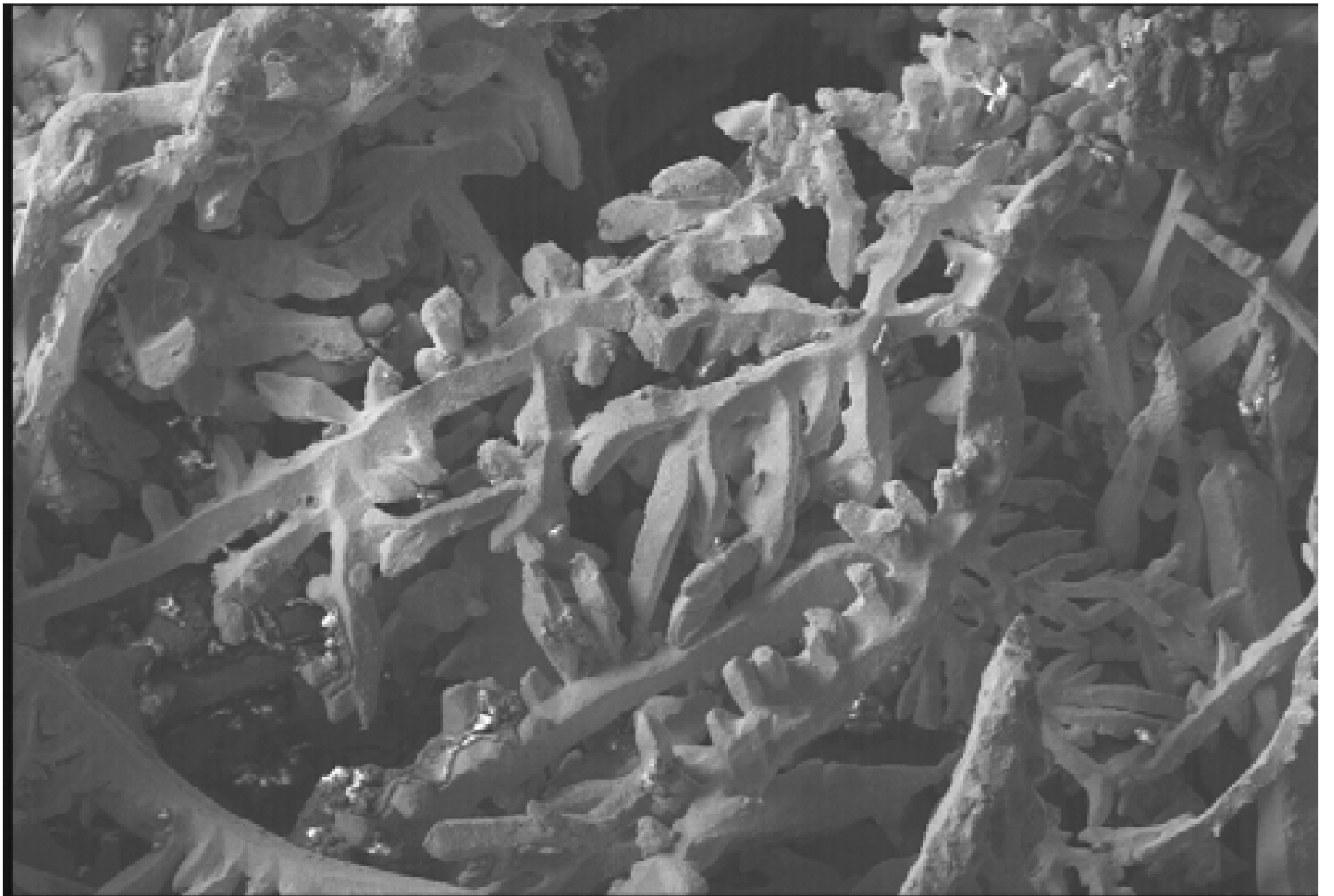


Au SP 02

00000

1000µm



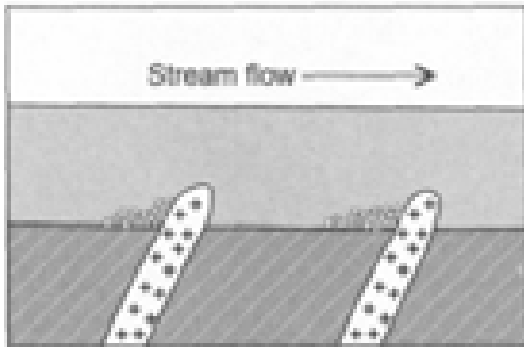


Au SP 02

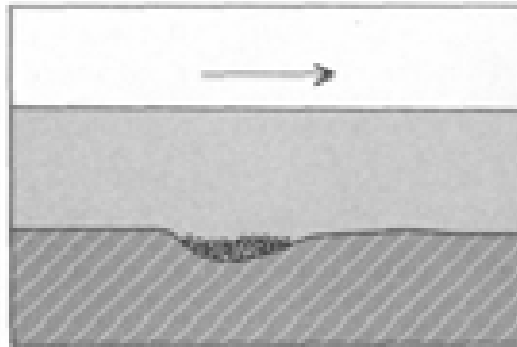
00000

300µm

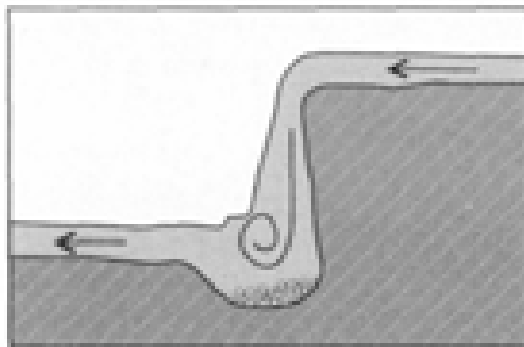




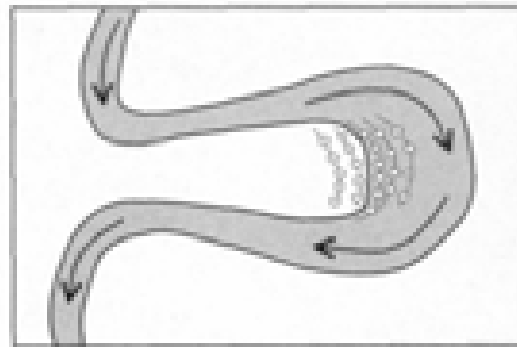
Behind covered bars



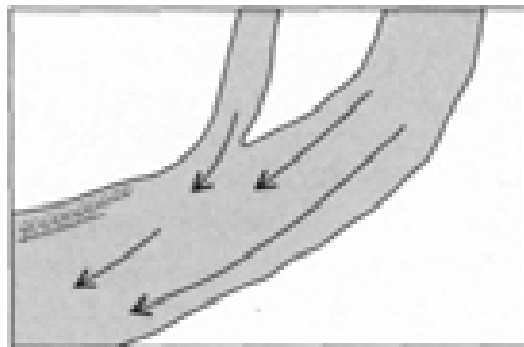
In bedrock depressions



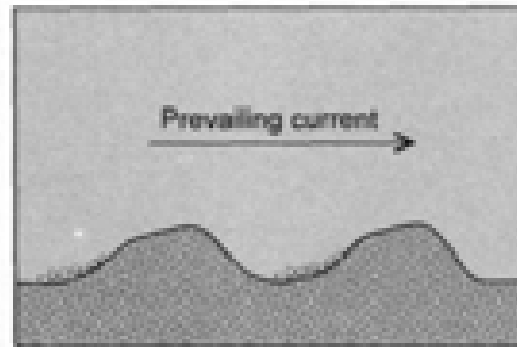
In potholes below waterfalls



On the inside of meander loops



Downstream from the mouth of a tributary



In the ocean behind bars against the prevailing current

Heavy minerals:

Insoluble:

Gold (17-19 g/cm³)

Pt-Fe alloy (18-21 g/cm³)

Diamond (3.5 g/cm³)

Cassiterite (7.0 g/cm³)

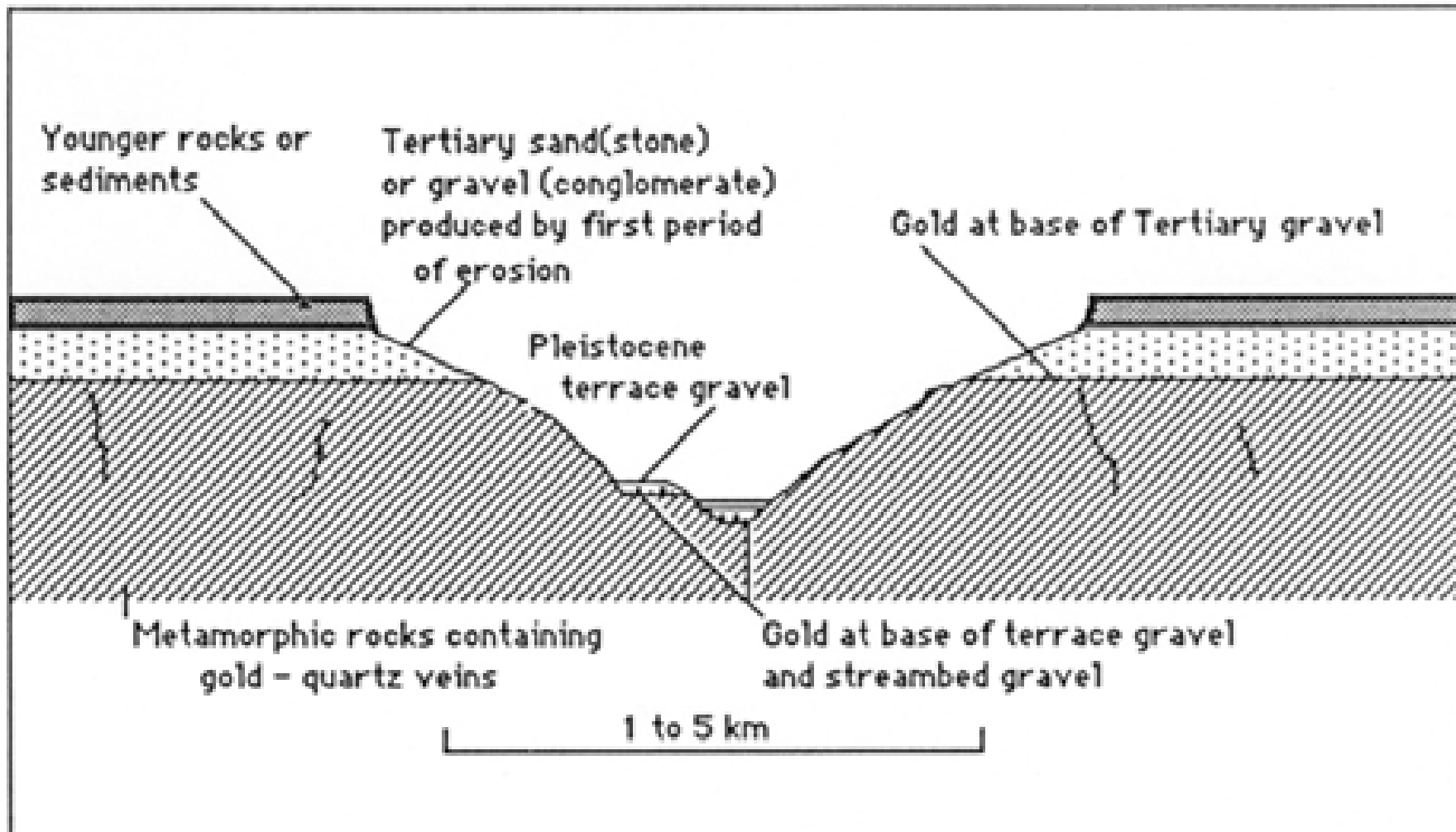
Zircon (4.7 g/cm³)

Soluble:

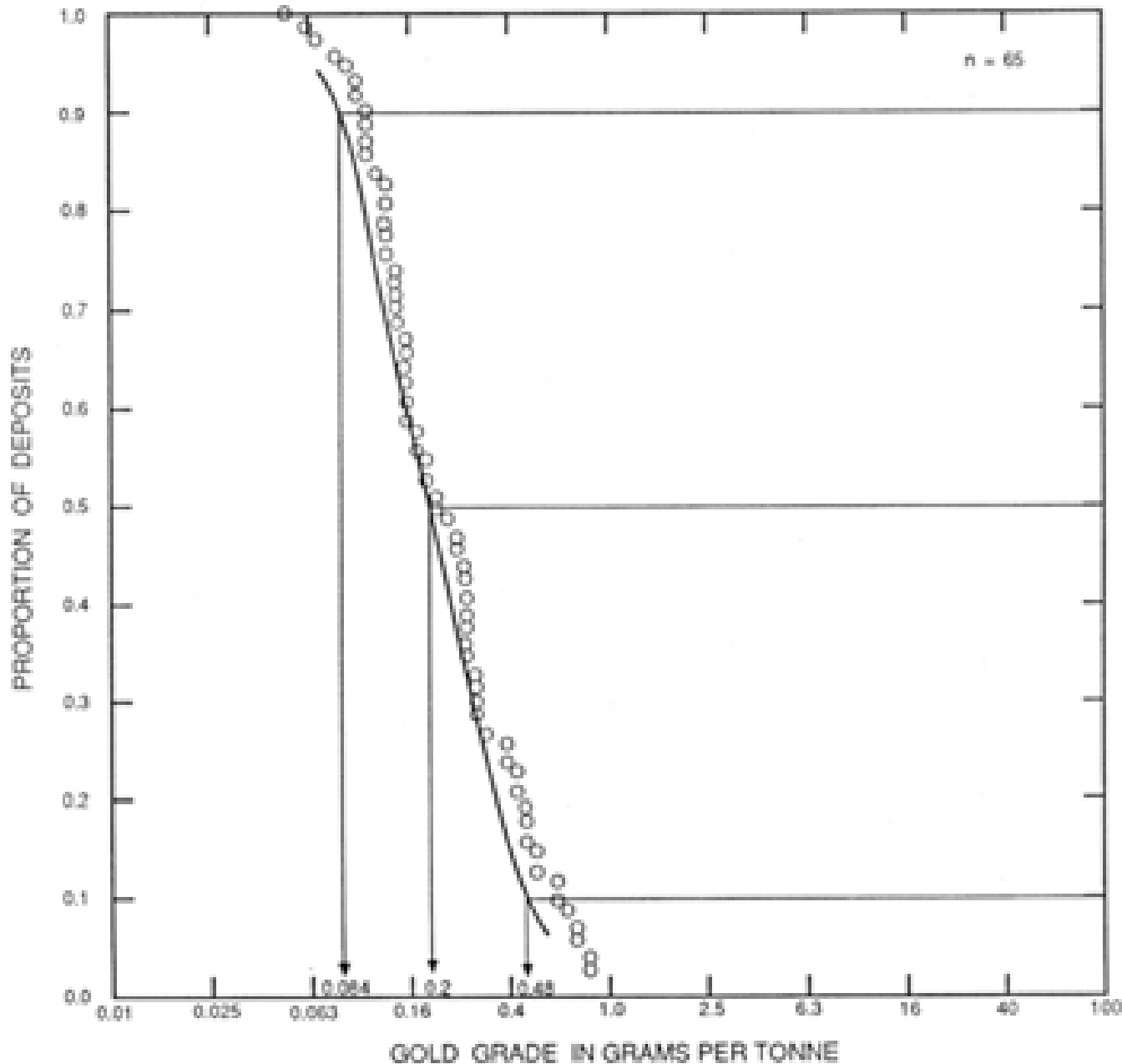
Pyrite (5.0 g/cm³)

Uraninite (11 g/cm³)

Placer deposits



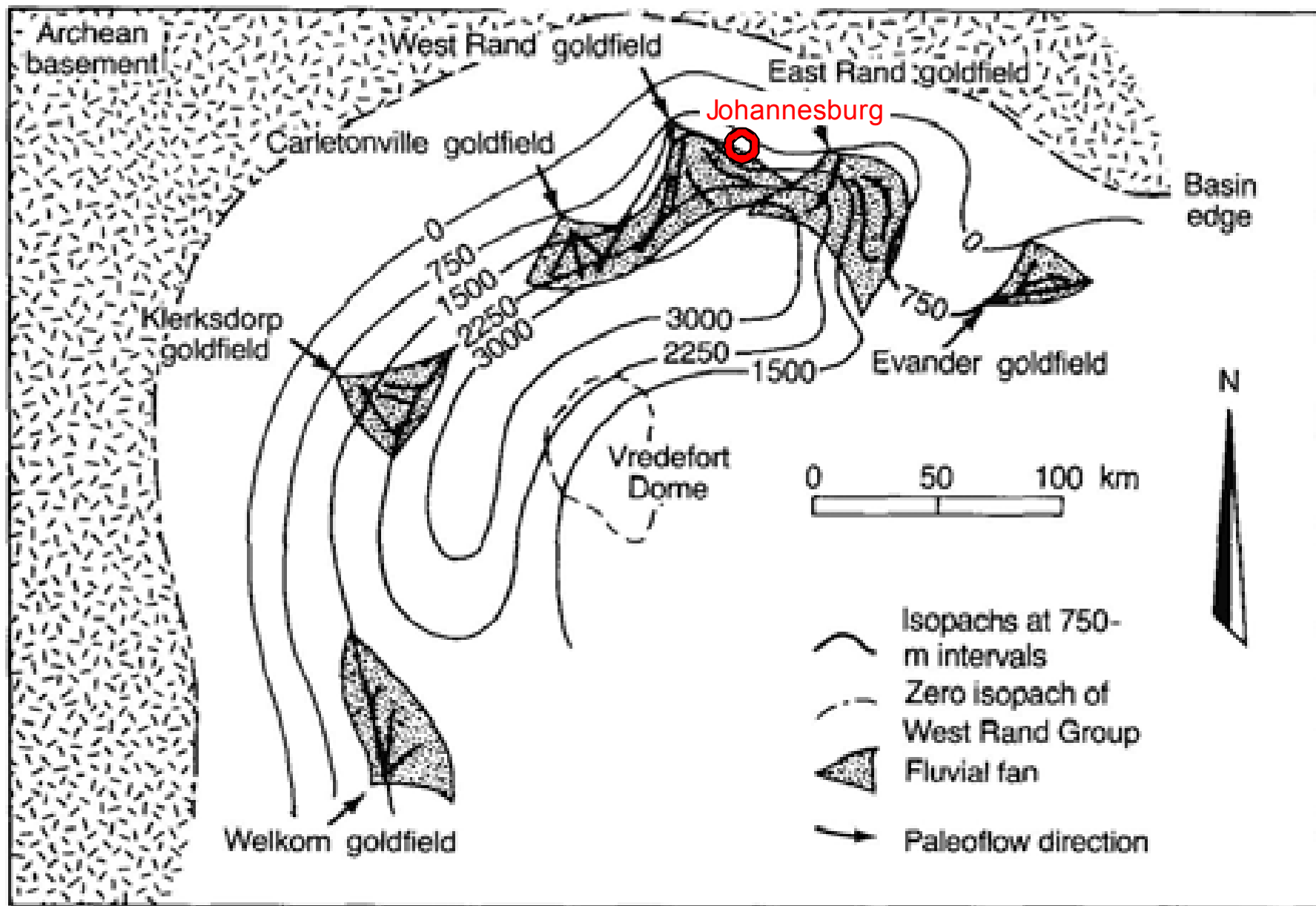
PLACER GOLD-PGE

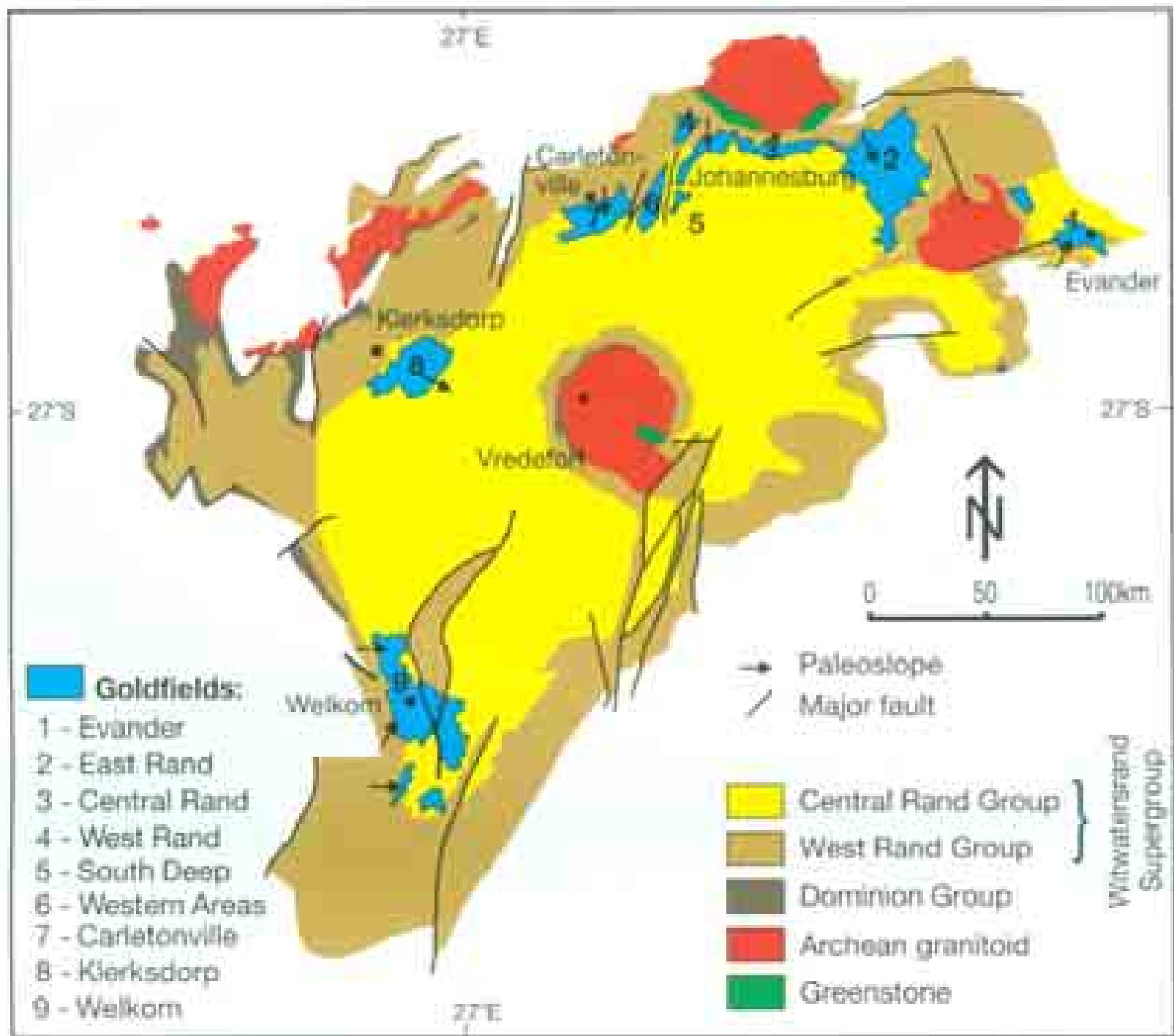


Distribution of ore grade:

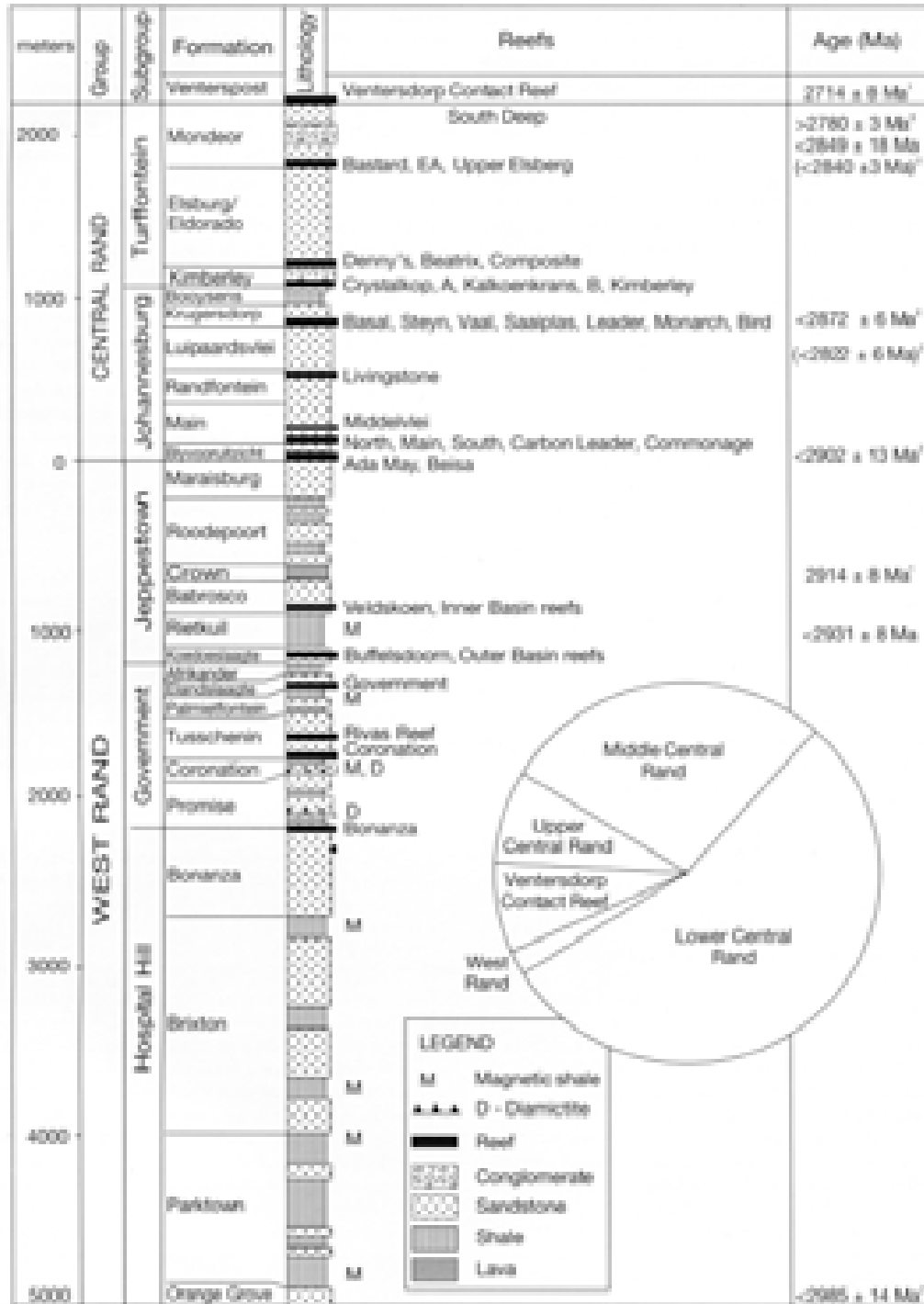
80 % of all deposits are in the range of 0.1-0.4 g/t Au

But Witwatersrand: 8 g/t Au!

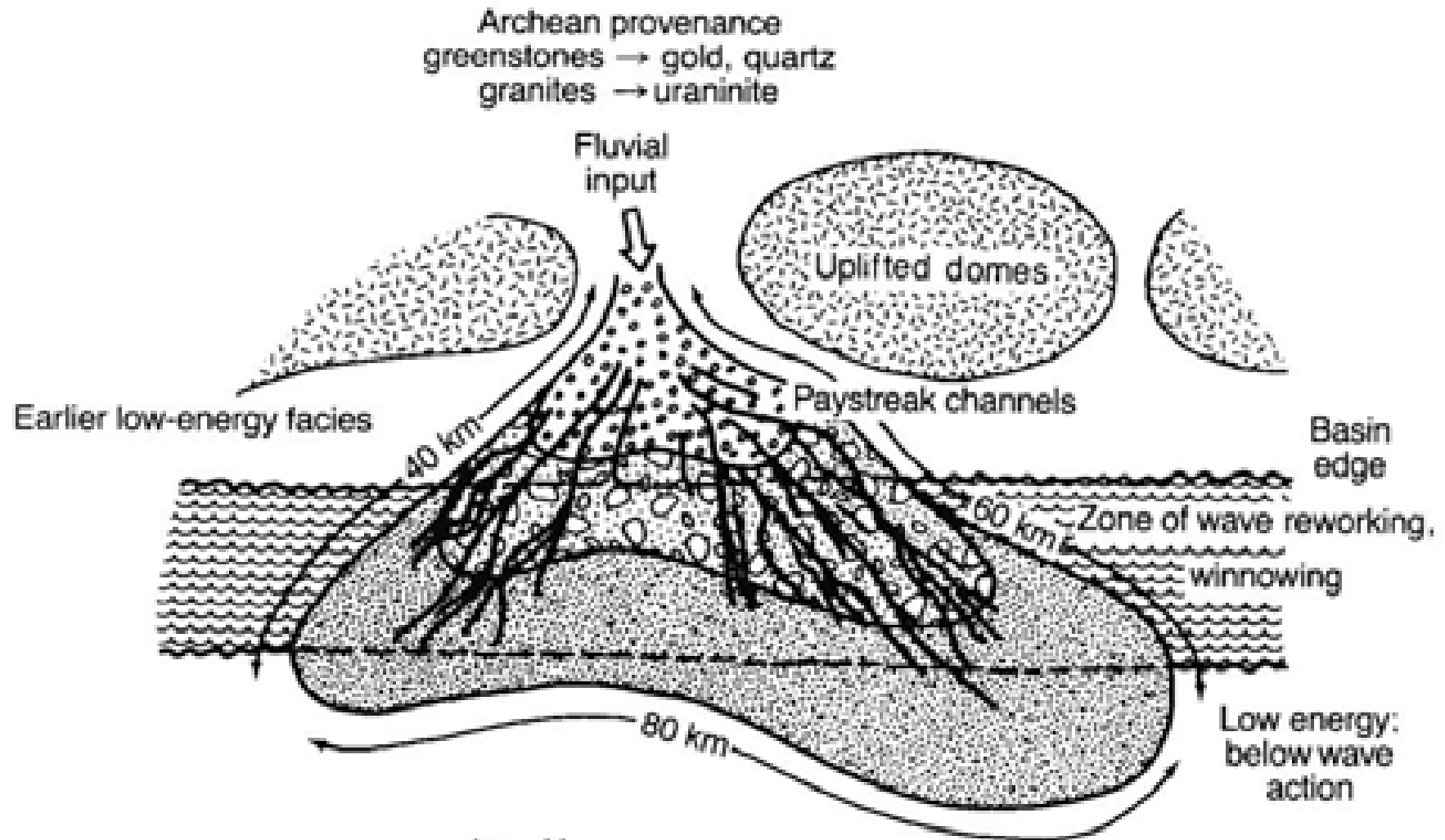




Witwatersrand Supergroup







	Au	U	
Fan head facies			Coarse channel conglomerates
Midfan facies			Finer channel conglomerates, trough cross-bedded channel sands
Fan base facies			Sand sheets, algal mats

Witwatersrand Basin:

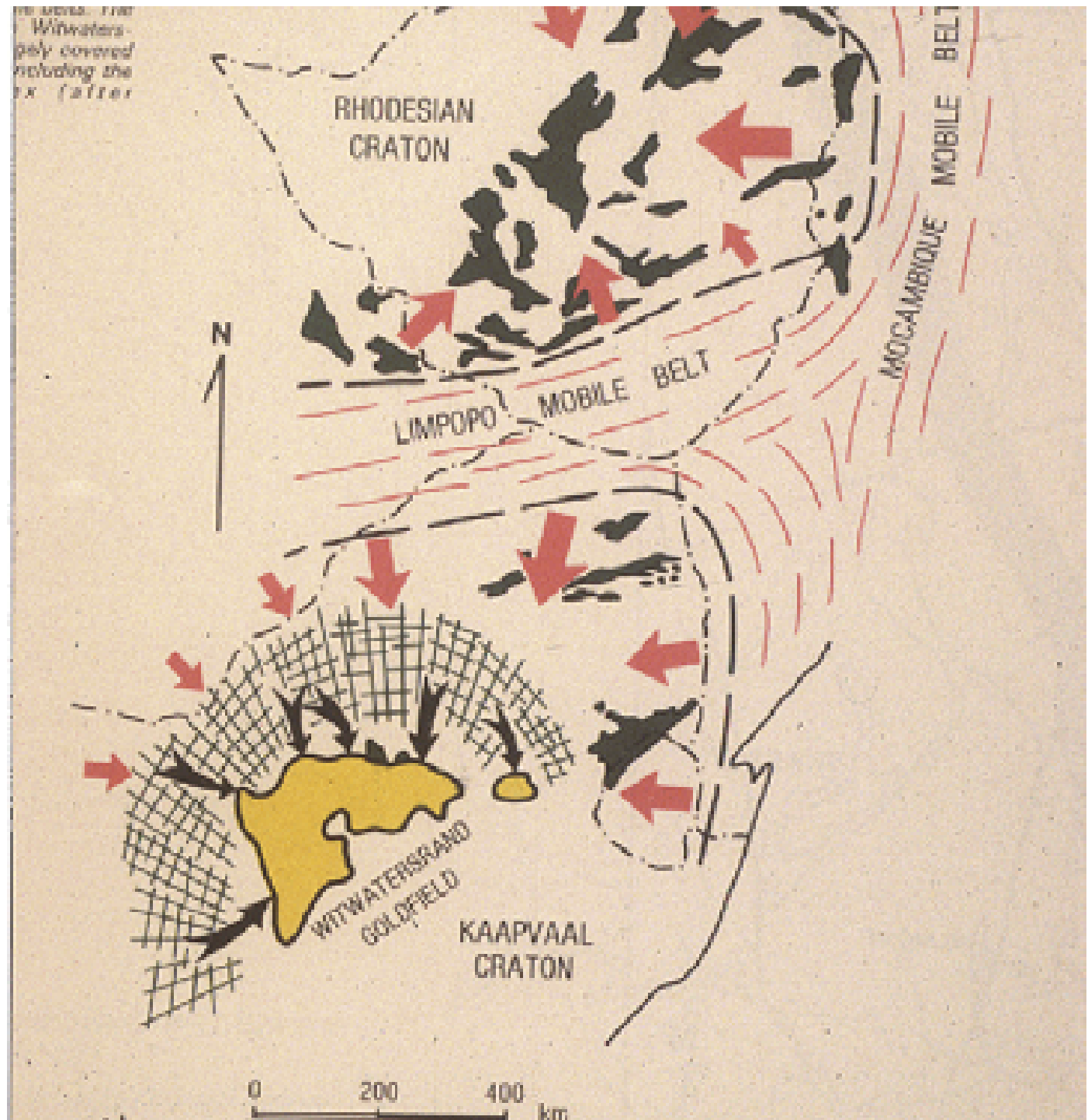
40 % of all gold mined,
and 35 % of global gold
resources

Gold-uranium bearing
meta-conglomerate
(2.89-2.76 Ga)
~8 g/t Au, 200 g/t U

Re-Os age of gold:
3.03 Ga

Kirk et al., Science 297:
1856 (2002)

Historical production
1887-today:
~55,000 t Au
[value 1600 billion USD
in 2008]
60,000 fatal accidents







Amazon mine



Mponeng mine: Ventersdorp Contact Reef (-3200 m), cut-off at 1000 g/t x cm
Overlying meta-basalt: 2714 ±8 Ma (SHRIMP U-Pb on zircon)

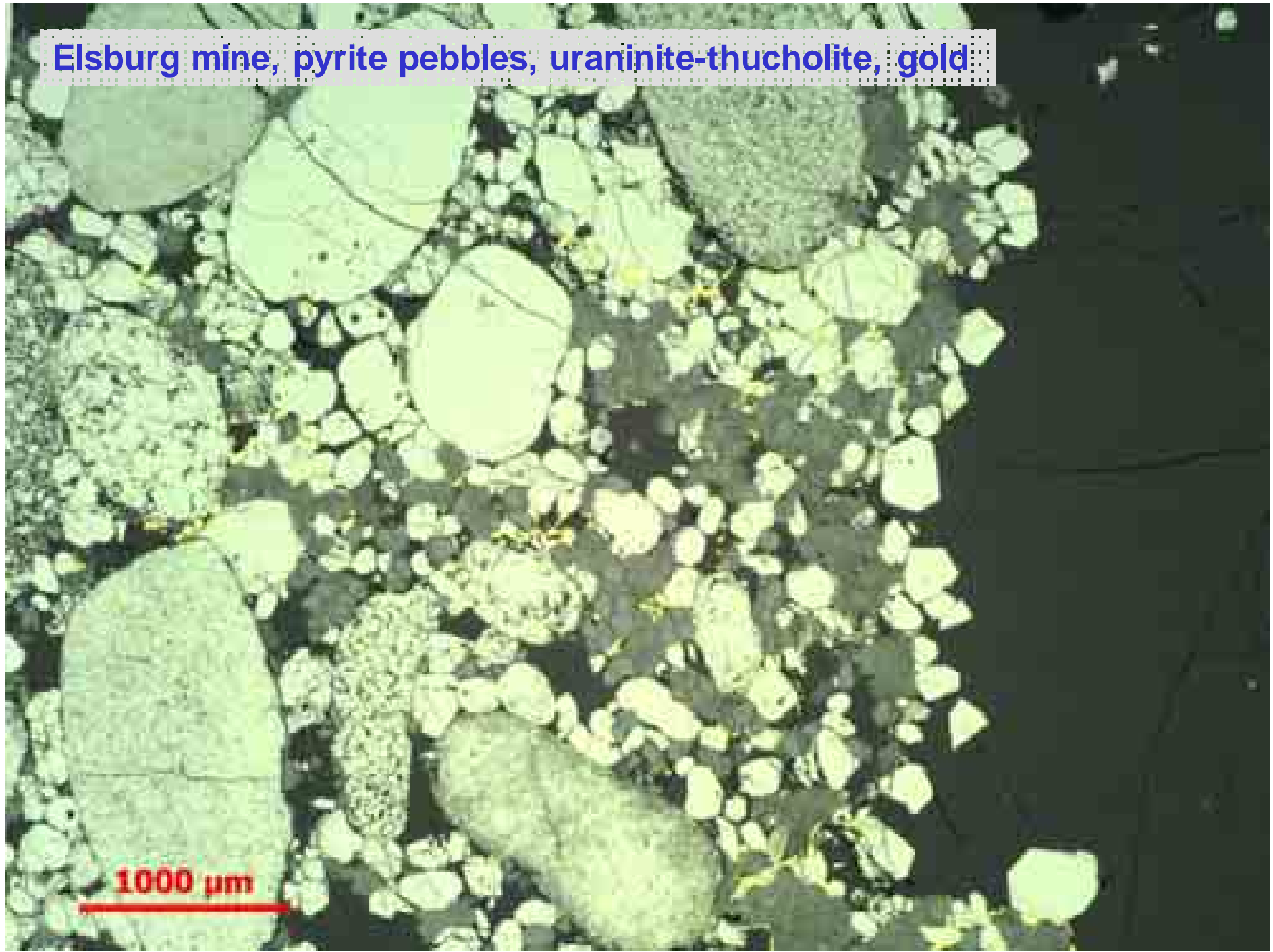






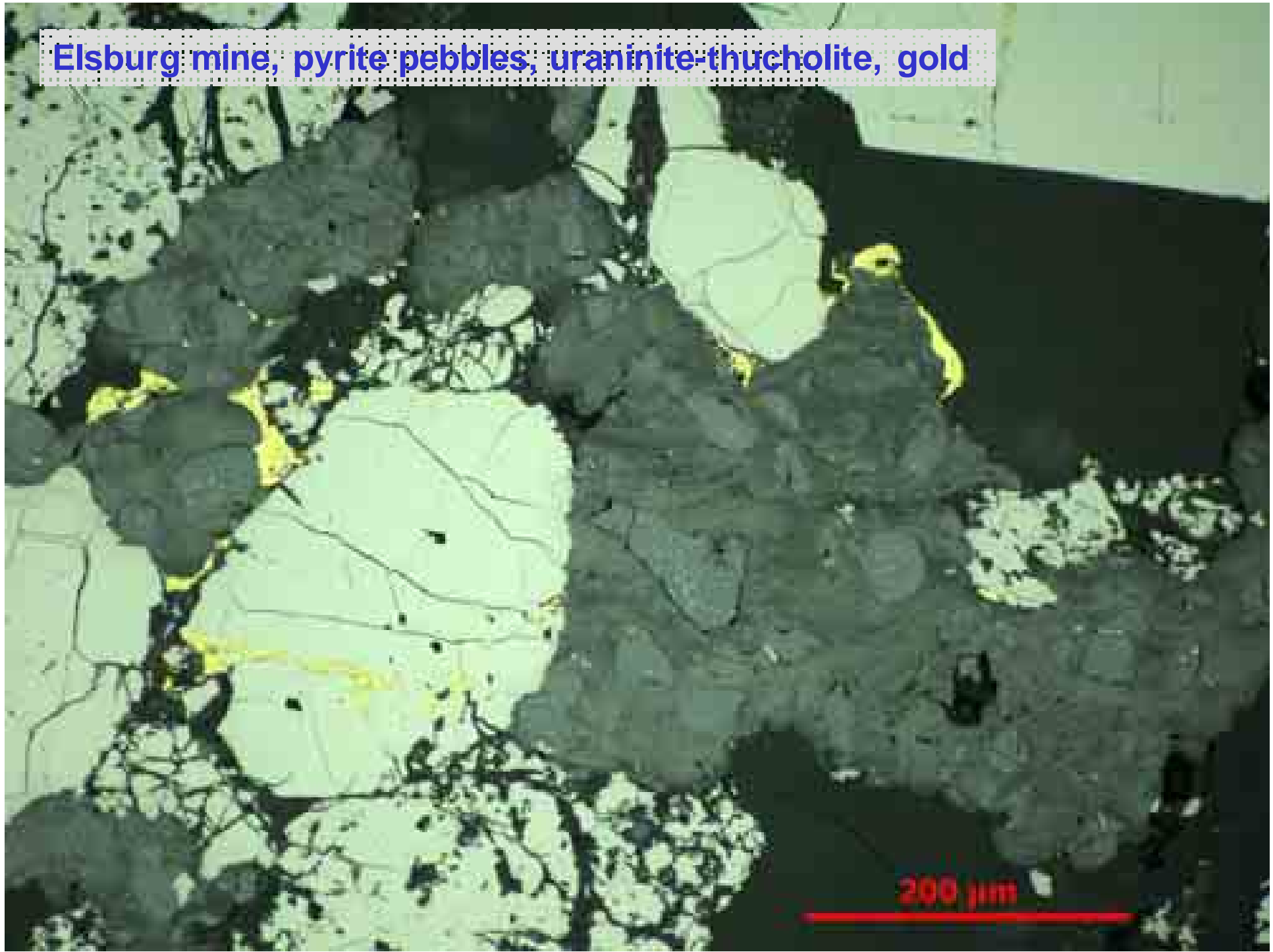


Elsburg mine, pyrite pebbles, uraninite-thucholite, gold

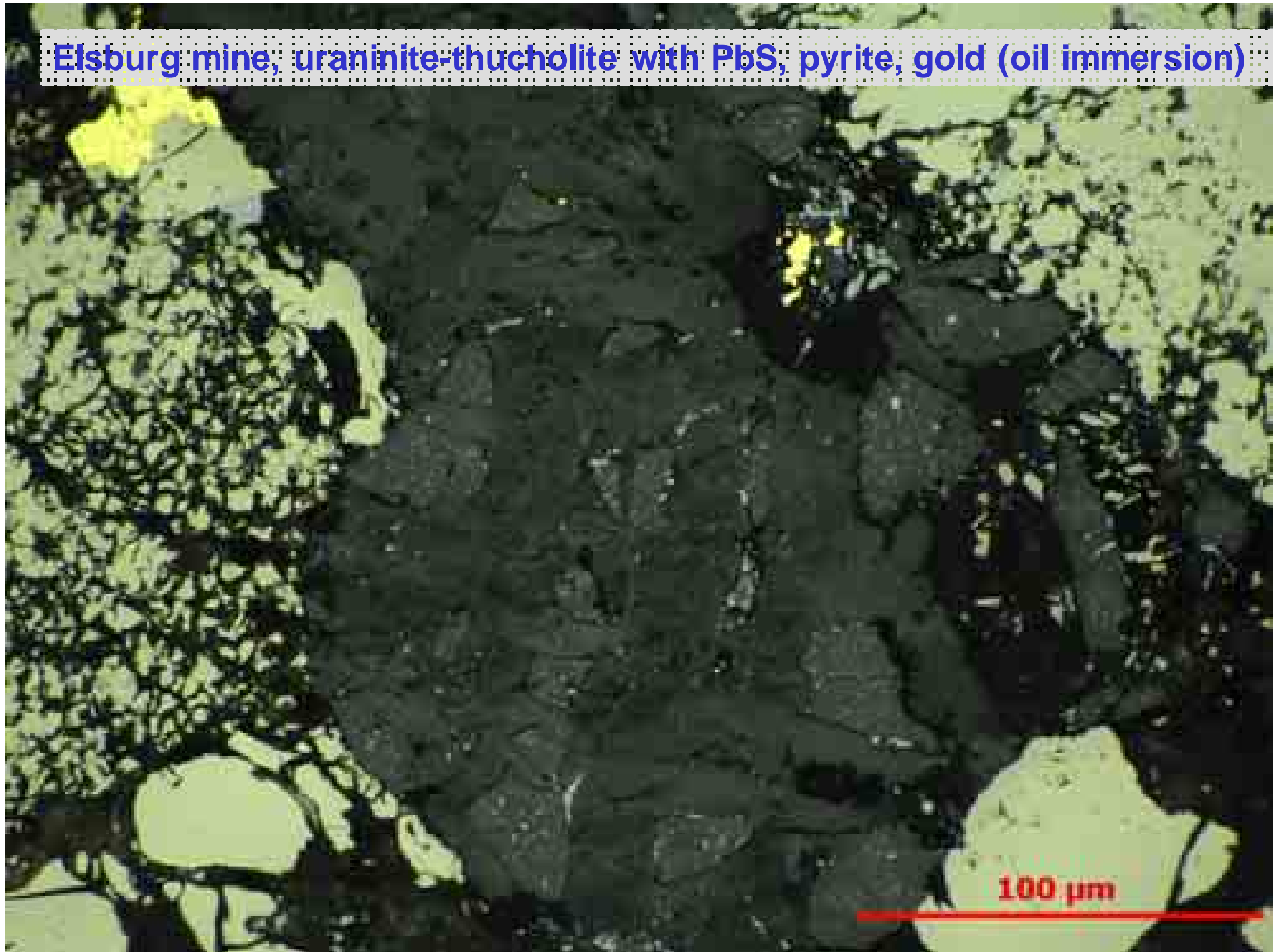


1000 μm

Elsburg mine, pyrite pebbles, uraninite-thucholite, gold



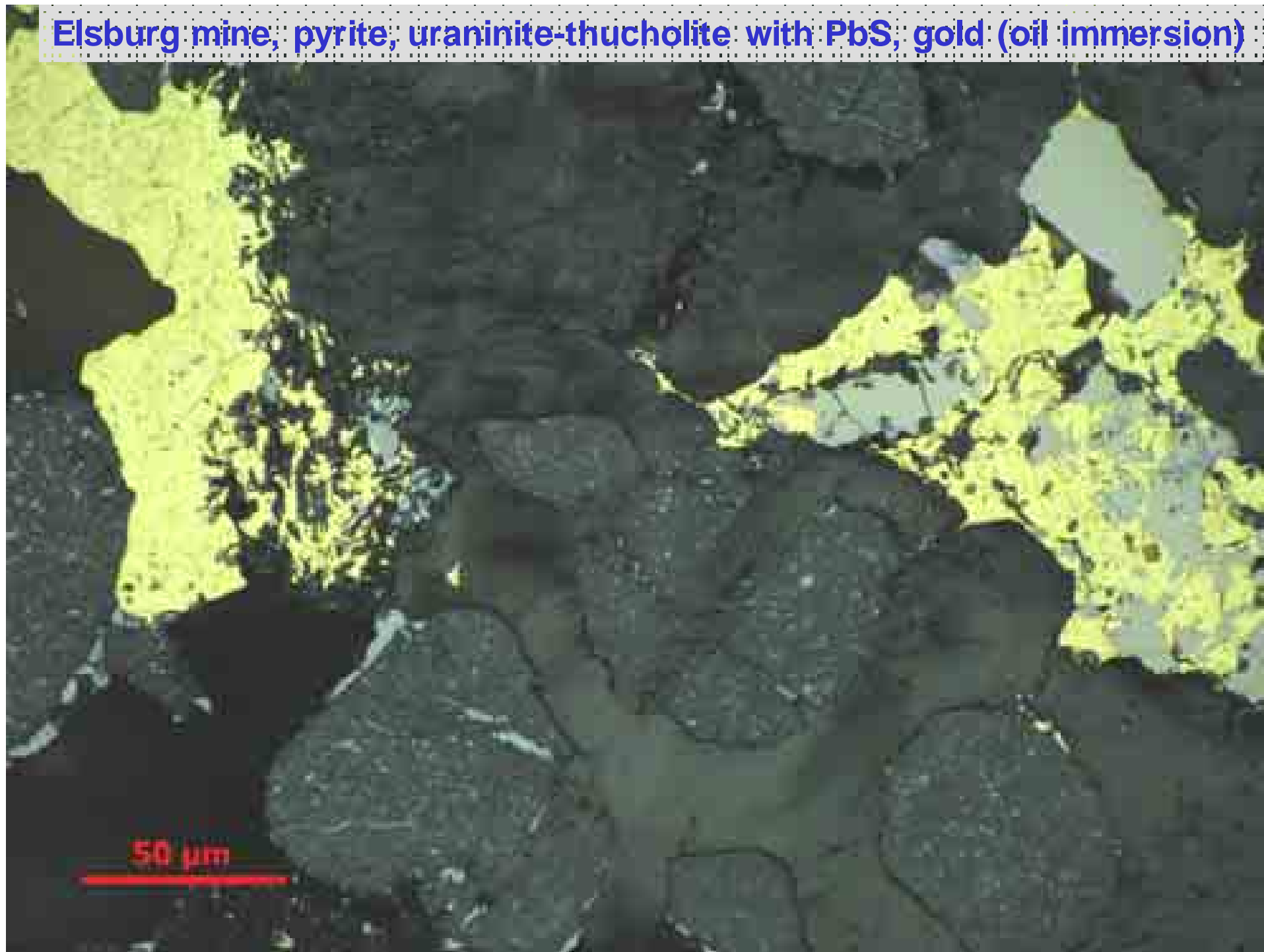
Elsburg mine, uraninite-thucholite with PbS, pyrite, gold (oil immersion)



Elsburg mine, pyrite, uraninite-thucholite with PbS, gold (oil immersion)



Elsburg mine, pyrite, uraninite-thucholite with PbS, gold (oil immersion)



The Great Oxidation Event (GOE): 2.4-2.0 Ga

Oxygen from photosynthesis is essentially fixed in Fe-oxides and gypsum. Free oxygen in the atmosphere ($>10^{-5}$ PAL) only after the GOE.

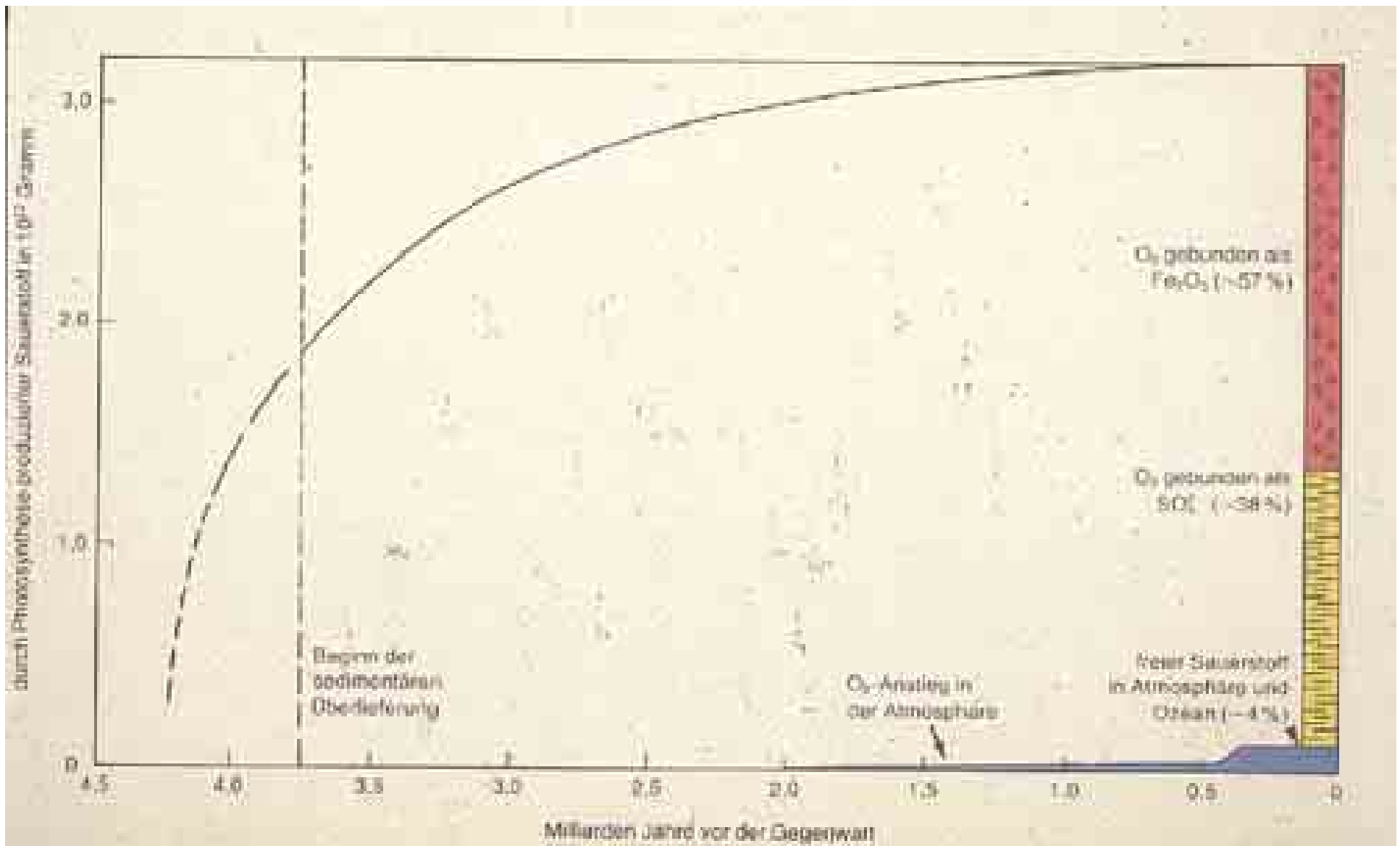
(1) Oxygen from oxygenic photosynthesis is fixed in BIF



(2) Anoxygenic photosynthesis by reduction of CO₂



The two mechanisms for formation of iron ore deposits of the „Banded Iron Formation“ (BIF) family



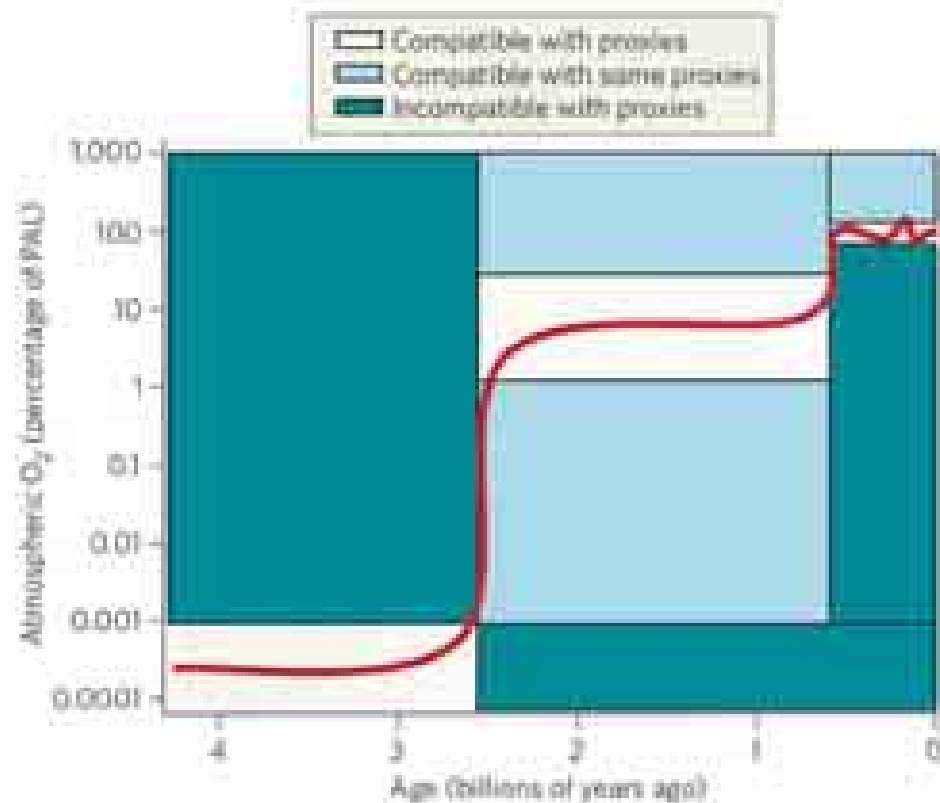
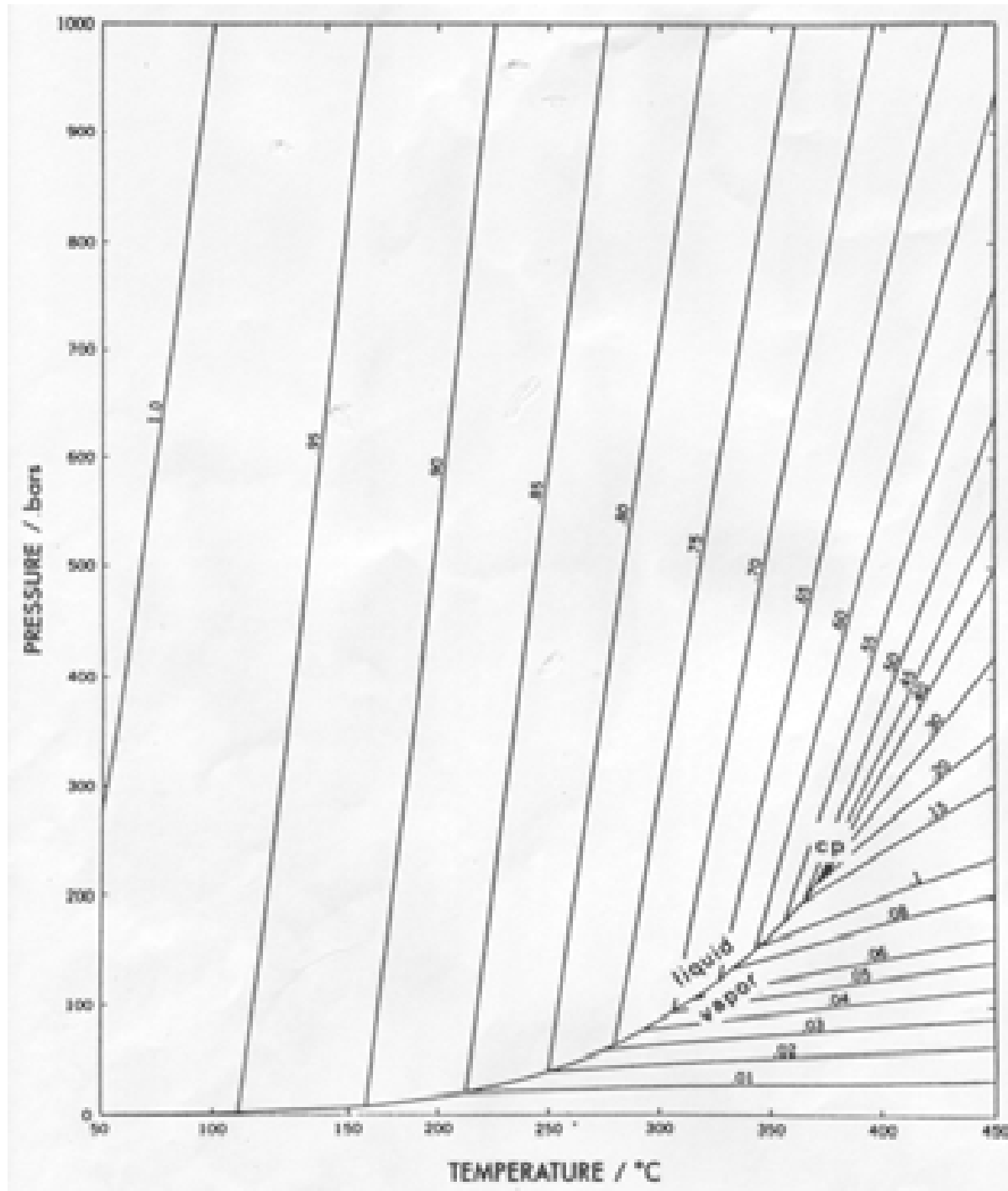


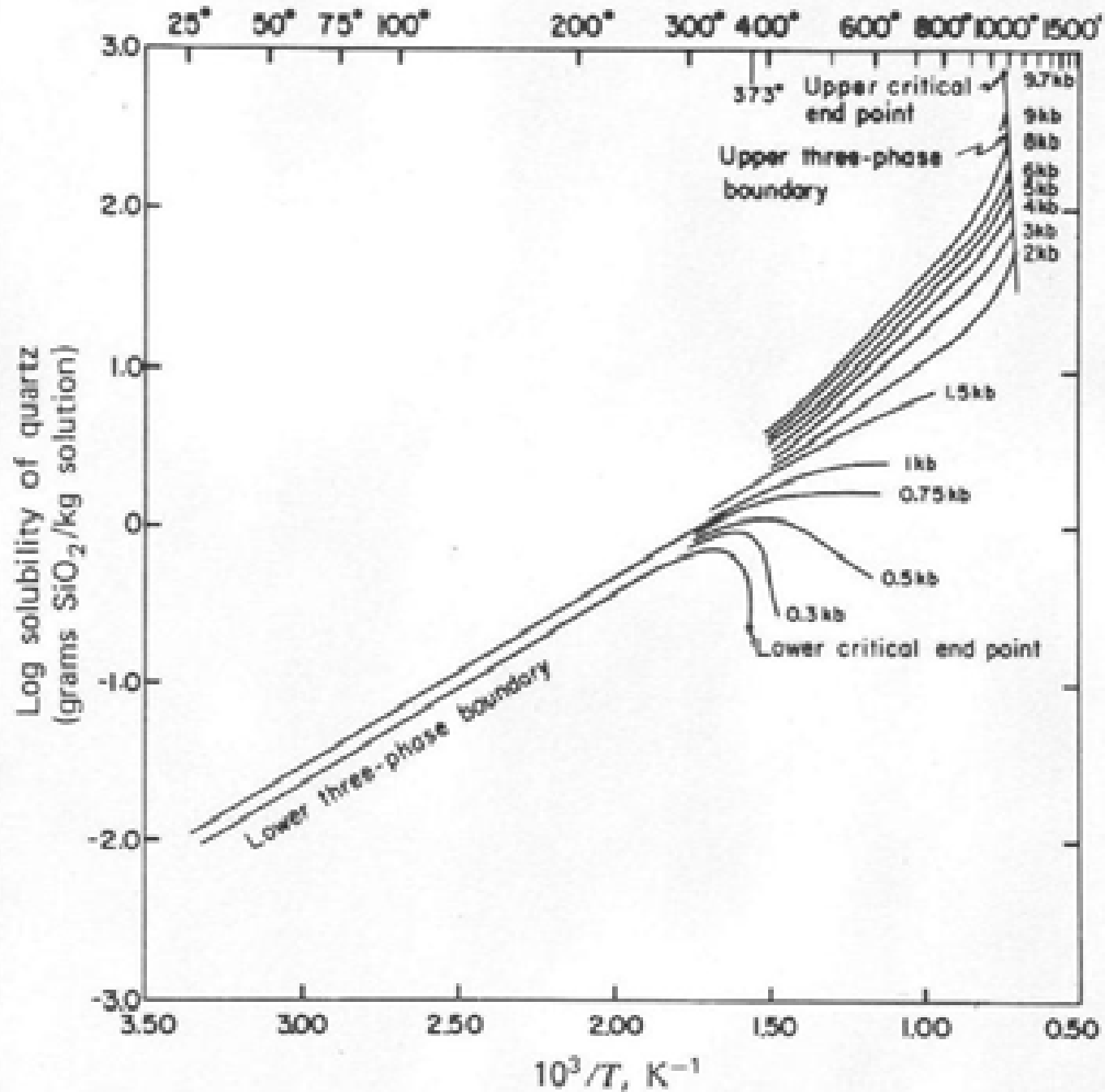
Figure 2 | Prevailing view of atmospheric oxygen evolution over time. The red line shows the inferred level of atmospheric oxygen bounded by the constraints imposed by the proxy record of atmospheric oxygen variation over Earth's history²⁰. The signature of mass-independent sulphur-isotope behaviour sets an upper limit for oxygen levels before 2.45 billion years ago and a lower limit after that time. The record of oxidative weathering after 2.45 billion years ago sets a lower limit for oxygen levels at 1% of PAL, whereas an upper limit of 40% of PAL is inferred from the evidence for anoxic oceans during the Proterozoic. The tighter bounds on atmospheric oxygen from 420 million years ago to the present is set by the fairly continuous record of charcoal accumulation²¹: flames cannot be sustained below an oxygen level of 60% of PAL, and above about 160% of PAL the persistence of forest ecosystems would be unlikely because of the frequency and vigour of wildfires²¹.

Kump (2008)
Nature 451: 278



PT diagram of
water and
isochores
(lines of equal
density)
cp = critical point

Temperature, °C



Solubility of quartz in water

**Yellowstone
River, Wyoming,
USA**





Mammoth hot springs, Yellowstone Park, Wyoming



Mammoth hot springs, Yellowstone Park, Wyoming



Old Faithful
(1 eruption/h)

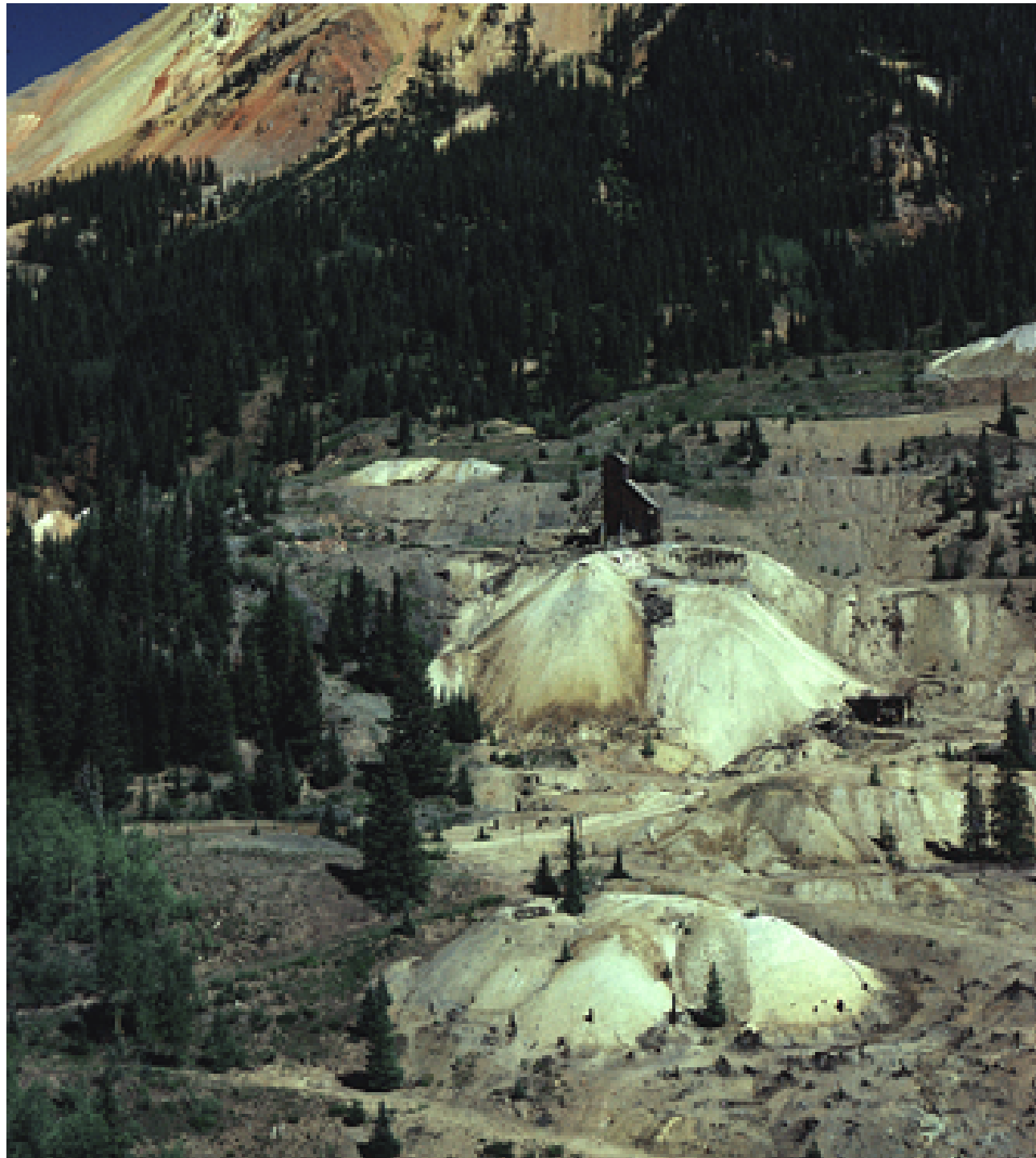




Mud pot/mud volcano (water-deficient hot spring, $\text{CO}_2 + \text{SO}_2$)

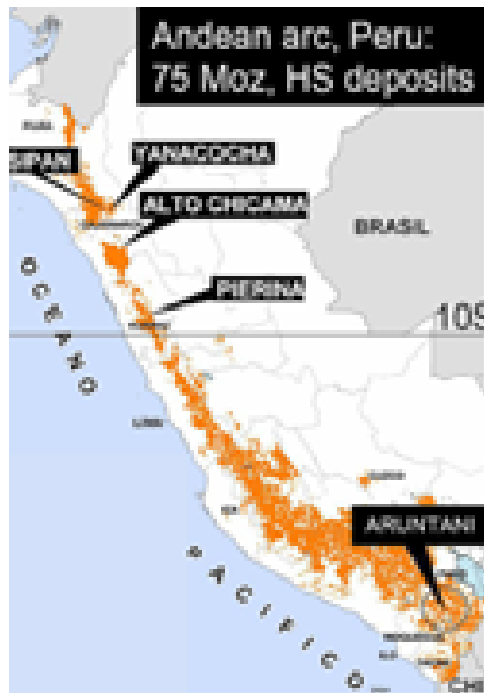


Red Mountain, Colorado





Julcani, Peru





Laurani, Bolivia: high-sulfidation gold (quartz-alunite alteration)



Cerro Rico de Potosí. Bolivia



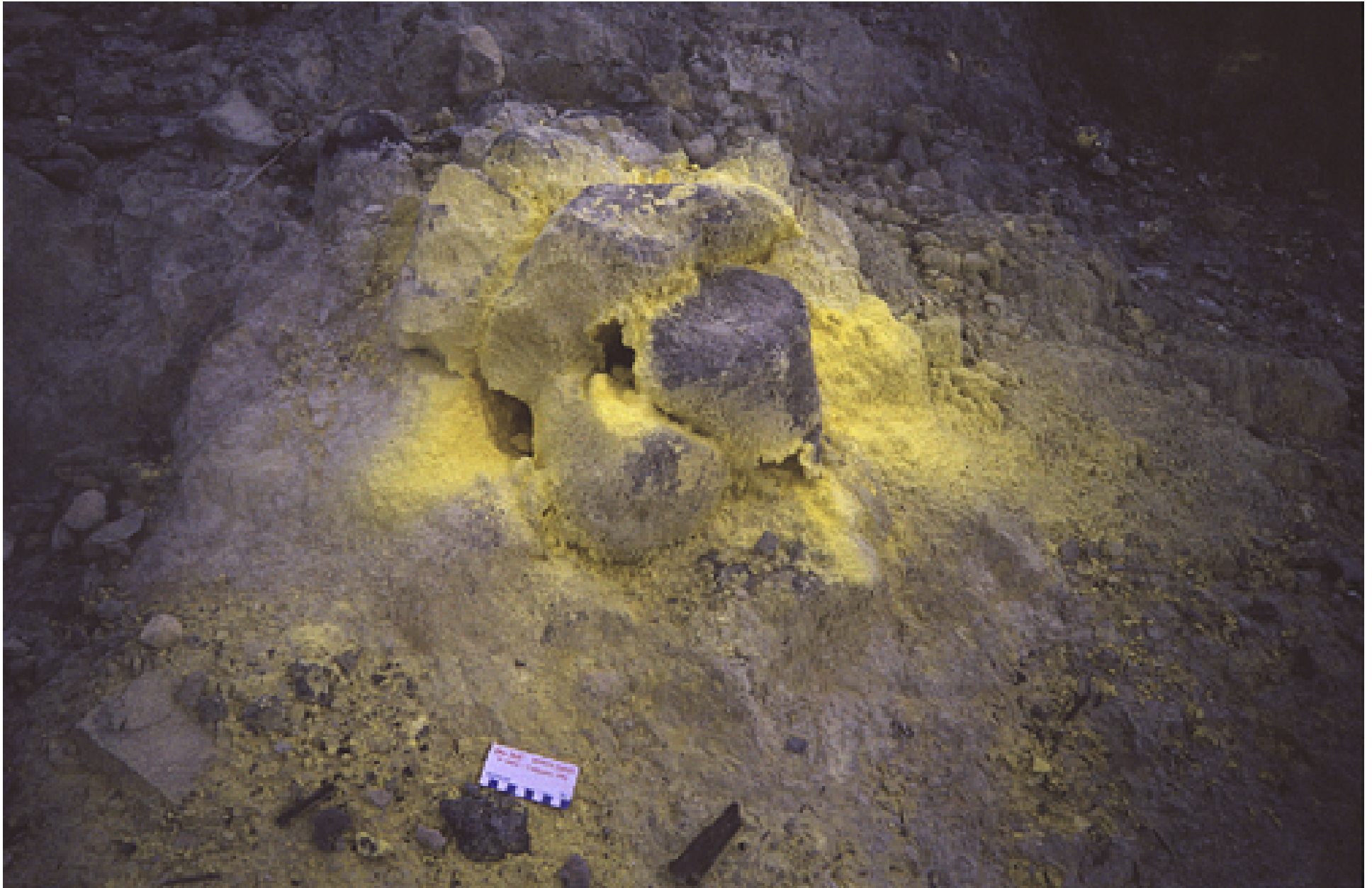
Osorezan, Japan



Osorezan, Japan



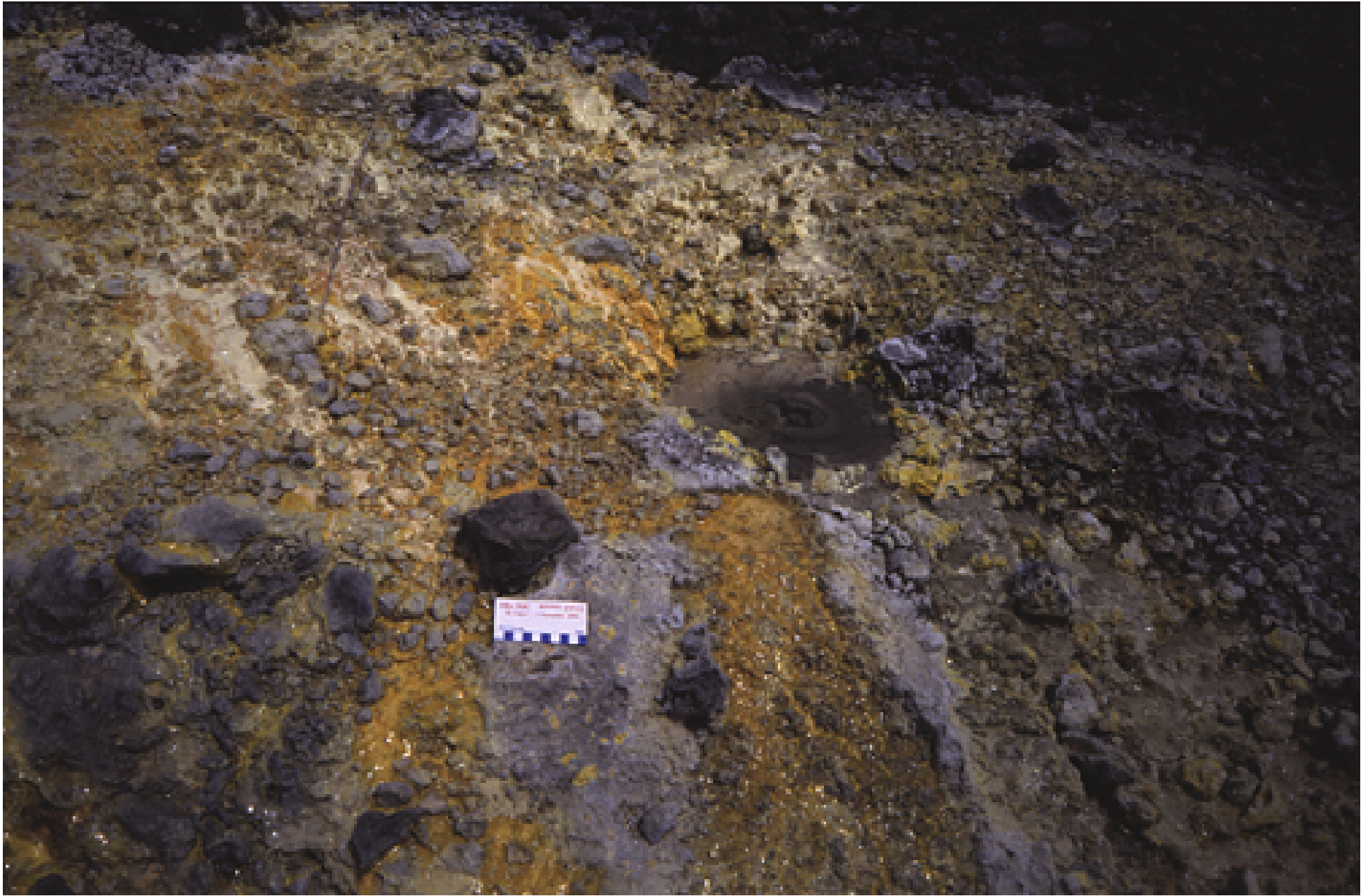
Osorezan, Japan



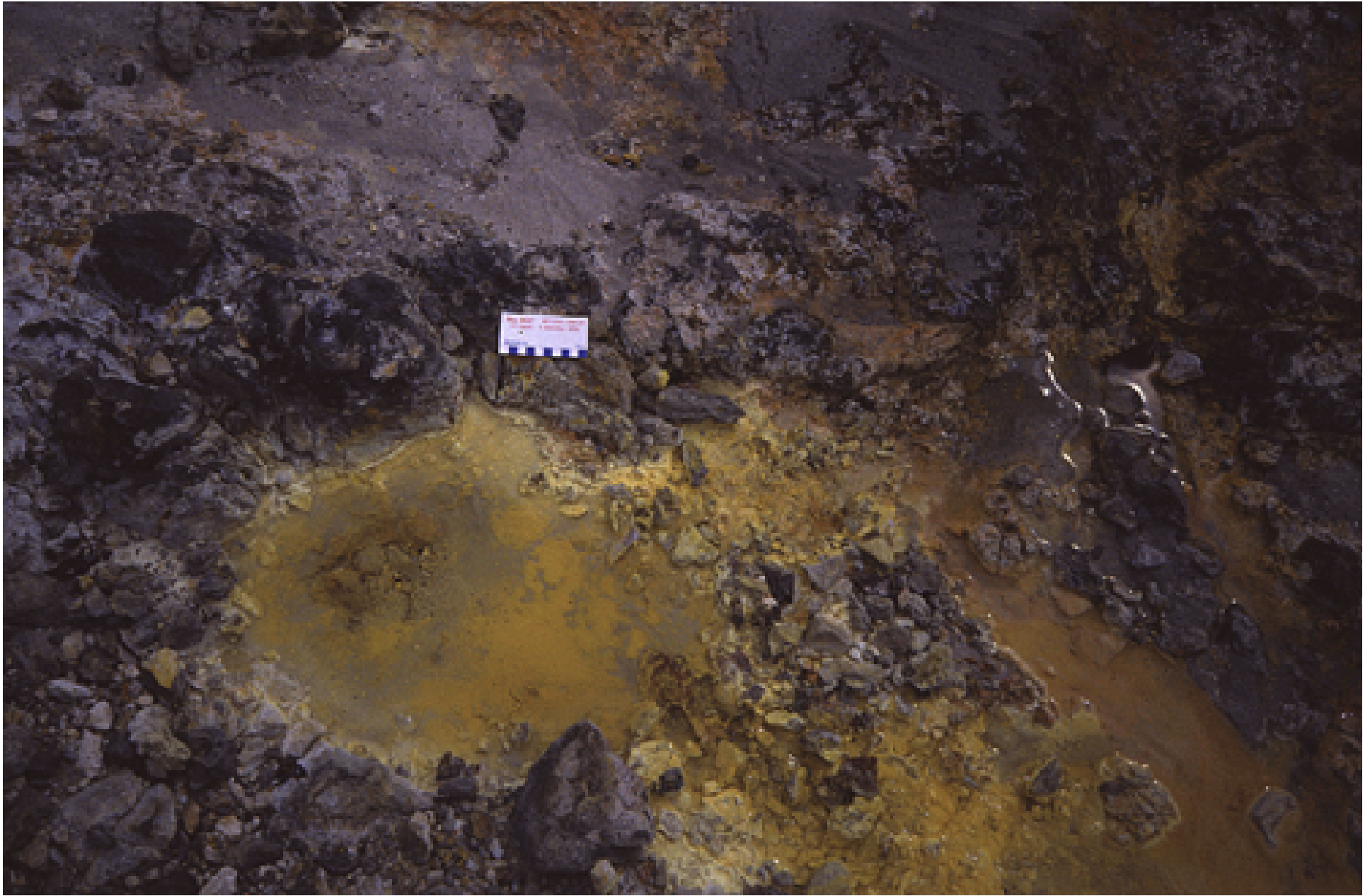
Osorezan, Japan



Osorezan, Japan



Osorezan, Japan



Osorezan, Japan

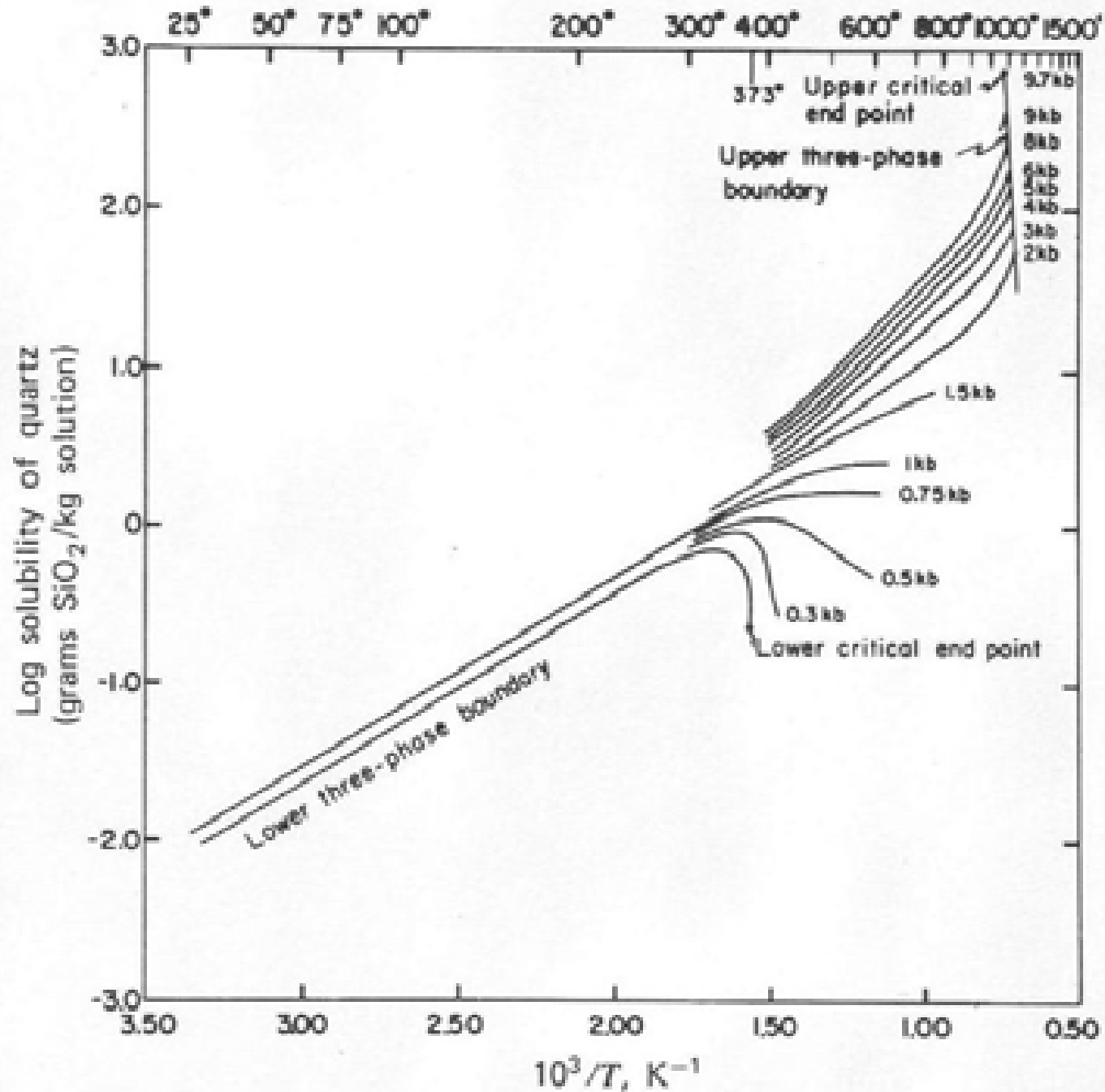


Osorezan, Japan

Hishikari,
Japan



Temperature, °C



Solubility of
quartz
in water

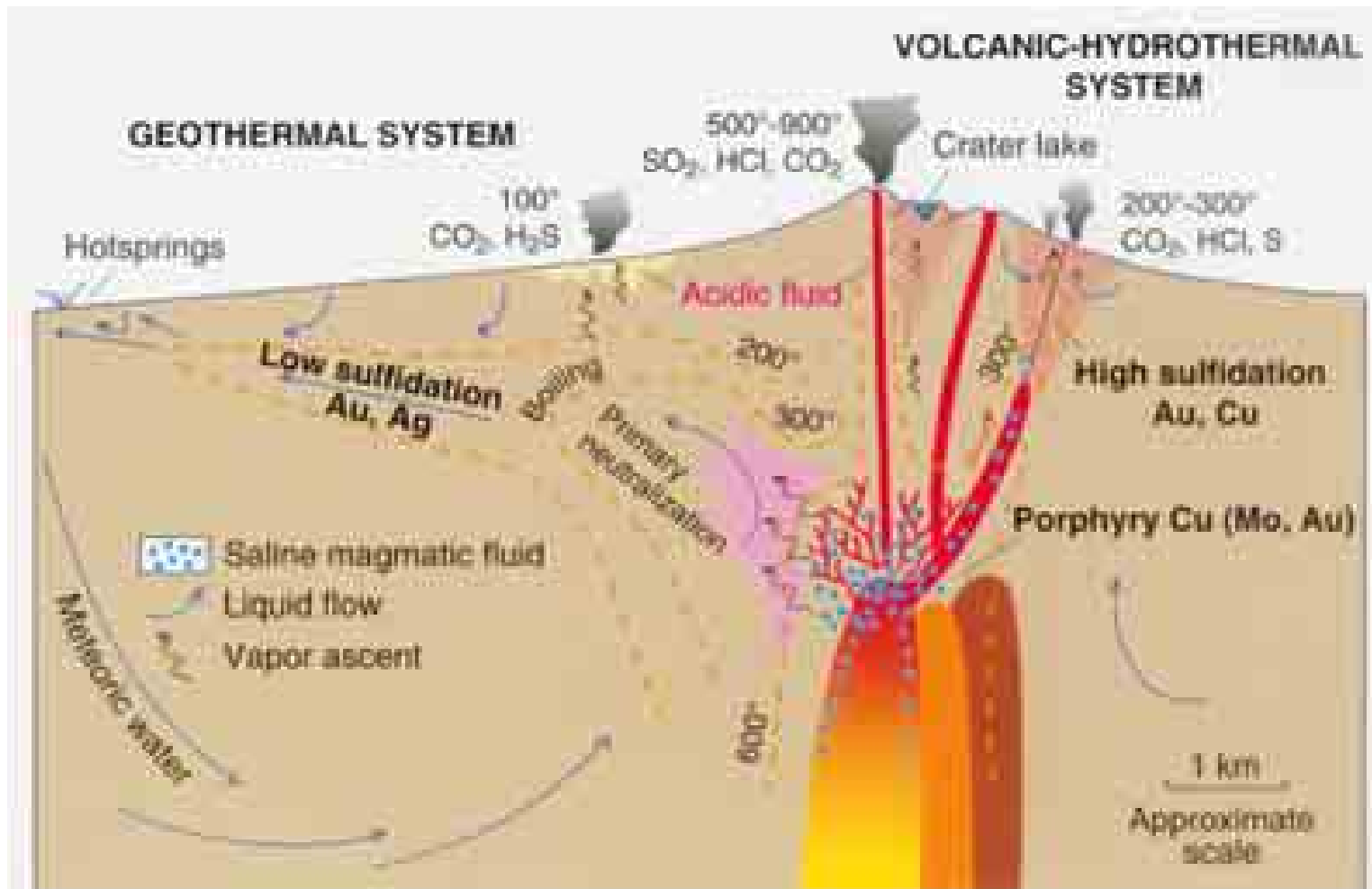
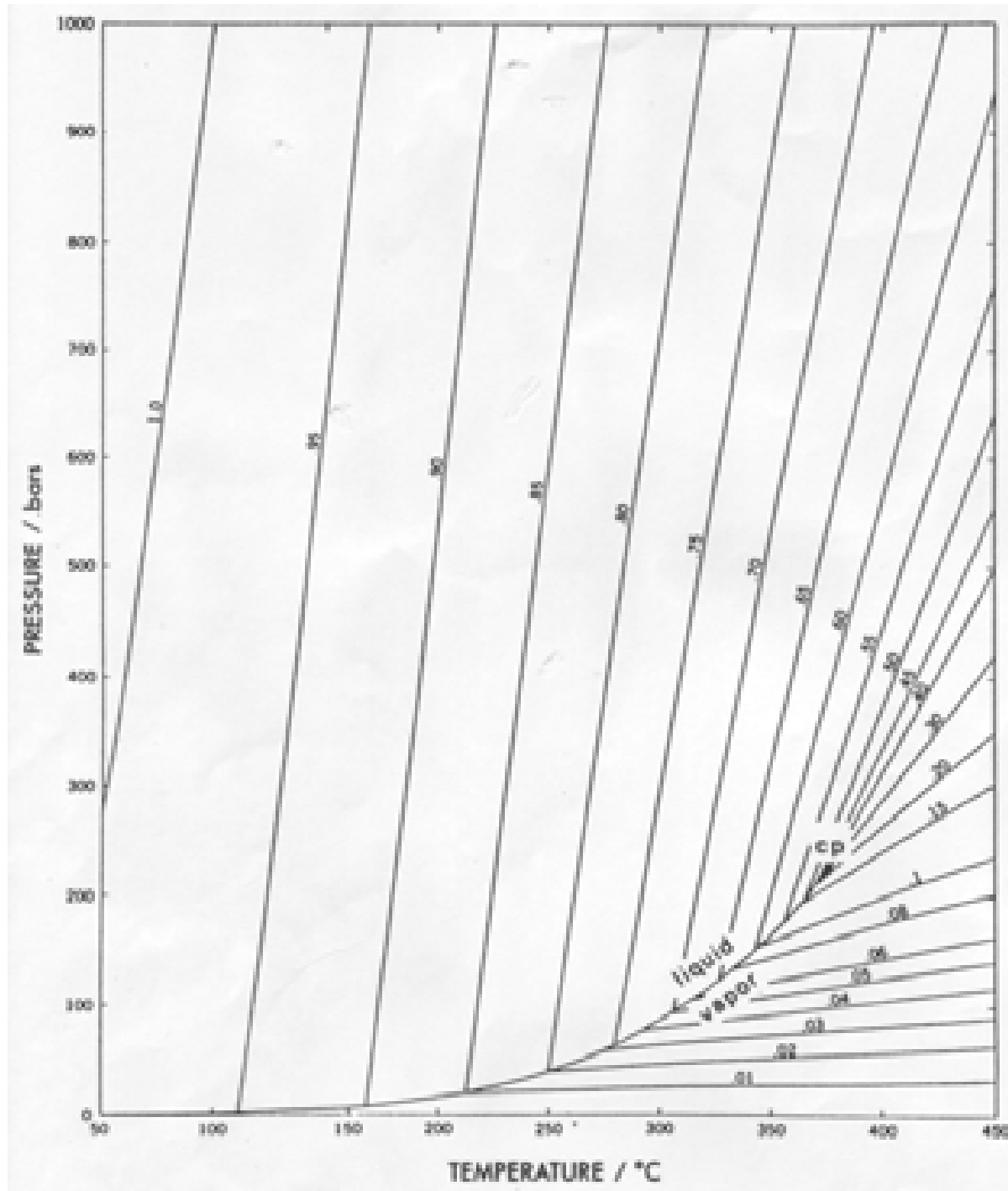


Fig. 1.1 Schematic cross-section showing shallow sub-volcanic intrusions and associated stratovolcano, and environments deduced for formation of porphyry Cu, and high- and low-sulfidation epithermal ore deposits [20,25]. Active volcanic-hydrothermal systems extend from degassing magma to fumaroles and acidic springs, and incorporate porphyry and/or high-sulfidation ore environments, whereas low-sulfidation ore deposits form from geothermal systems characterized by neutral-pH waters that may discharge as hot springs.



PT diagram of
water and
isochores
(lines of equal
density)
cp = critical point



Kori Kollo, Altiplano, Bolivia



Kori Kollo, Altiplano, Bolivia



Kori Kollo, Altiplano, Bolivia



**Kori Kollo, Bolivia: 59 Mt @ 2.3 g/t Au + 14 g/t Ag
Annual production: 10 t Au/a, worked out in 2002**



Kori Kollo, Bolivia: Leach pads



Kori Kollo, Bolivia: Leach pads



Kori Kollo, Bolivia: Leach pads



Kori Kollo, Bolivia: Pregnant ponds



Kori Kollo, Bolivia: Pregnant ponds































Basin and range province, Nevada



Round Mountain gold mine, Nevada





Round Mountain, 300 Mt @ 0.8 g/t Au (0.18 g/t Au cut-off in final pads), 200-250 USD/oz



Round Mountain mine in 1990: 320 t Au until 2006



Round Mountain, 24 t Au in 2002, 100,000 t/d ore + 100,000 t/d waste











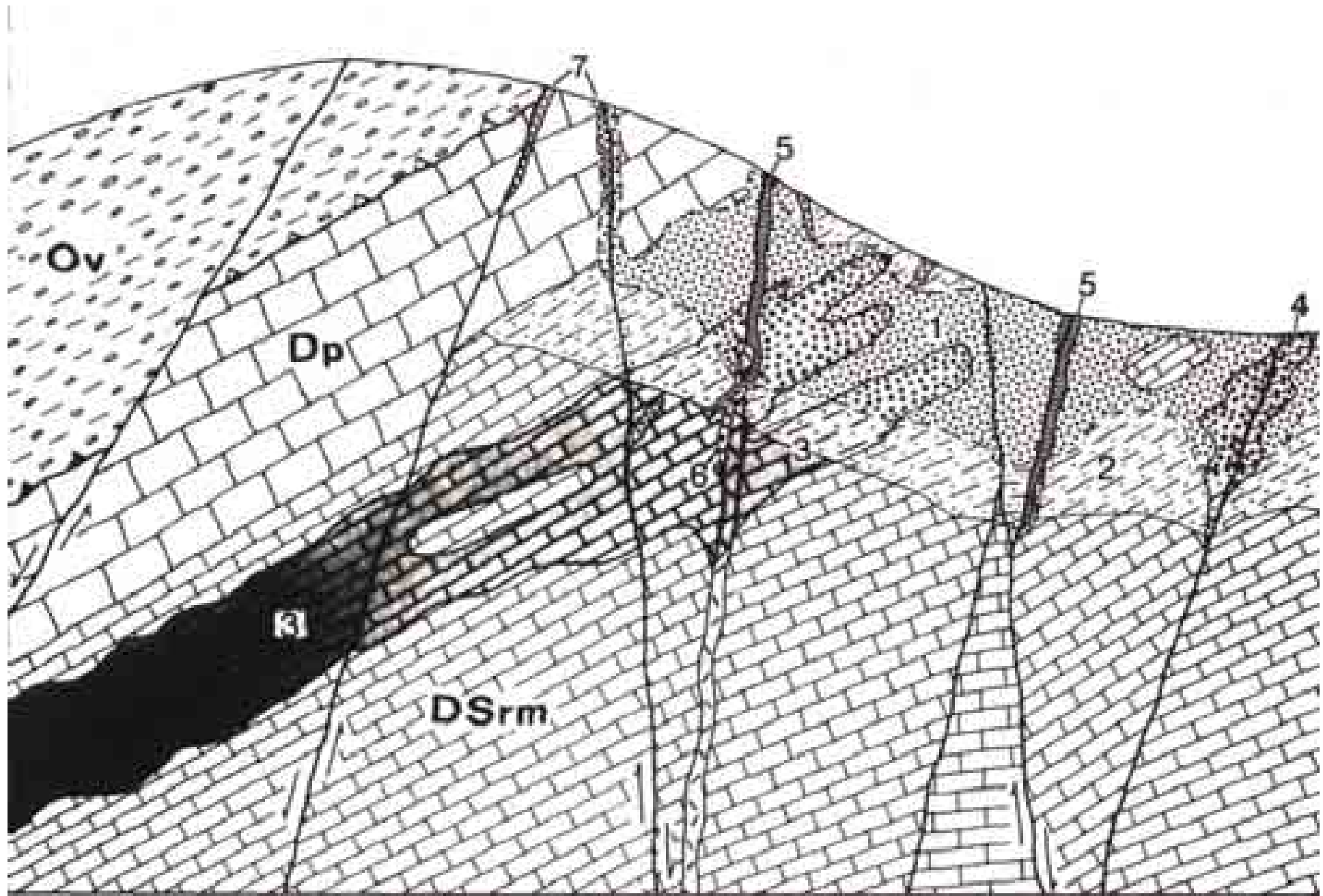


Round Mountain open pit in July 2004





Experimental biooxidation-bioleaching reactor at the Gold Quarry Mine



Carlin type: „invisible“ gold in carbonaceous, decarbonated limestone



Alchem Pit, Jerritt Canyon, Nevada



Alchem Pit, Jerritt Canyon, Nevada

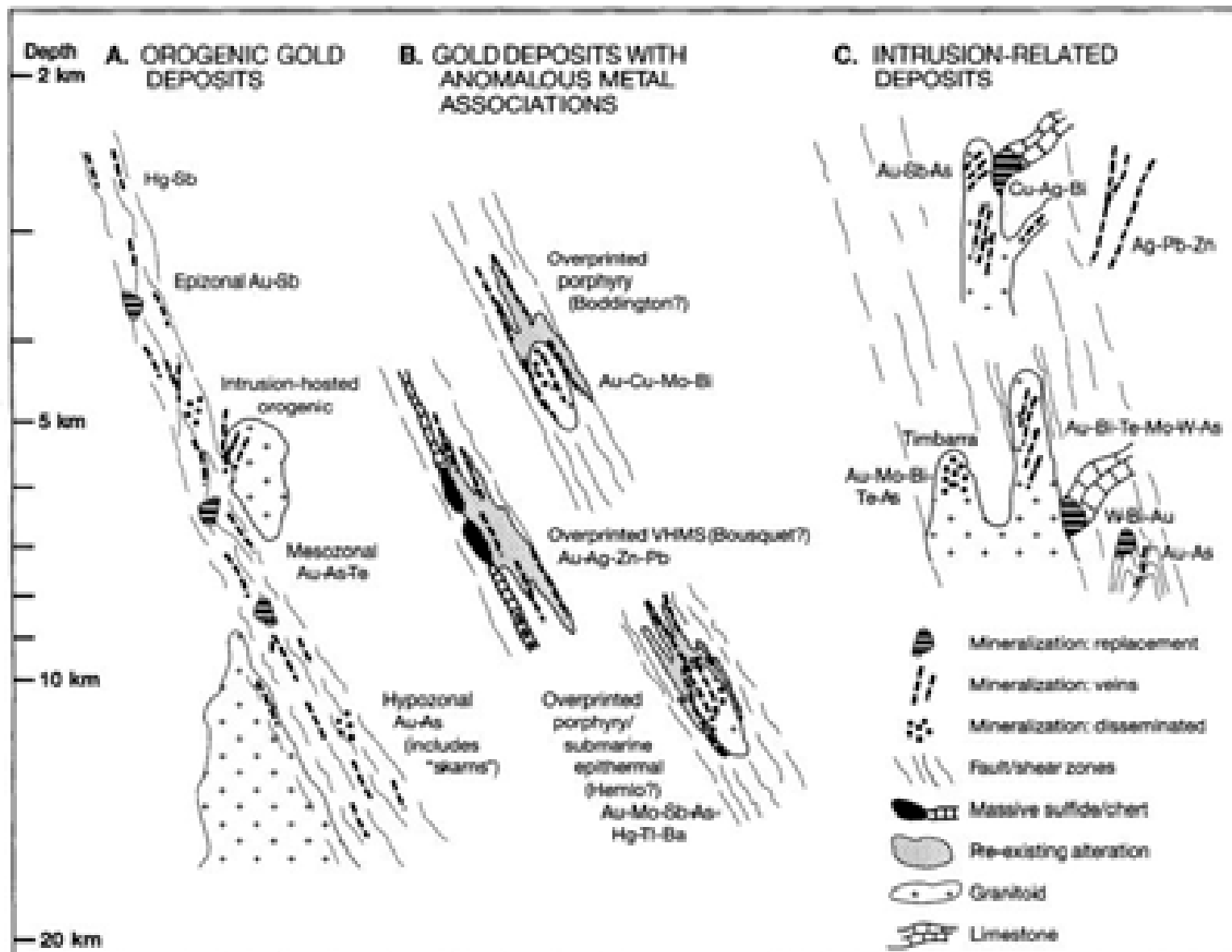


FIG. 2. Schematic representation of crustal environments of orogenic gold deposits, gold deposits with anomalous metal associations, and intrusion-related gold deposits, in terms of depth of formation and structural setting. The figure is, by necessity, stylized. Adapted partly from Groves et al. (1998) and Lang et al. (2000). Abbreviations: VHMS = volcanic-hosted massive sulfide.

Groves et al., Econ Geol 98: 5 (2003)

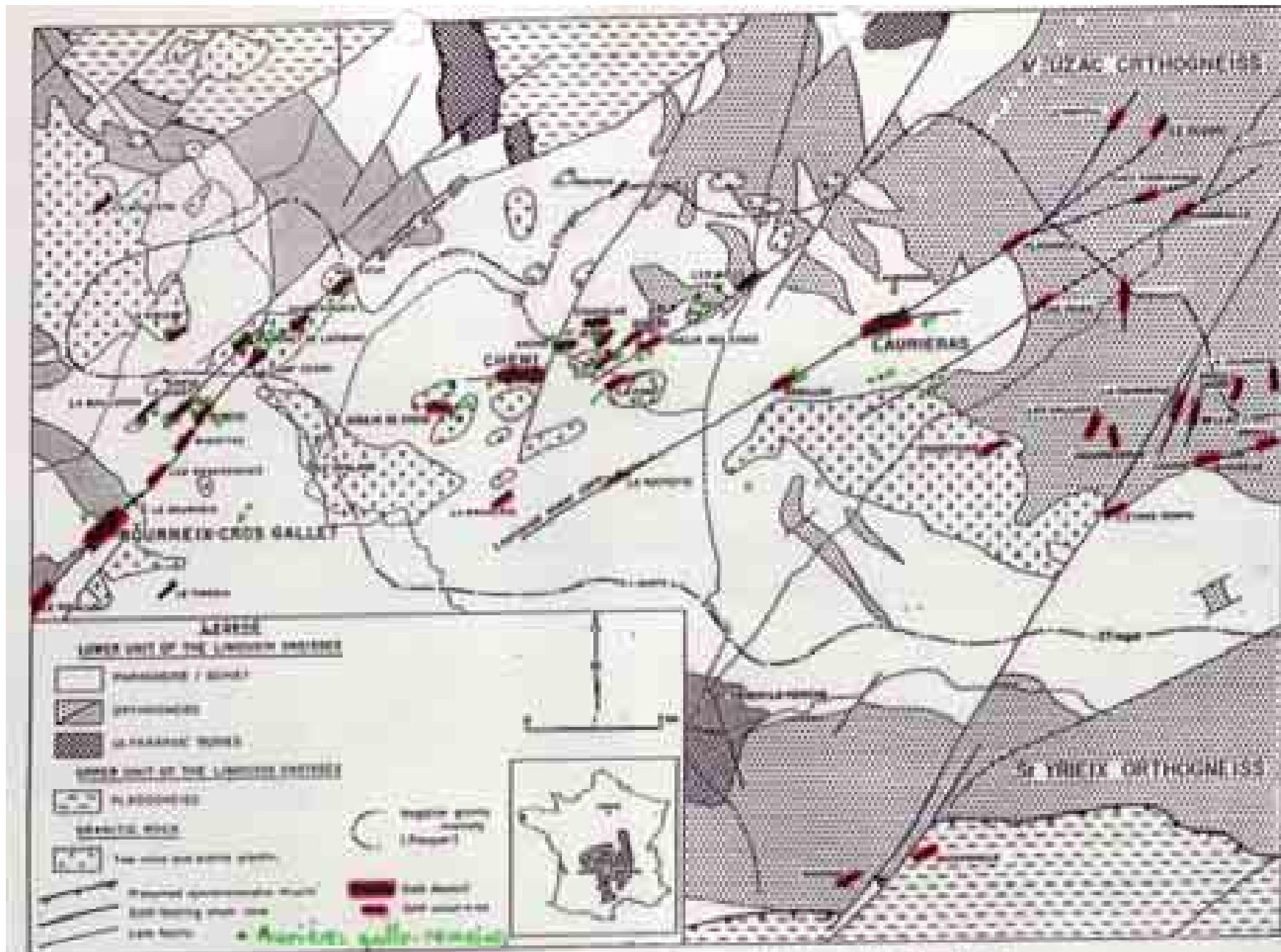
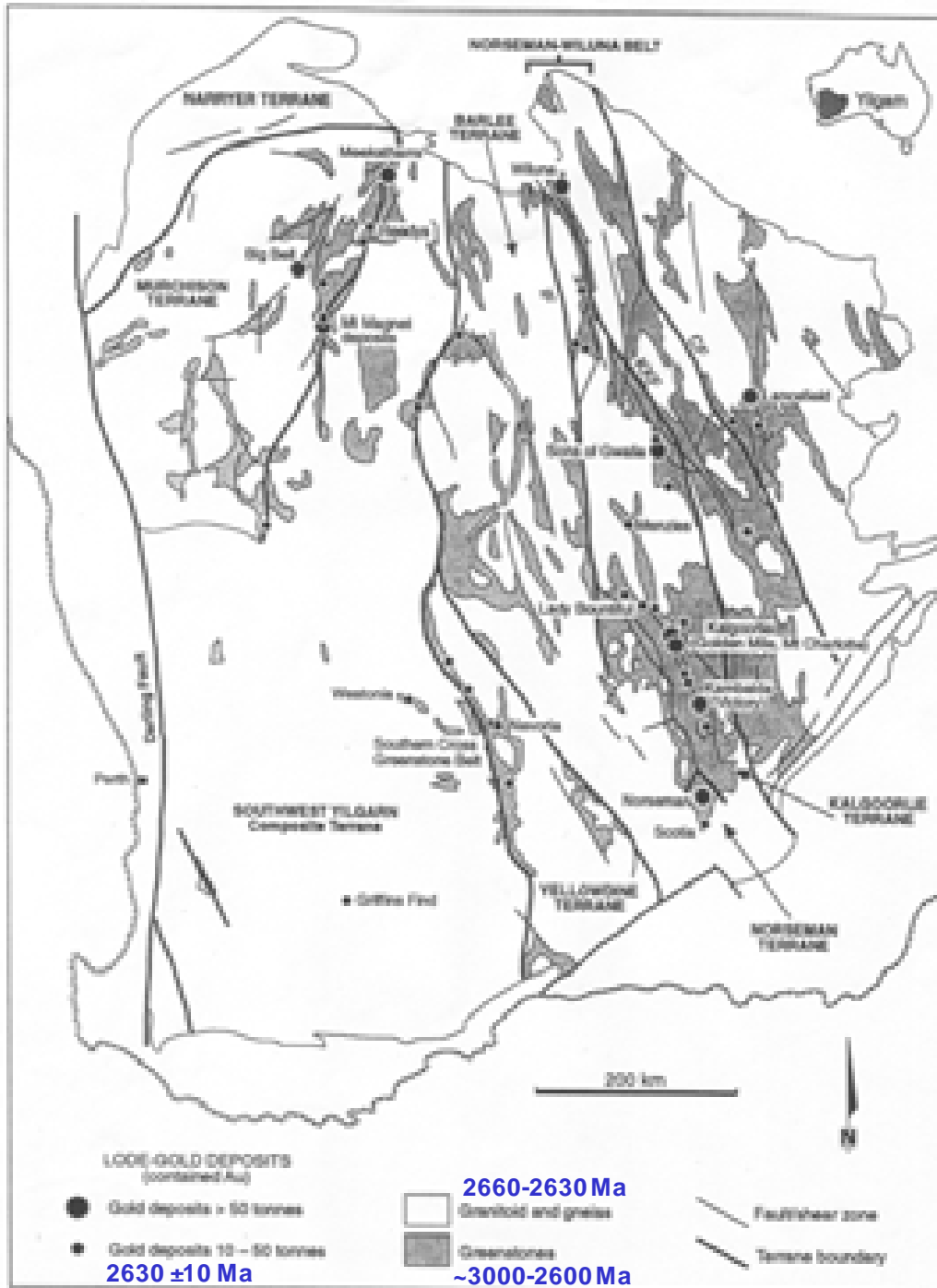


FIG. 3-1 - Carte géologique et géologique synthétique de l'ouest du district de St-Yrieix. Localisation du gisement de Cros Gallet.

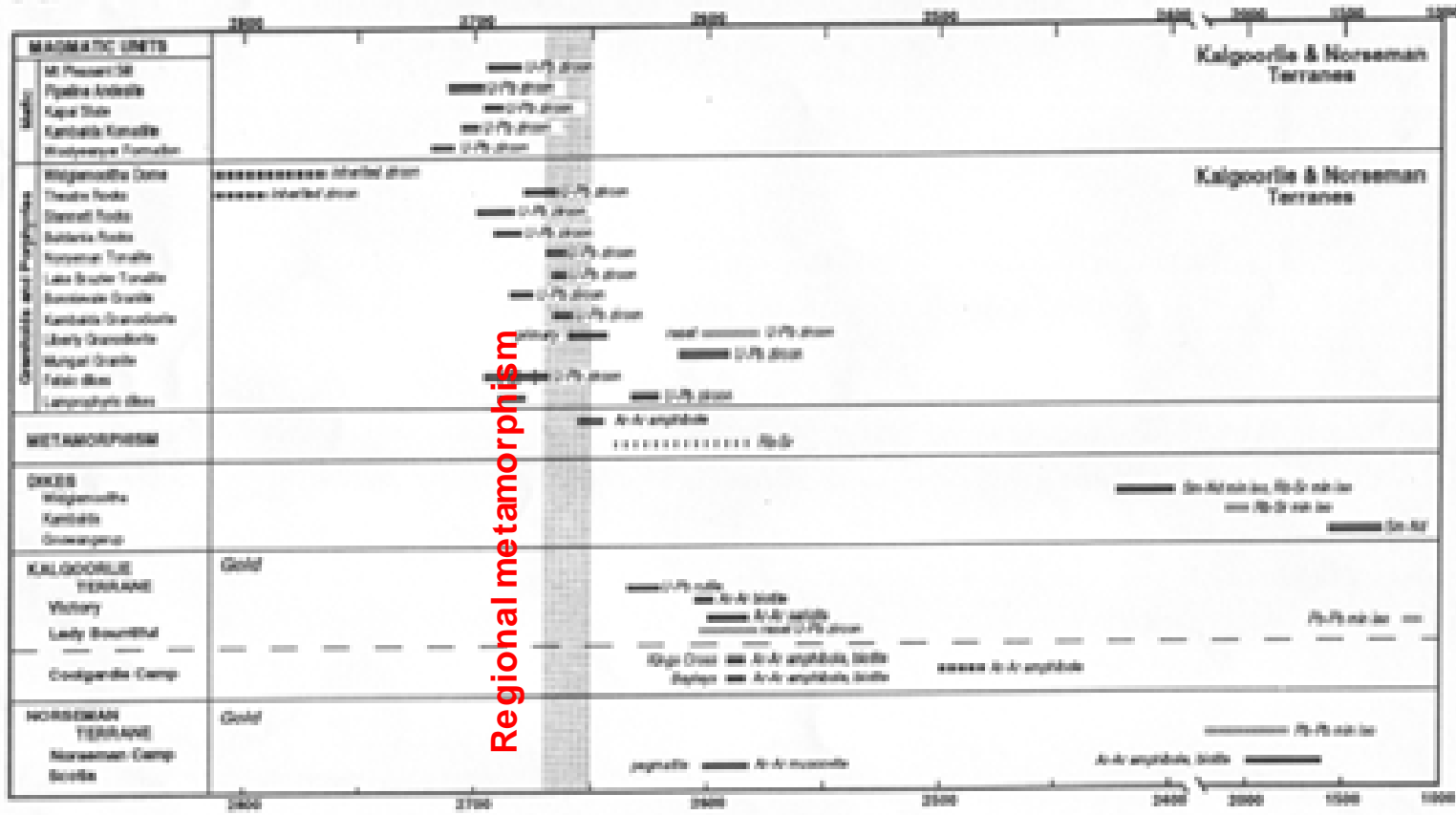
Yilgarn Craton, western Australia



Golden Mile: ~1200 t Au

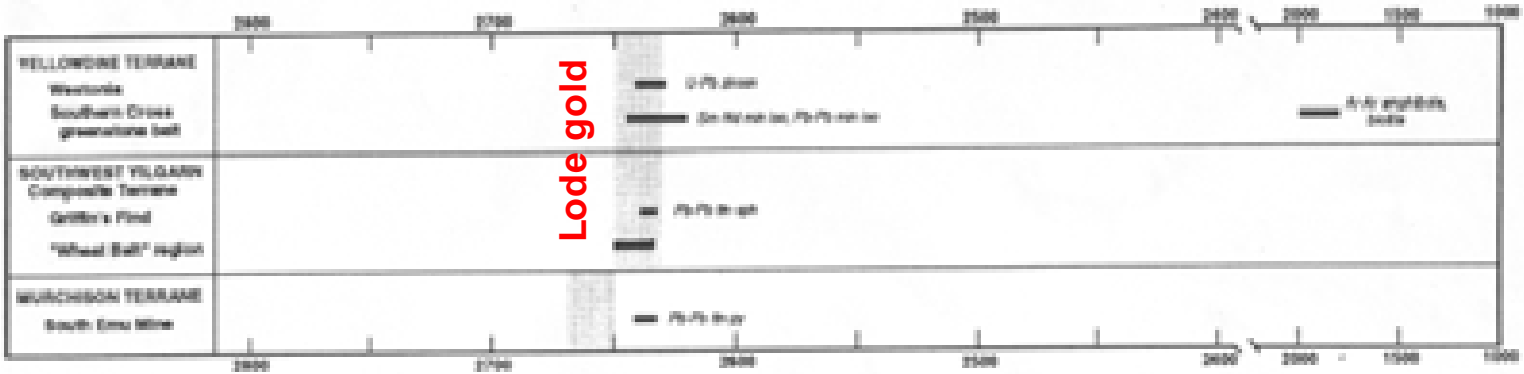
Kerrich and Cassidy (1994) OGR 9: 277

A. Magmatic and thermal evolution of the eastern Yilgarn Craton, and gold mineralization and resetting events



Regional metamorphism

B. Temporal relationships of lode gold mineralization in the Yilgarn Craton

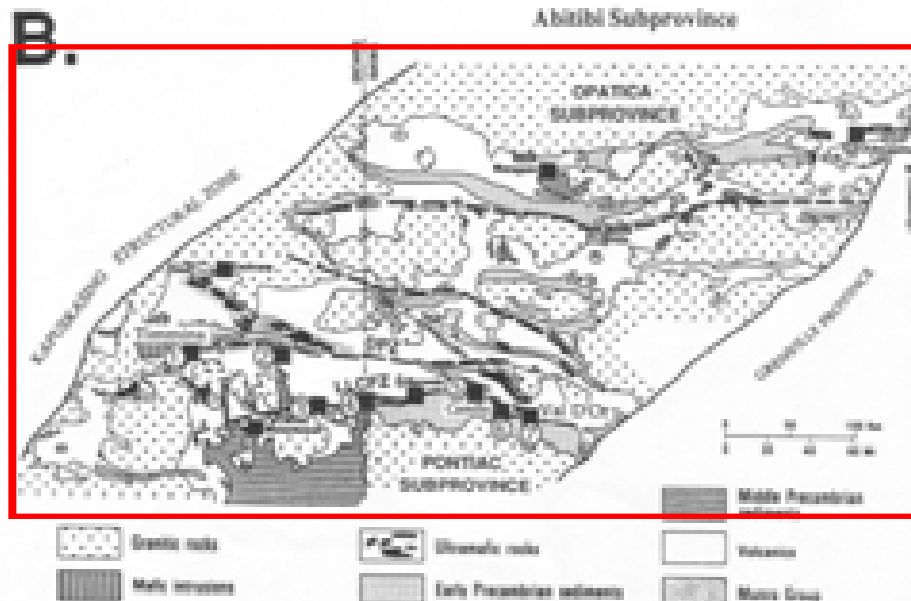


Lode gold



Superior Province, Canada

Hemlo: >300 t Au

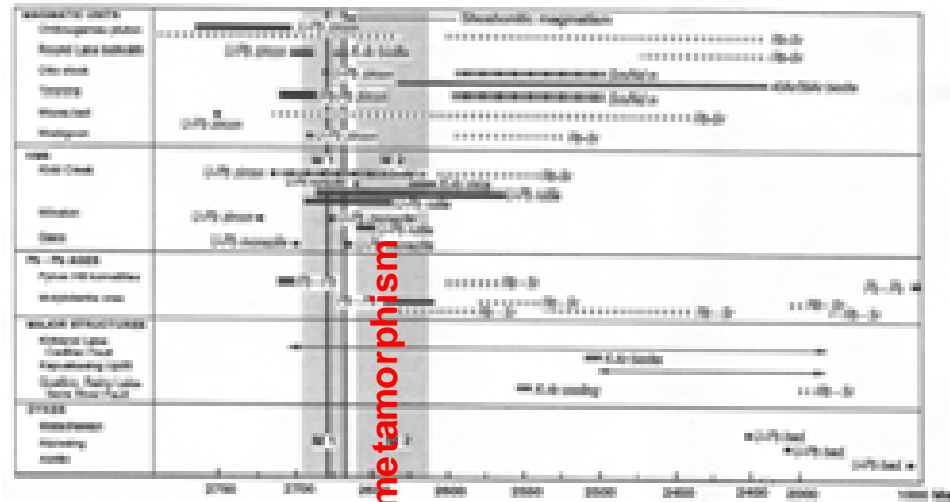


Timmins-Hollinger: >600 t Au

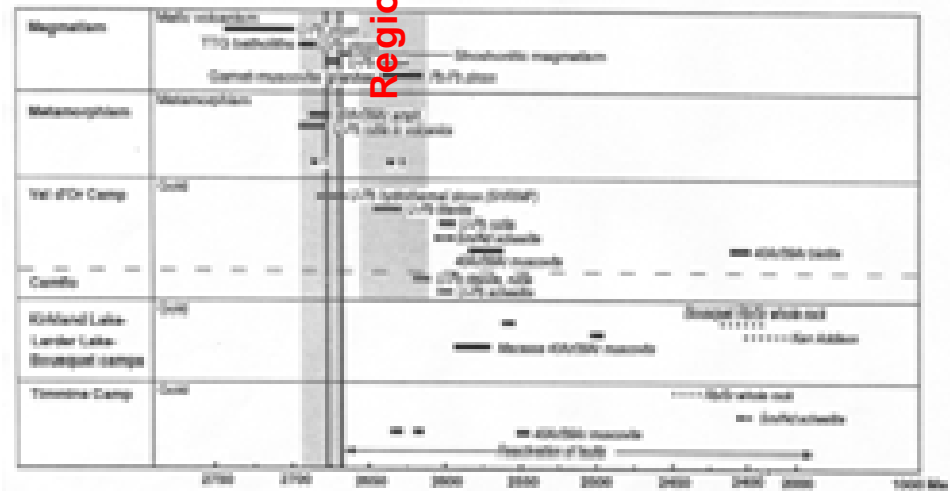
Larder Lake Shear Zone:
Larder Lake: >300 t Au,
Val d'Or >100 t Au

Kerrich and Cassidy (1994) OGR 9: 268

A. Magmatic, thermal, fluid, and structural chronology of the southern Superior Province, based on different isotopic systems and minerals



B. Magmatic and thermal evolution of the southern Abitibi subprovince and lode gold mineralization and resetting events

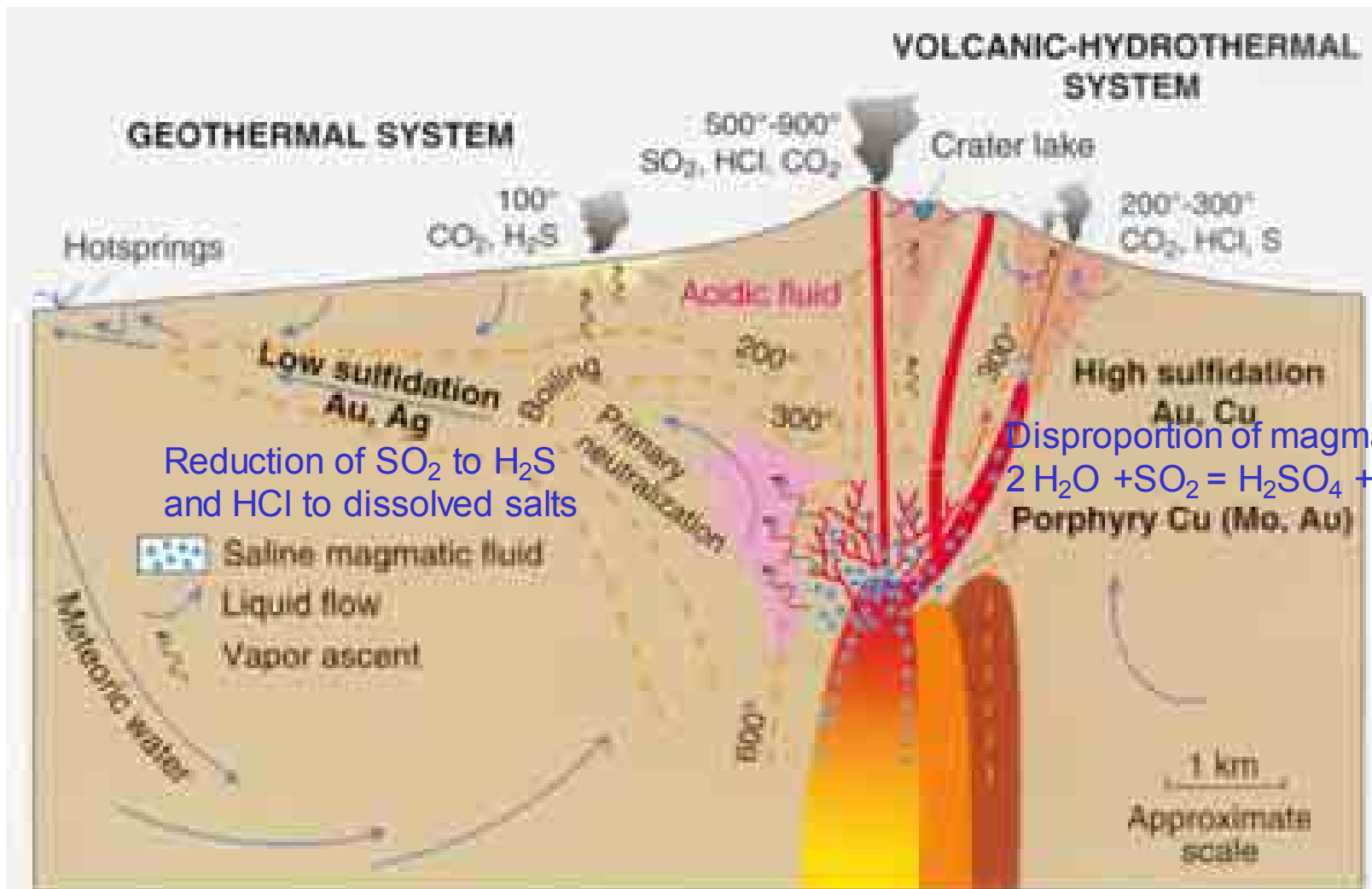


C. Superior Province gold timing constrained by cross-cutting dikes






Regional metamorphism

Lode gold

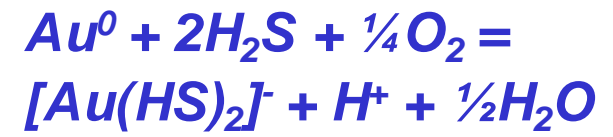
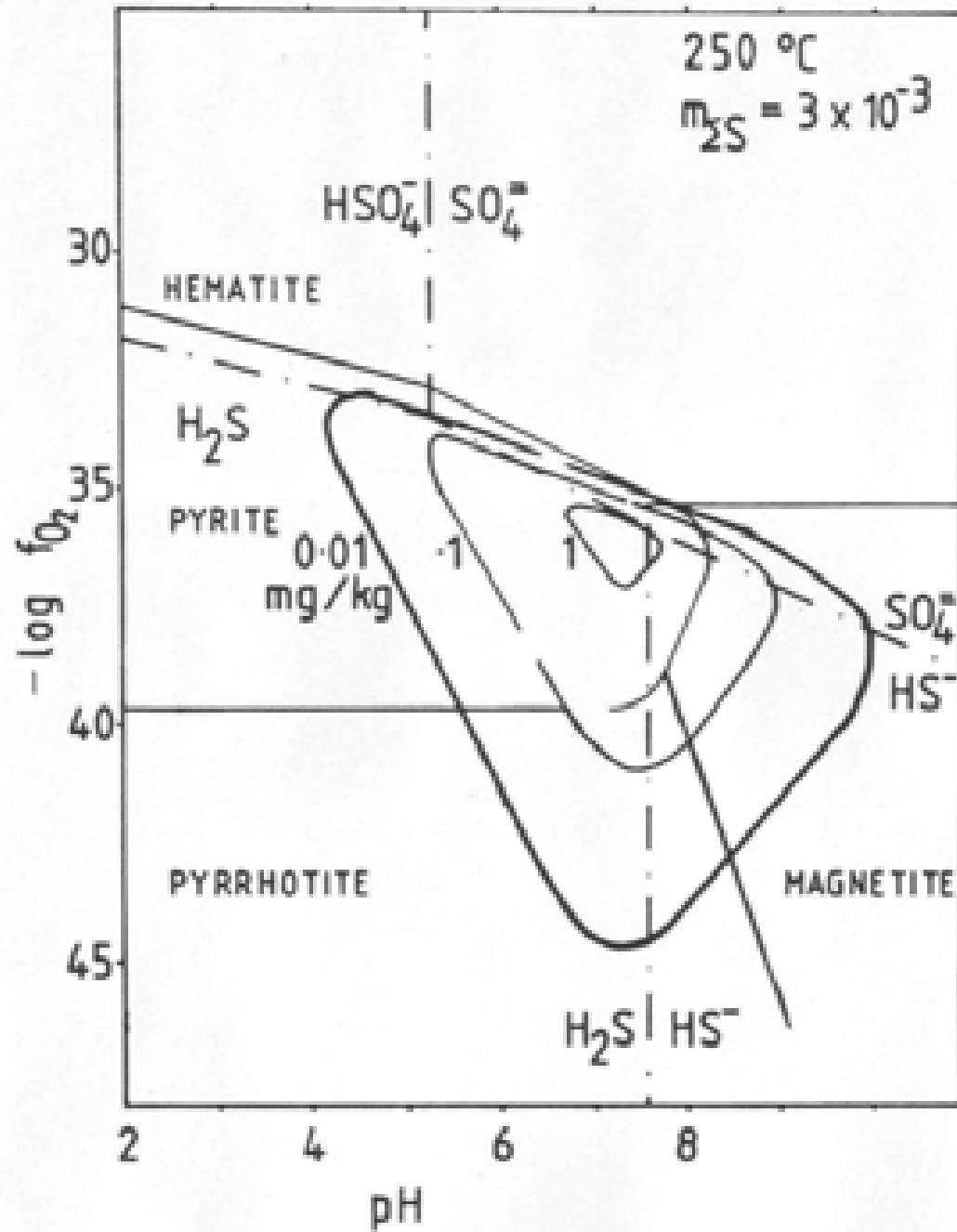


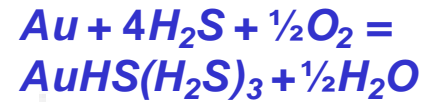
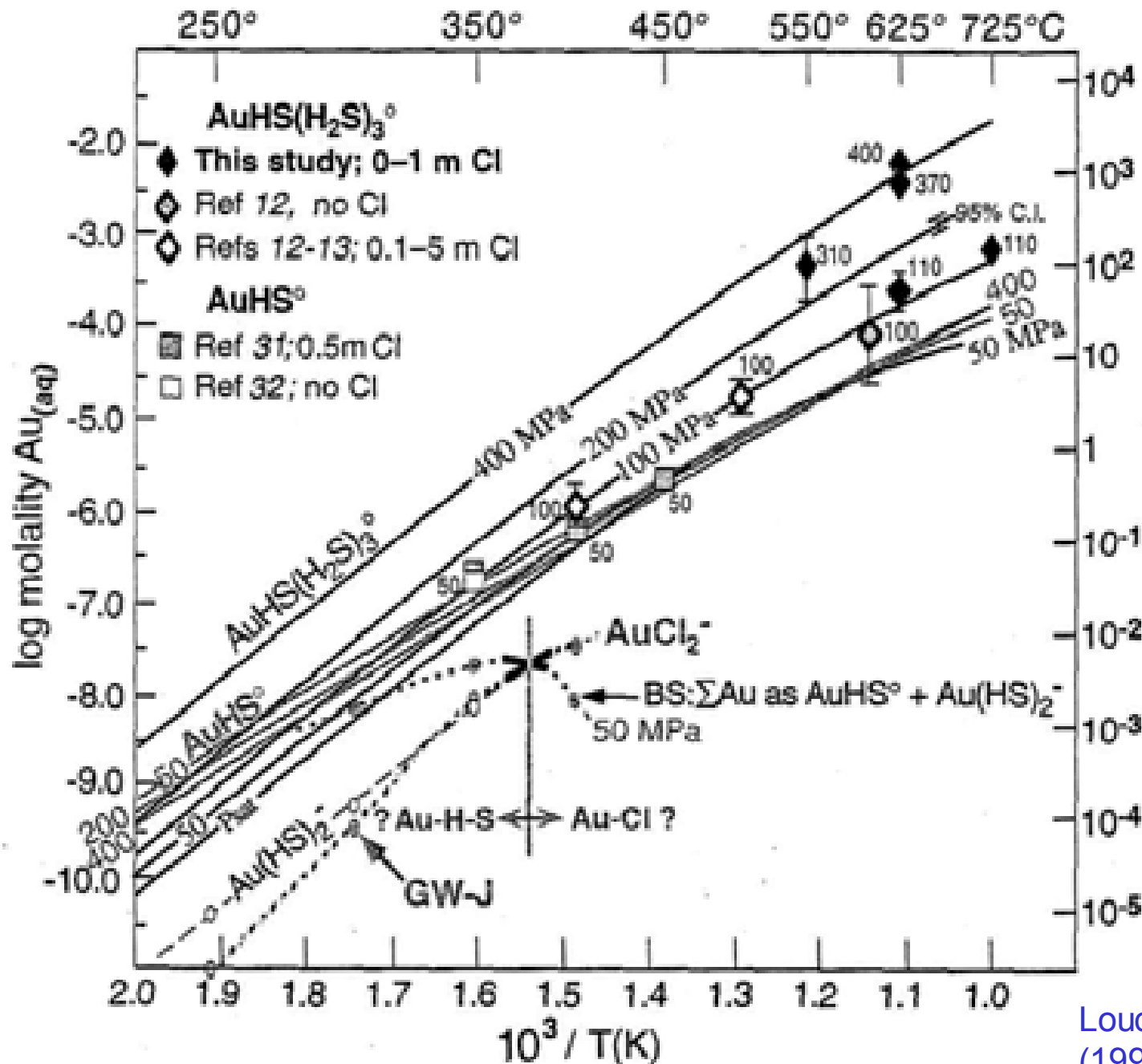
Reduction of SO₂ to H₂S
and HCl to dissolved salts

-  Saline magmatic fluid
-  Liquid flow
-  Vapor ascent

Disproportion of magmatic SO₂:
 $2\text{H}_2\text{O} + \text{SO}_2 = \text{H}_2\text{SO}_4 + \text{H}_2\text{S}$
Porphyry Cu (Mo, Au)

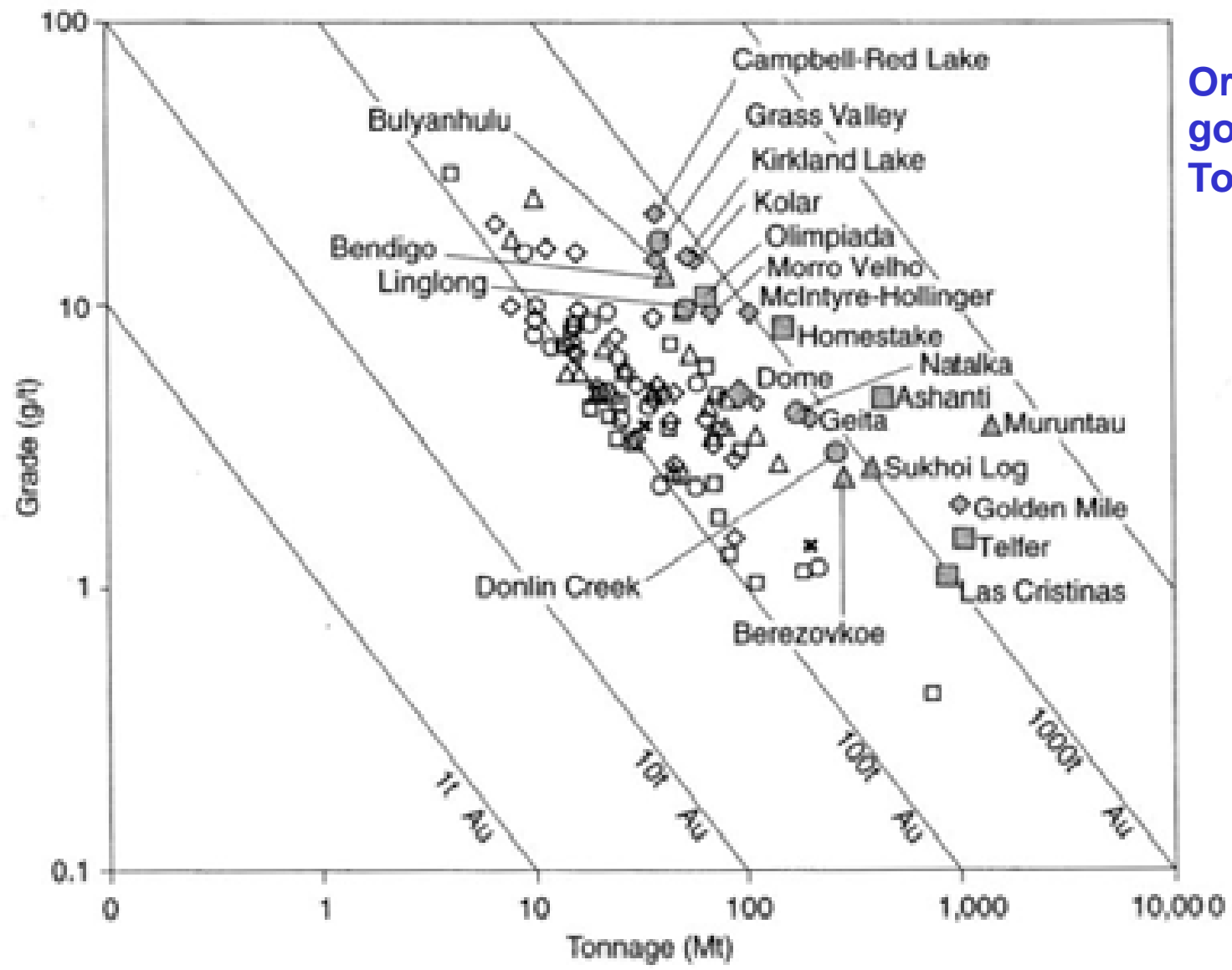
Fig. 1.1 Schematic cross-section showing shallow sub-volcanic intrusions and associated stratovolcano, and environments deduced for formation of porphyry Cu, and high- and low-sulfidation epithermal ore deposits [20,25]. Active volcanic-hydrothermal systems extend from degassing magma to fumaroles and acidic springs, and incorporate porphyry and/or high-sulfidation ore environments, whereas low-sulfidation ore deposits form from geothermal systems characterized by neutral-pH waters that may discharge as hot springs.





Gold solubility oxygen-buffered (pyrrhotite-pyrite-magnetite) and pH-buffered (orthoclase-muscovite-quartz) as typical of orogenic gold deposits

Orogenic
gold deposits:
Tonnage-grade plot



Age of deposit

- Archean
- Proterozoic
- △ Paleozoic
- Mesozoic
- × Cenozoic

Size of deposit

- ◇ □ △ 70t to 499t Au
- ◆ ■ ▲ > 500t Au



Road to Grasberg (Freeport McMoRan) in Irian Jaya



Irian Jaya: Grasberg road



Grasberg



**Grasberg open pit (Aug 1999), 1.2 Gt @ 1.41 % Cu + 1.5 g/t Au, 1 Gt overburden
Production in 2003: 600,000 t Cu + 80 t Au, 26 ct/pound Cu, 113 USD/oz Au**



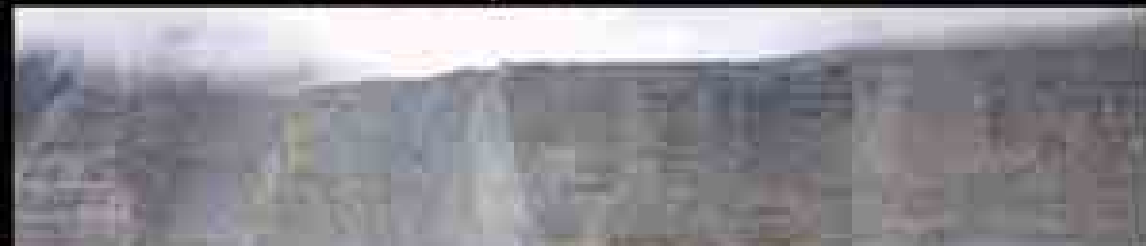
Grasberg open pit (Aug 99)



Grasberg Open Pit

View Looking South

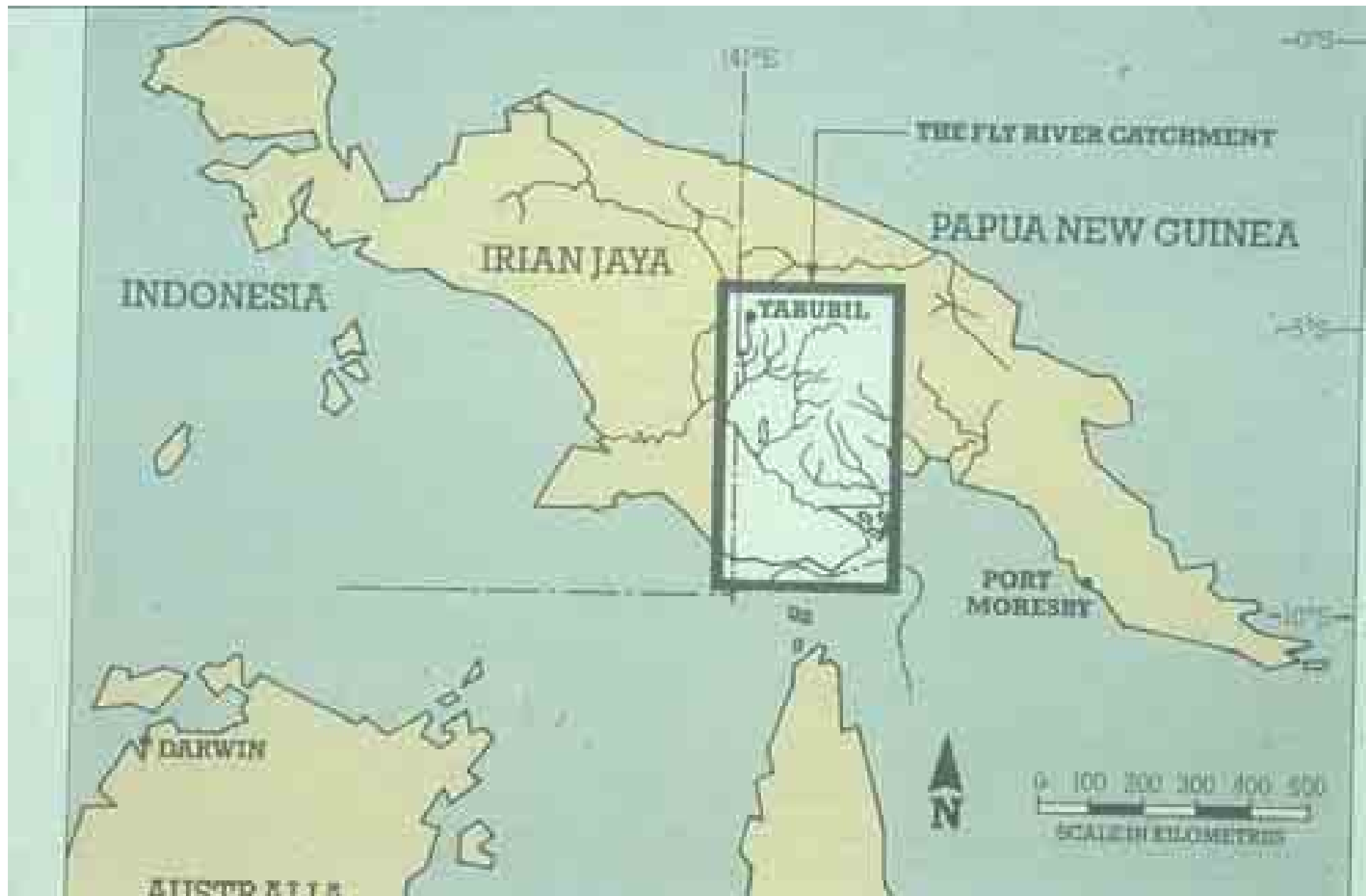
October 9, 2003

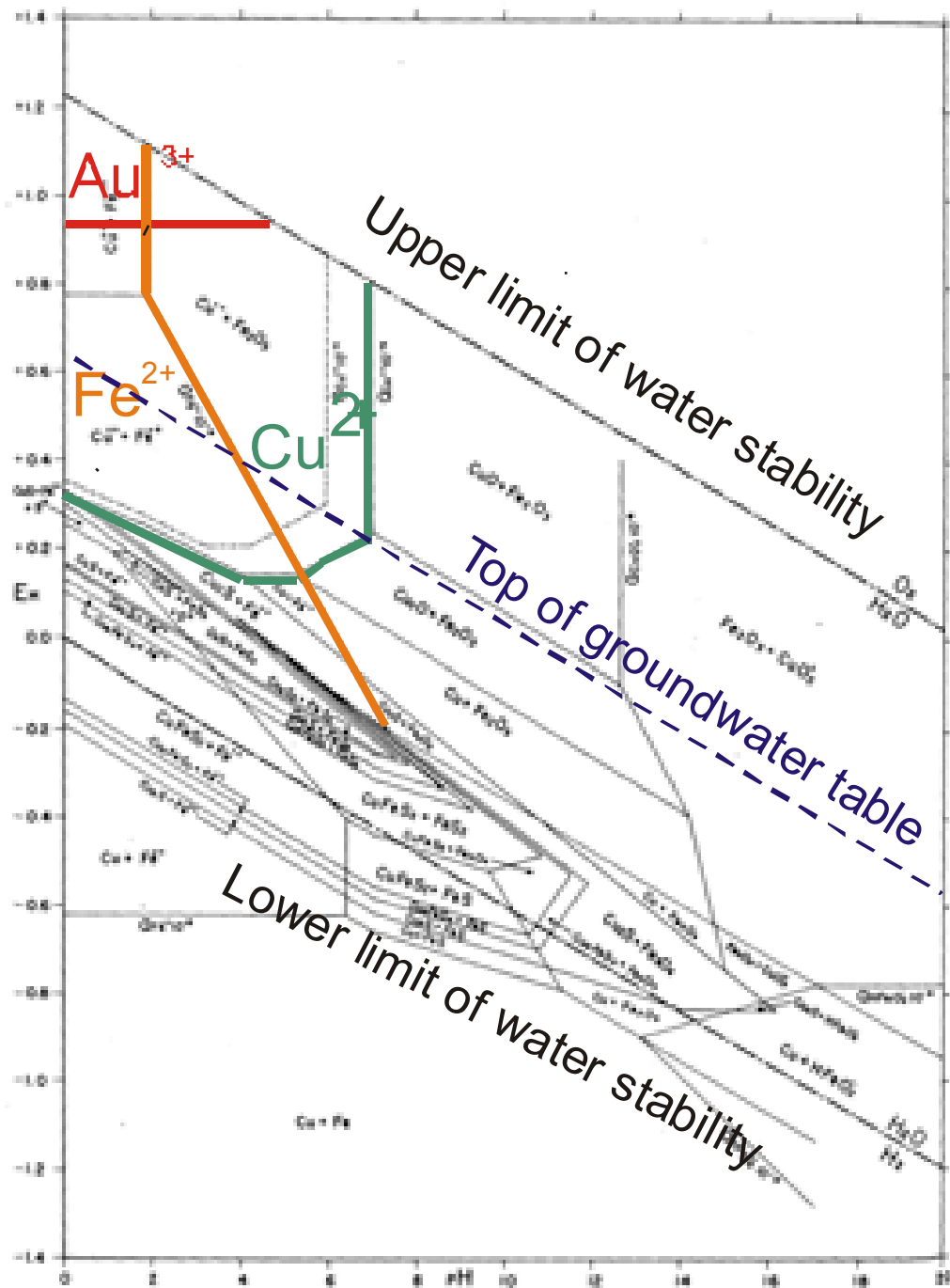


65

55

Ramp
Access





The system Cu-Fe-S-O-H
 at 25°C and 1 bar.
 Total dissolved sulfur = 10^{-4} m
 From Garrels and Christ (1965: 231)

The colored solubility limits of
 Au³⁺, Fe²⁺ and Cu²⁺ are drawn
 at 10^{-6} m Fe (56 ppb Fe), 10^{-6} m Cu
 (64 ppb Cu) and 10^{-8} m Au (2 ppb Au).



**OK Tedi, Papua New Guinea (1976) Drill sites, helicopter landing pads
EG 73: 597 (1978)**



OK Tedi (1992)



**OK Tedi, Papua New Guineas (1994), 265 Mt @0.82 % Cu + 0.65 g/t Au
Production in 2003: 210,000 t Cu + 16 t Au**

Davies et al. (1978)
Econ Geol 73: 796-809



Ok Tedi/ Papua New Guinea

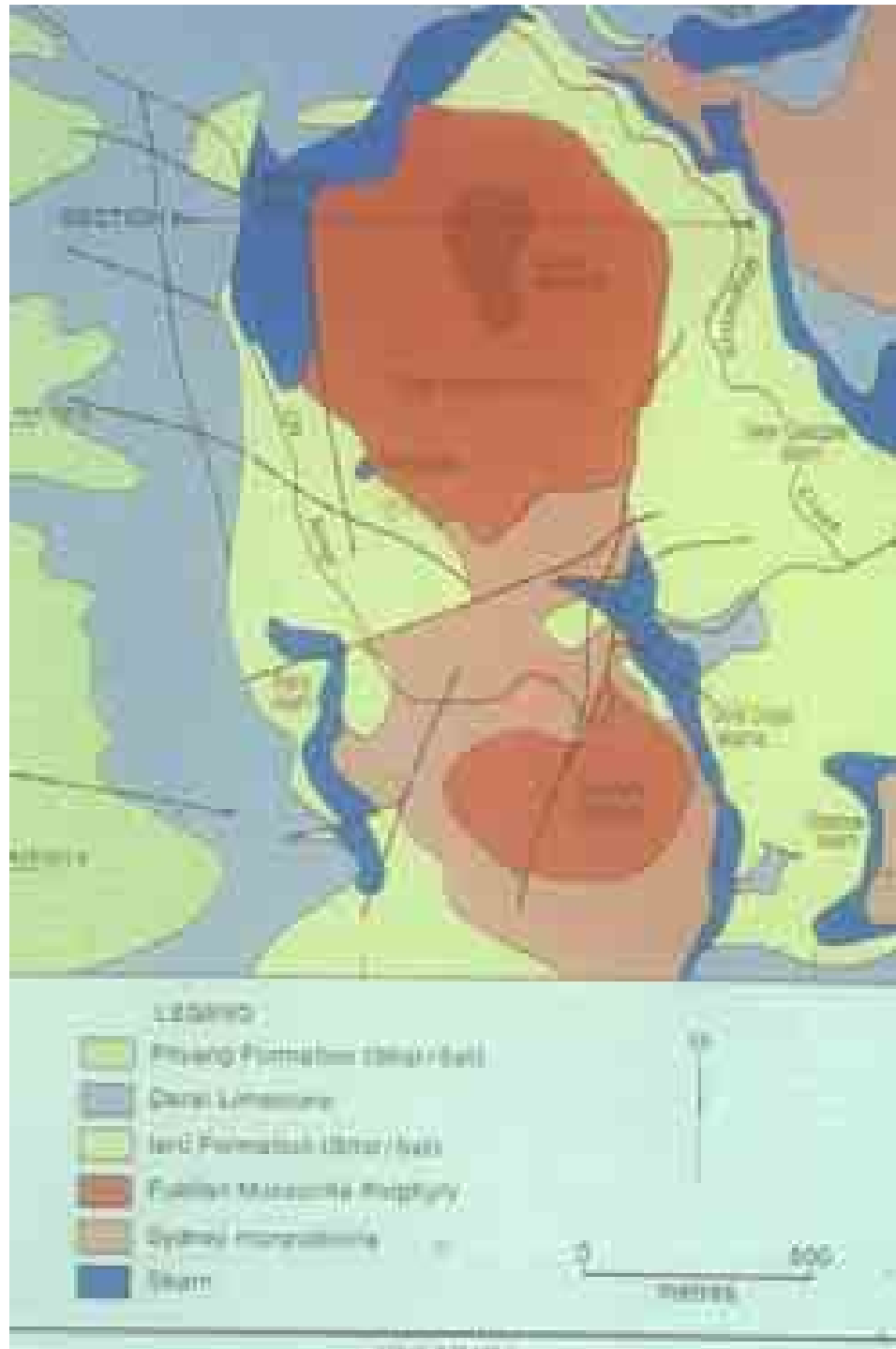
**460 Mt @ 0.72 % Cu,
0.7 g/t Au**

Gossan ore:
30 Mt x 3 g/t Au =
90 t Au
~ 2.5 billion USD

Secondary enrich-
ment zone:
265 Mt x 0.82 % Cu =
2 Mt Cu
~ 14 billion USD

265 Mt x 0.65 g/t Au =
170 t Au

Protore:
0.2-0.4 % Cu
0.3-0.5 g/t Au



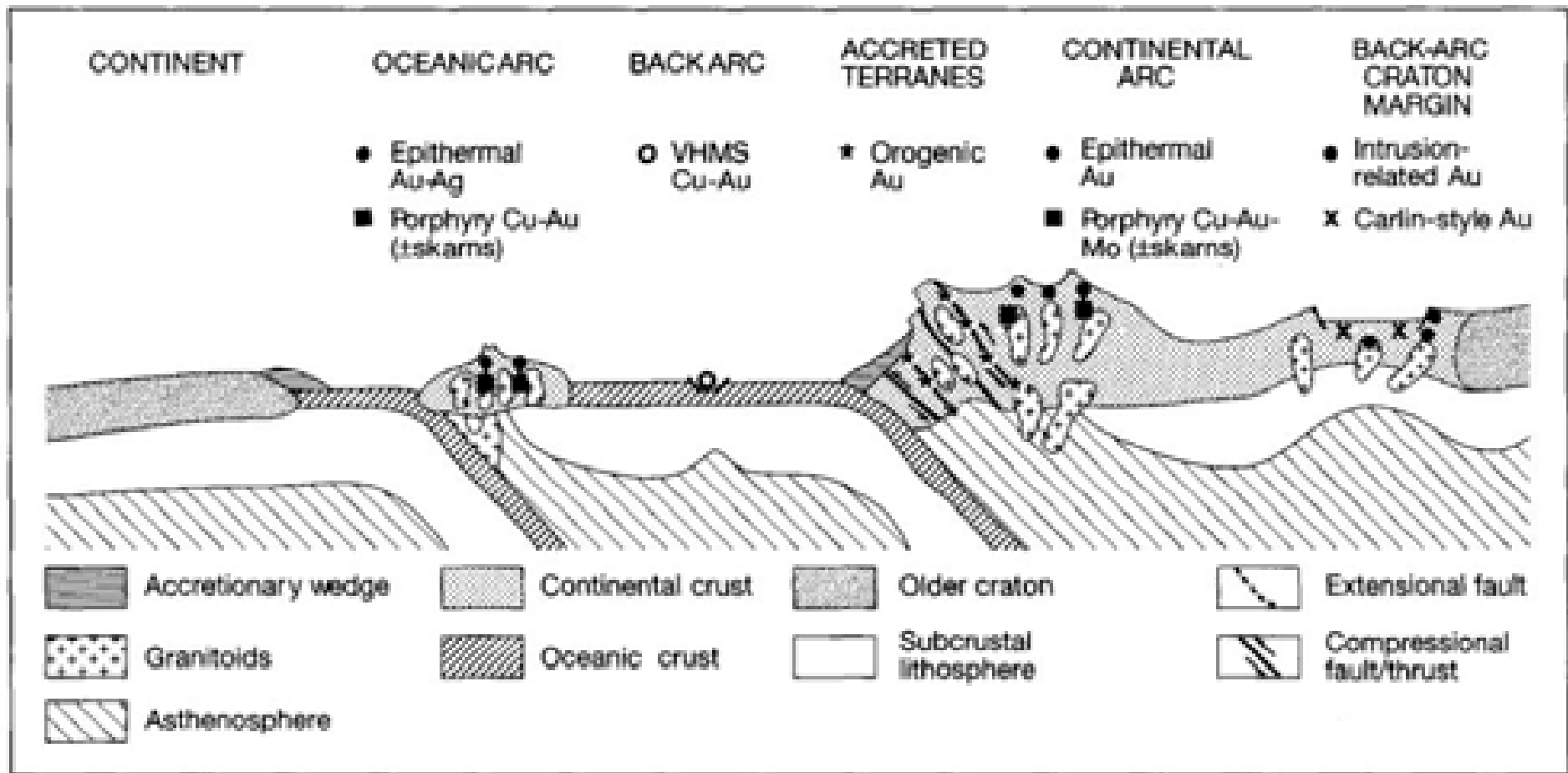
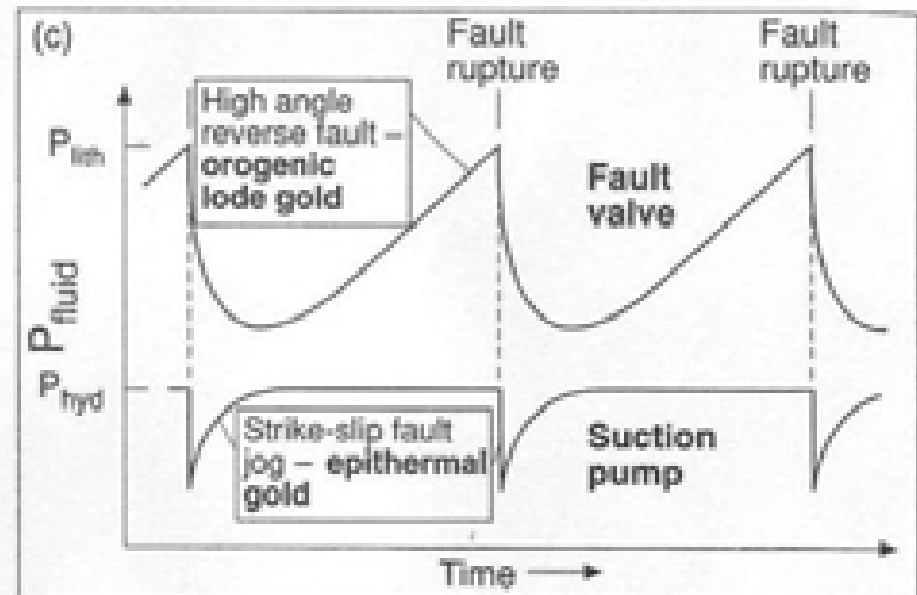
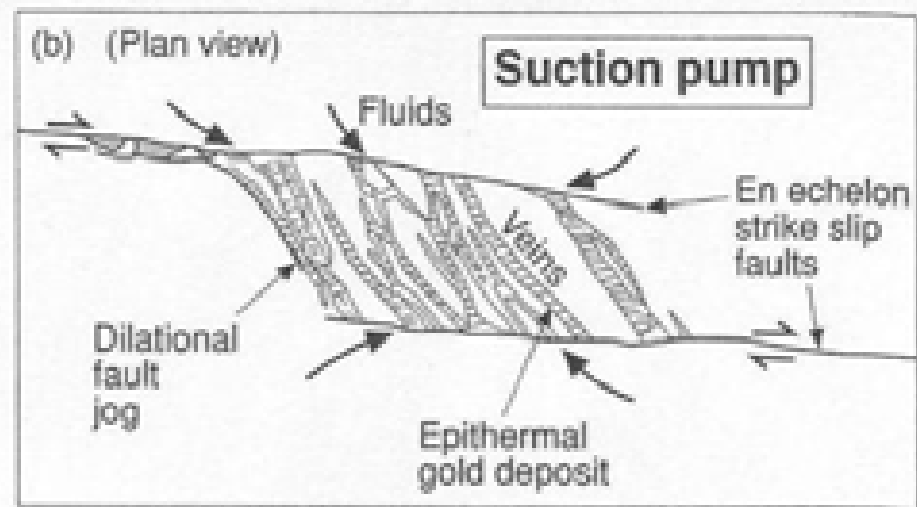
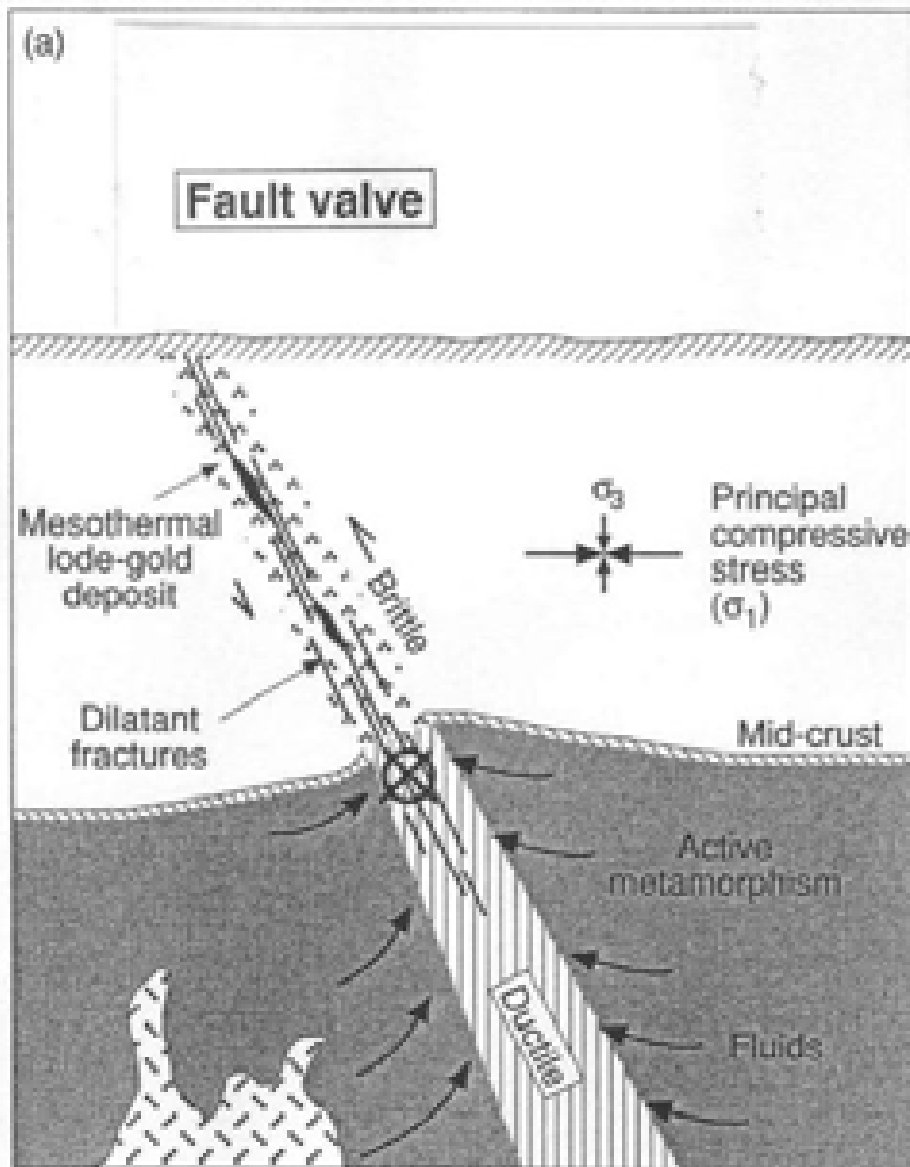


FIG. 1. Tectonic settings of gold-rich epigenetic mineral deposits. Vertical scale is exaggerated to allow schematic depths of formation of various deposit styles to be shown. Adapted from Groves et al. (1998). Abbreviations: VHMS = volcanic-hosted massive sulfide.



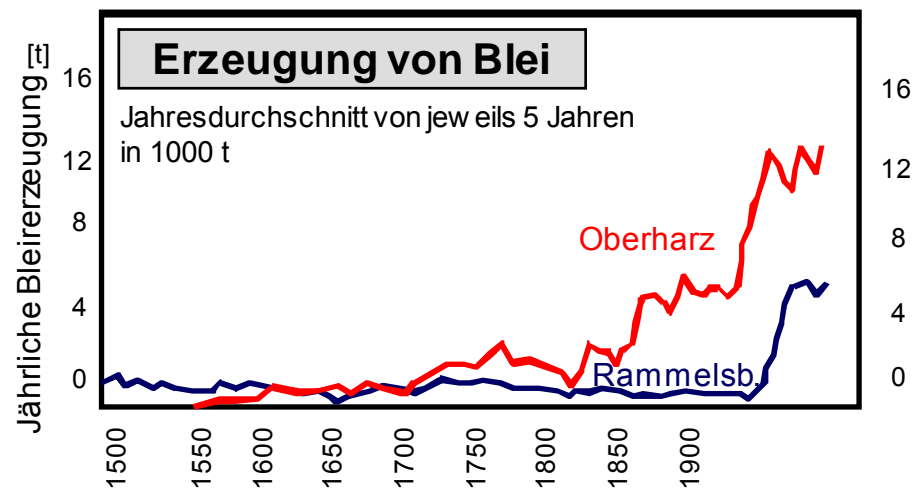
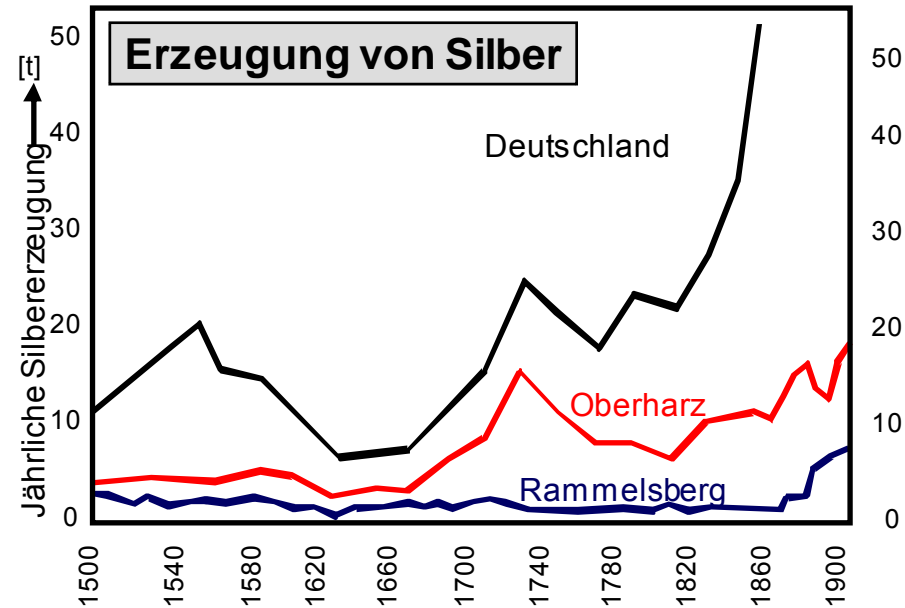
Hydrothermal fluid flow at deep levels (compressive stress regime at several km depth) » **Fault valve model**: orogenic gold/mesothermal gold; and at shallow levels (extensional regime) » **Suction pump model**: epithermal gold

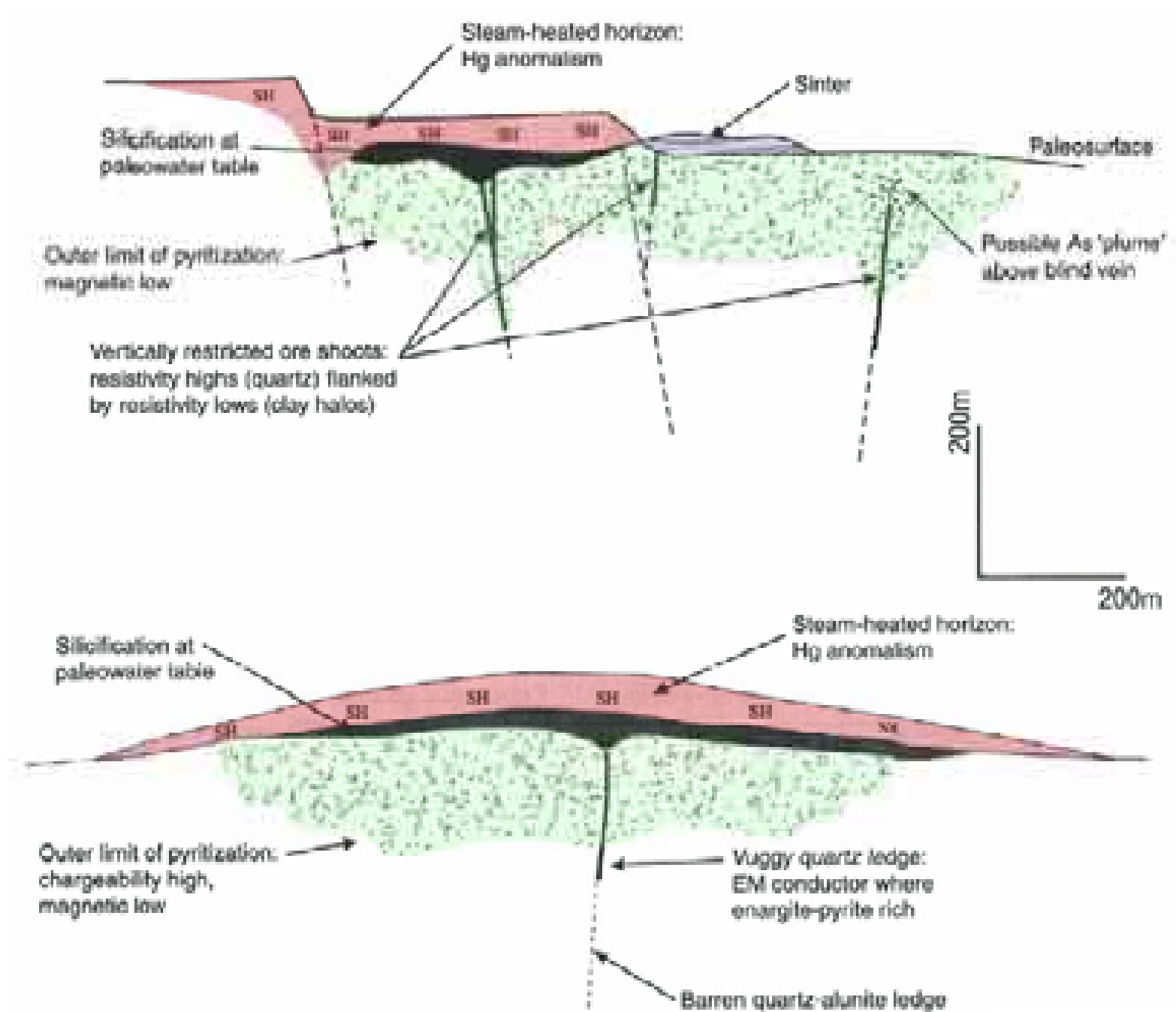
Wadi Hammamat,
Eastern Desert, Egypt

Turin Mine Papyrus,
Museo Egizio
ca. 1200-1000 A.D.
(XXth Dynasty)

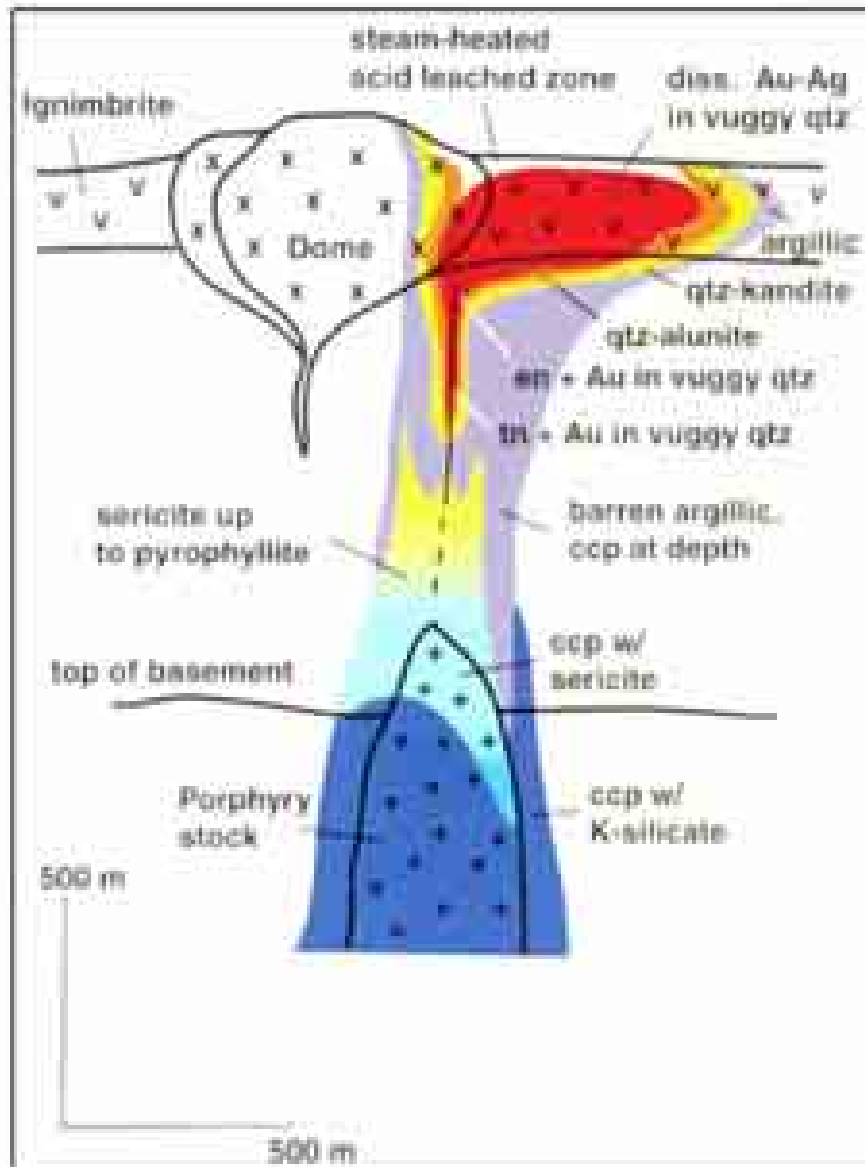


Die Oberharzer Blei- und Silbererzeugung von 1500 bis 1900



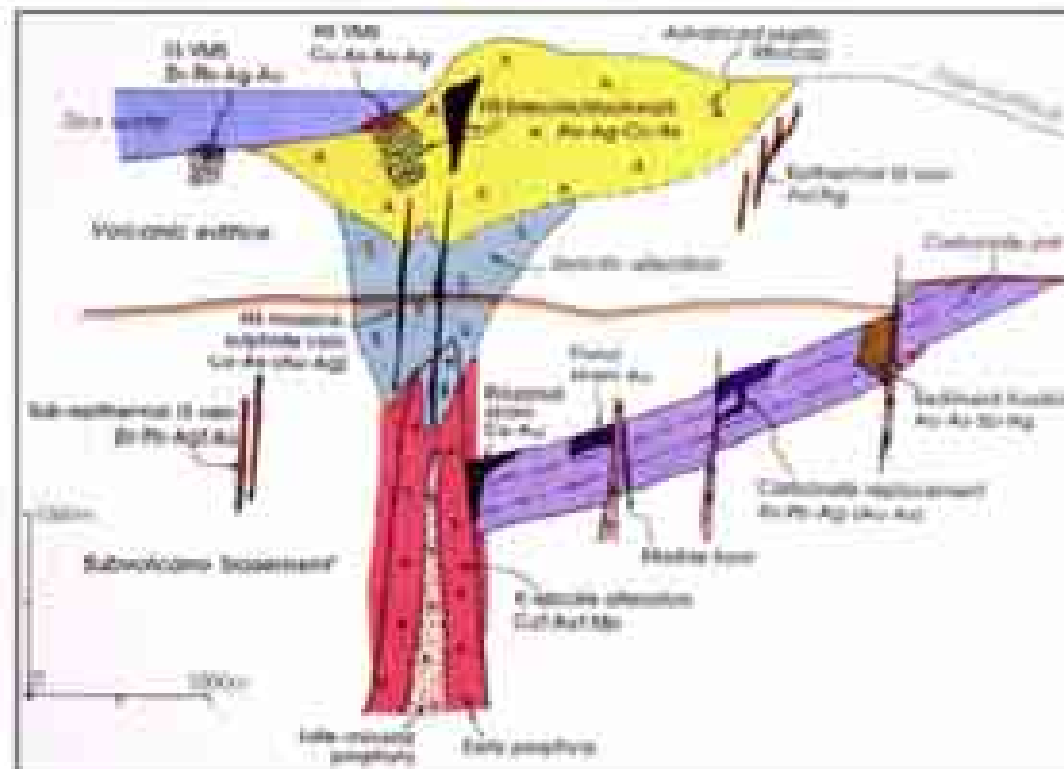


High-sulphidation - porphyry transition



- 1.5 – 2 km vertical interval represented from paleo-surface to porphyry deposit
- Vuggy quartz → quartz-alunite → quartz-pyrophyllite → quartz-sericite from top downwards
- Au-dominated → Cu-dominated from top downwards

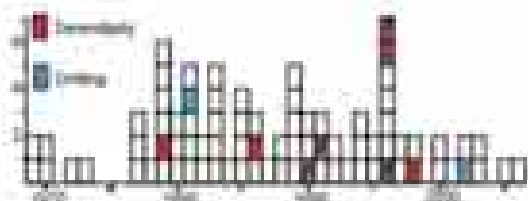
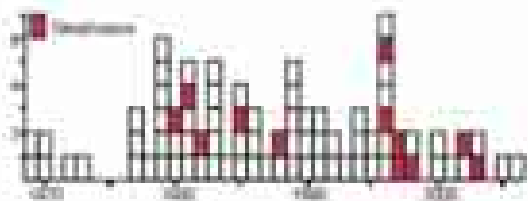
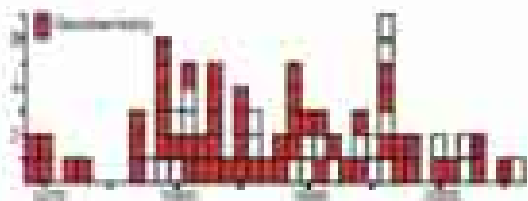
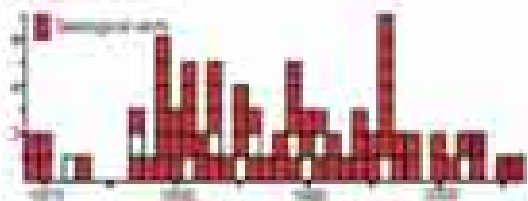
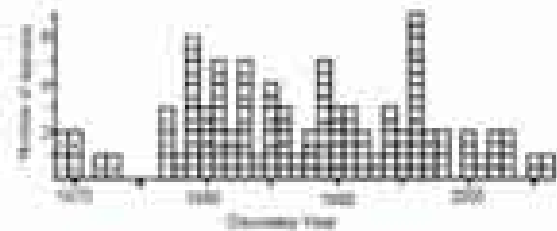
Porphyry-epithermal relationships



Linkages between porphyry, high- and intermediate-sulphidation epithermal, skarn, carbonate-replacement, and Carlin-like environments now widely appreciated.

The necessary information was supplied by worldwide exploration activities.

Key role of geology in porphyry and epithermal exploration



Circum-Pacific Region

Parameters

- 37-year history
- 81 deposits
- Mainly porphyry, epithermal, & sediment-hosted gold (minor VMS & orogenic gold)

Main conclusions

- Notwithstanding exploration changes, little overall evolution in discovery methodology (but see next slide)
- Geologic fieldwork: 90% of discoveries
 - routine observation, mapping, & interpretation
 - familiarity with deposit models (since 1980s)
- Geochemistry: 70% of discoveries
 - stream sediment, soil, & rock chip
- Geophysics: 15% of discoveries (only 50% of programs)
 - Ground IP & EM
- Drilling & serendipity: 12% of discoveries
- Remote sensing (satellite imagery, airborne scanners): 0%